Institut für Hydrologie
Albert-Ludwigs-Universität Freiburg

Matthias Gaßmann

Measuring and Modelling Erosion and Suspended Sediment.

Diplomarbeit unter der Leitung von

Prof. Dr. Ch. Leibundgut
Freiburg, Dezember 2007

Institut für Hydrologie

Albert-Ludwigs-Universität Freiburg

Matthias Gaßmann

Measuring and Modelling Erosion and Suspended Sediment.

Referent: Prof. Dr. Ch. Leibundgut

Koreferent: Dr. J. Lange

Diplomarbeit unter der Leitung von

Prof. Dr. Ch. Leibundgut

Freiburg, Dezember 2007

Acknowledgments

I would like to thank some people for their support during the thesis and the studies:

- Professor Dr. Leibundgut for the allocation of the thesis' theme.
- Dr. Jens Lange for the supervision of the thesis and the discussions.
- Tobias Schütz for the precious discussions about the thesis.
- Emil Blattmann for the support with the measurement instruments.
- All people from 'Rheinstrasse 10' for the discussions.
- My parents, that they were always behind me and for their financial support during the whole studies.
- My girlfriend Sarah for her love and her emotional support on the phone.

Contents

List of Figures

List of Tables

List of Symbols

λ	Brooks-Cores grain size distribution index
ν	kinematic viscosity
$\partial h(\theta)$	soil water matric potential head (m)
∂z	soil depth
ϕ	porosity
ϕ	angle in partially filled pipes
θ	water content
θ_r	residual water content
$\bar{Q}_{obs}$	average of measured runoff
a	distance between drainage pipes
a_{fish}	concentration time in Fisher-Tippet distribution
$areaDep$	influence of area on b_{fish} (%)
B	channel width (m)
b_{fish}	width factor in Fisher-Tippet distribution
C	percentage of clay
C	C-factor of USLE
C_1, C_2, C_3	weighting factor of the Muskingum-Cunge routing method
C_s	suspended sediment concentration ($\frac{g}{l}$)
D	pipe diameter
d	flow depth in partially filled pipes
$depth\_full$	water depth when inner channel is full
E	kinetic energy of a raindrop ($\frac{J}{m^2h}$)
ETA	monthly actual evapotranspiration
ETA_d	monthly actual evapotranspiration derived after distribution
FC	field capacity
$frac\_chan$	fraction of inner channel
$fric$	friction velocity in partially filled pipes
g	acceleration due to gravity
I	infiltration capacity
IL	initial loss (mm)
K	storage constant of the Muskingum-Cunge routing method
$K(\theta)$	unsaturated hydraulic conductivity
K_f	saturated hydraulic conductivity

k_s	surface roughness length (m)
m	mass of raindrop (g)
m_{dry}	mass of dry water samples (g)
m_{glass}	mass of glass (g)
m_{wet}	mass of wet water samples (g)
n	Manning roughness coefficient
NTU	Nephelometric Turbidity Unit
P	water level (m)
P_{eff}	effective porosity
PI	rainfall intensity
PI_{max}	maximum rainfall intensity
PWP	permanent wilting point
Q	runoff ($\frac{l}{s}$)
q	depp infiltration
Q_{i+1}^{j+1}	runoff of the next segment j and the next timestep i
Q_i^{j+1}	runoff of this timestep in the next segment
Q_i^j	runoff of this timestep and this segment
Q_{max}	maximum runoff $\frac{l}{s}$
Q_{obs}	observed runoff
Q_{REF}	estimated reference discharge
Q_{sim}	modelled runoff
Q_s	sediment yield ($\frac{g}{s}$)
r^2	coefficient of determination
R_{eff}	Nash-Suttcliffe efficiency
R_{hy}	hydraulic radius
S	percentage of sand
S_0	energy slope
S_f	hydraulic gradient
SL	soil loss
$slopeDep$	influence of slope on a_{fish} (%)
SSC	suspended sediment concentration
U	percentag of silt
v	velocity ($\frac{m}{s}$)
v_{full}	water velocity of the full pipes
v_{part}	water velocity of the partially filled pipe
v_k	kinematic wave velocity ($\frac{m}{s}$)
X	weighting factor of the Muskingum-Cunge routing method
x	segment length (m)

Summary

Pesticides enter the surface water with precipitation and overland flow. The EU project ArtWET (Mitigation of pesticides pollution and phytoremediation in Artificial WETland ecosystems) researches the possibility to reduce the amount of pesticides in surface water by means of artificial wetlands as some water plants are known to decay pesticides. For this matter, the Institute of Hydrology of the University of Freiburg built an artificial wetland at the outlet of the Loechernbach catchment near Eichstetten am Kaiserstuhl.
The aim of this thesis was a first step on the way to model the movement of pesticides in a catchment. This step contained the modelling of erosion and sediment transport as some pesticides are very strong adsorbed to soil particles. In addition, the possibility to measure suspended sediment concentration by means of turbidity measurements should be reviewed.

Turbidity was measured continuously over a period of two months at the outlet of the catchment as well as at the anthropogenic spring. By means of event water samples, turbidity could be calibrated to suspended sediment concentration by a regression. For comparative reasons, a laboratory calibration with soil taken from the catchment was done also. The result of the laboratory work was a regression equation similar to the equations found in literature (Holliday et al., 2003). A comparison of the two relationships derived in this thesis showed a better usability of the field relationship.
As there was no distributed model with temporal high resolution for erosion and the transport of sediment and pesticides within the existing models, the uncalibrated rainfall runoff model ZIN (Lange et al., 1999) was extended by an erosion and sediment transport module. Originally built for the application in arid catchments, the model had also to be extended by a baseflow module.
The baseflow module was based upon the assumption, that the average of groundwater recharge equals baseflow (Kille, 1970). However, this assumption is only valid for long time intervals. A module test and validation showed that the modelled baseflow approximately fit the measured on an average if the soil storage is large enough. But the dynamic and the recharge of the storage are to lazy to simulate

the rise in baseflow as reaction to a rainfall event.
The hydrological part of the model (except the baseflow module) was parameterised by literature values and own measurements. The validation showed very nice results for single event flow. However, it seems that runoff generation processes that are not integrated in the model play a role in the catchment, when more than one event takes place in short sequence.
The only input needed to run the erosion and sediment transport module is the relationship between rainfall intensity and erosion ($\frac{g}{m^2 s}$). This equation could be derived from rainfall simulator tests found in literature. As the tests were done on bare surface, the coverage and crop rotation factor C from the Universal Soil Loss Equation was taken to derive values for the vegetated areas. Module test and validation showed suitable results, whereas the validation runs underestimated the measured values.

To compare both approaches of this work to derive the suspended sediment concentrations, a further validation of the model results was done with sediment concentrations derived by turbidity measurements. The results showed a good agreement of both approaches.
So it could be suggested that the turbidity measurements as well as the modelling can be applied successfully in the Loechernbach catchment. For a common validation of the methods, an application in other catchments should be done in future.

Keywords:
suspended sediment concentration, erosion modelling, sheet erosion, sediment transport, rainfall-runoff modelling, turbidity measurements, ZIN model.

Zusammenfassung

Pestizide werden durch Niederschlag und Oberflächenabfluss in Oberflächengewässer eingetragen. Das europäische Projekt ArtWET (Mitigation of pesticides pollution and phytoremediation in Artificial WETland ecosystems) untersucht die Möglichkeit die Menge von Pestizide in Oberflächengewässern anhand von künstlich angelegten Feuchtflächen zu vermindern, da es bekannt ist, dass Wasserpflanzen in der Lage sind Pestizide abzubauen. Das Institut für Hydrologie der Universität Freiburg hat zu diesem Zweck eine künstliche Feuchtfläche am Auslass des Löchernbach Einzugsgebietes nahe Eichstetten am Kaiserstuhl eingerichtet.
Das Ziel dieser Arbeit war ein erster Schritt hin zur Modellierung des Transportes von Pestiziden. Dieser Schritt sollte in der Modellierung von Erosion und Sedimenttransport bestehen, da Pestizide teilweise sehr stark an Sedimentpartikel gebunden werden. Dazu sollte die Möglichkeit, suspendiertes Sediment anhand von Trübungsmessungen zu erfassen, überprüft werden.

Die Trübung wurde über einen Zeittraum von zwei Monaten kontinuierlich sowohl am Pegel als auch an der anthropogenen Quelle des Loechernbaches gemessen. Anhand von Ereigniswasserproben konnte die Trübung über eine Regressionsrechnung auf die Sedimentkonzentration kalibriert werden. Zu Vergleichszwecken wurde ebenso eine Kalibrierung anhand eines Laborversuches mit Boden aus dem Einzugsgebiet durchgeführt. Das Ergebnis war eine Regressionsbeziehung, die ähnlich den in der Literatur (Holliday et al., 2003) angegebenen Beziehungen war. Ein Vergleich der beiden hier gewonnen Beziehungen erbrachte, dass die im Feld gewonnene Beziehung besser zu gebrauchen war.
Da unter den bestehenden Modellen kein flächenverteiltes zeitlich hoch aufgelöstes Modell für Erosion und den Transport von Sediment und Pestiziden gefunden werden konnte, wurde das unkalibrierte Niederschlags-Abfluss Modell ZIN (Lange et al., 1999) um ein Erosions- und Sedimenttransport Modul erweitert. Ursprünglich für den Einsatz in ariden Gebieten entwickelt, musste ebenfalls ein Modul für die Simulation von Basisabfluss in das Modell integriert werden.
Dem Basisabflussmodul liegt die Annahme zu Grunde, dass die Grundwasserneubildung im Mittel gleich dem Basisabfluss ist (Kille, 1970). Jedoch gilt diese Annahme

nur für lange Zeiträume. Modultest und -validierung zeigten, dass bei einem genügend großen Bodenspeicher der Basisabluss im Mittel getroffen werden konnte, die Dynamik und das Auffüllen des Speichers aber zu träge sind, um einen Anstieg im Basisabfluss als Reaktion auf ein Niederschlagsereignis richtig modellieren zu können.
Der hydrologische Teil des Modells (neben dem Basisabfluss-Modul) wurde anhand von Literaturdaten und eigenen Messungen parametrisiert. Eine Validierung zeigte sehr gute Ergebnisse für die Simulation von Einzelereignissen. Jedoch scheinen bei dicht aufeinander folgenden Ereignissen auch Abflussbildungsprozesse eine Rolle zu spielen, die das Modell nicht erfassen kann.
Der einzige Input der zur Benutzung des Erosions- und Sedimenttransport Moduls erforderlich ist, ist die Beziehung zwischen Niederschlagsintensität und Erosion ($\frac{g}{m^2 s}$). Diese Beziehung konnte aus in der Literatur gefundenen Beregnungsversuchen gewonnen werden. Da die Beregnunsversuche auf naktem Boden durchgeführt wurden, wurde der Bedeckung- und Fruchfolgefaktor C aus der allgemeinen Bodenabtragsgleichung (Universal Soil Loss Equation) benutzt um die Werte für die bewachsenen Flächen zu erhalten. Modultest und -validierung zeigten befriedigende Ergebnisse, wobei bei der Validierung die Werte unterschätzt wurden.

Um die beiden Ansätze dieser Arbeit, Sedimentkonzentrationen zu gewinnen, miteinander vergleichen zu können, wurde eine erneute Validierung der Modellergebnisse mit den aus Trübungsmessungen gewonnen Sedimentkonzentrationen durchgeführt. Die Resultate zeigten eine deutliche Übereinstimmung der beiden Ansätze. So konnte geschlossen werden, dass sowohl die Trübungsmessung als auch die Modellierung im Löchernbachgebiet angewandt werden können um Sedimentkonzentrationen zu gewinnen.
Zur allgemeinen Validierung der Methoden steht eine Anwendung in anderen Einzugsgebieten für die Zukunft aus.

1. Introduction

Pesticides and herbicides are widley used in agriculture to destroy weeds and vermin. With this practice a better growth of plants should be enabled.
In areas where pesticides are applicated, they are often found in surface water, which should be avoided according to the european Water Framework Directive of the year 2000. There are two main pathways for pesticides to get into the surface water (Schulz, 2007):

- spray drift by wind
- overland flow by water.

The EU-Project ArtWET (Mitigation of pesticides pollution and phytoremediation in Artificial WETland ecosystems) researches the possibility to fate pesticides in the surface water by artificial wetlands as some water plants are known to decay pesticides. The Institute of Hydrology of the University of Freiburg is predominantly responsible for the hydrological and hydraulical part, that means also the modelling of pesticide movement with water at events (hydrological model) and the allocation within the wetland (hydraulic model). The modelling is always associated with measurements, partly classical hydrometric measuring, partly tests with natural (Nippgen, 2007) and dye tracers and natural tracers taken as dye tracers (e.g. temperature).
For the purpose of the project an artificial wetland was constructed in the flood detention basin 'Breitenweg' near Eichstetten, which is located some meters below the catchment outlet of the Loechernbach. In this catchment extensive agriculture is practiced, and so it is a good test catchment for the aims of the ArtWet project.

2. Deriving objectives - model decision

The objectives of this thesis were defined as the modelling of pesticide movement in the Loechernbach catchment. Before a modelling can be done, a model has to be searched for. In this chapter some models are reviewed and the model requirements are defined. The question has to be asked if there exists a model for the requirements. Just when this question is answered and a model is found, the objectives of the thesis can be defined clearly with taking the abilities of the chosen model into account.

There is a mass of models available for pesticide movement in overland water. Some models, with origin mostly in the USA, are discussed in Borah and Bera (2003) as well as Borah and Bera (2004). These models are the partly very often used AnnAGNPS, AGNPS, HSPF, SWAT und DWSM.
The Group FOCUS, 'FOrum for Co-ordination of pesticide fate models and their USe', is an international expert group, that deals with the application of pesticide-models for the authorisation of new pesticides (Adriaanse et al., 1997). It consists of four workgroups for the different fields Groundwater, Surface Water, Landscape and Mitigation and Degradation Kinetics. The workgroup Surface Water suggests a combination of different models (MACRO, PRZM_SW, TOXSWA, Drift Calculator) to compute the exposure of pesticides in streams (URL1, 12.07.2007).

2.1. Event based models

2.1.1. AGNPS

The event-based model AGNPS (Agricultural Nonpoint Source Pollution) is a distributed model developed by the USDA Agricultural Research Service to estimate the pollution from agricultural sources and to find a best management practice for the application of fertilizers (Shoemaker et al., 2005). It is able to simulate point

and non-point sources. The temporal resolution of the model is restricted to one value per event. The Input of the data is mostly GIS-based.
The pesticide-module is working with a first-order kinetic reaction for degradation of pesticides as well as a linear sorption-equation.
The hydrology of the model, which is infiltration excess overland flow and channel routing, is based upon the SCS-CN-Method(Borah and Bera, 2003).
AGNPS is free and can be downloaded at http://www.ars.usda.gov.

2.1.2. DWSM

The mainly physical based model DWSM (Dynamic Watershed Simulation Model) was developed by the Illinois State Water Survey. In literature the model is said to be distributed (Borah and Bera, 2003; Shoemaker et al., 2005). However, before the modeling is done, the catchment is divided into subbasins and by means of hydrological attributes into hydrological response units (Shoemaker et al., 2005). This is typical for semi-distributed models.
DWSM is able to simulate single events and to divide these into timesteps of any length, for example one minute.
The infiltration excess is either represented by the SCS-CN-method (Soil Conservation Service - Curve Number) or by a complex approach by Smith and Parlange (1978) as it is described in Borah et al. (1999). Overland flow and routing are integrated as an analytical solution of the kinematic wave. Interflow, drainage as well as baseflow are computed in the same module, a storage based approach.
An erosion module calculates the channel sediment yield in fife grain sizes. The amount of pesticides adsorbed to the sediment particles is computed as an equilibrium between dissolved and adsorbed phase with a linear isotherm. Degradation of pesticides is neglected (Borah et al., 1999).

2.2. Long term models

2.2.1. AnnAGNPS

The Annualized Agricultural Nonpoint Source Pollution Model (AnnAGNPS) is a further development of the AGNPS and is based upon it. AnnAGNPS is, as well as AGNPS, distributed and integrated in a GIS. It is working on a basis of daily values. In contrast to AGNPS it is thought for simulating long time and therefore there are partly other hydrological components integrated (Borah and Bera, 2003).
Infiltration excess is calculated as a water balance of a soil with two layers, over-

land flow - again - with the SCS-CN-method. Unlike AGNPS, interflow is computed separately as lateral flow with the Darcy-equation. The channel flow module is also modified in the AnnAGNPS. It is simulated with the Mannig-equation and assumed trapezoid profiles. Evapotranspiration is derived with the Penman-equation.
Erosion and sediment transport are described as well as pesticide transport. Pesticide transport is derived by a mass balance of dissolved and adsorbed species (Shoemaker et al., 2005). The pesticide module is the same as in the antecessor. Shoemaker et al. (2005) pointed out a limiting effect for the application: 'All runoff and associated sediment, nutrient, and pesticide loads for a single day are routed to the watershed outlet before the next day simulation.'

2.2.2. HSPF/WinHSPF

The model HSPF (Hydrological Simulation Program Fortran) respectively the graphical interface WinHSPF, is based upon the 'Stanford Watershed Model' (SWM). As integral part of the model package BASINS it gets data from the MapWindow GIS. HSPF divides a basin in subbasins and landuse, whereas the landuse of a single subbasin is treated as lumped. Therefore the model is settled in the group of semi-distributed models. Mostly it is run in a temporal resolution of one hour, but it may be run with shorter timesteps, too (Shoemaker et al., 2005).
The hydrology of the model is integrated very detailed, however often with empirical equations, that require a very elaborate calibration process (Shoemaker et al., 2005).
Infiltration excess is derived from the water balance in consideration of evapotranspiration and interception, overland flow as an empirical storage outflow and with the Cezy-Manning equation. Interflow, percolation and groundwater outflow are computed as empirical storage outflows, channel flow with an empirical equation in dependence of catchment parameters (Borah and Bera, 2003).
HSPF is able to simulate erosion and sediment transport. Pesticides are modelled in three phases: dissolved, adsorbed and crystallised and are degraded by a first-order kinetic reaction or two different Freundlich-Isotherms. Transport occurs with water movement or sediment dynamics. Also dry and wet atmospheric deposition of pesticides can be simulated (Bicknell et al., 2001).

2.2.3. SWAT

A mainly for prediction of the impacts of landuse changes to water, sediment and agricultural chemicals in discharge of big catchments developed model is the 'Soil and Water Assessment Tool' (SWAT). It is a semi-distributed model with a temporal

resolution of one day (Shoemaker et al., 2005).
The hydrology of the model is based upon the SCS-CN-method, whereas interception, infiltration (Green-Ampt equation) and evapotranspiration (Penman-Monteith, Priestley-Taylor or Hargreaves-approach) are considered (Shoemaker et al., 2005). Interflow and baseflow are separately simulated. Channel flow is based upon the Manning-equation.
Pesticides are transported with overland flow to the channel as adsorbed or dissolved phase. The equations were adopted from the model GLEAMS. Solubility, half-life time, as well as a coefficient which describes adsorption to organic carbon in the soil rule the dynamic of pesticides. Erosion as well as sediment transport are based upon the MUSLE (Modified Universal Soil Loss Equation) (Neitsch et al., 2005).

2.3. FOCUS-models

The models of the group FOCUS are not intended for a single application on pesticides, because each covers just parts of the hydrological cycle. Figure 2.3.1 shows the mesh of the different models. Some scenarios for the permission of new pesticides have been developed. The models MACRO and PRZM are used alternatively depending on the scenario (URL1, 12.07.2007).

The 'Surface WAter Scenarios Help' (SWASH) is a graphical interface to handle with the FOCUS-software. While SWASH prepares the output data of one model as input data for an other model, it is the linkage between the FOCUS models, as it is shown in figure 2.3.1. Scenarios of different agricultural situations can be chosen to run the models (URL1, 12.07.2007).
The only model running directly in SWASH is the "Drift Calculator". It computes the direct pesticide input from winddrift when pesticide is allocated at fields (URL1, 12.07.2007).

MACRO is a physically based one-dimensional numeric soil water model based upon the Richards-equation. It calculates saturated as well as unsaturated flow in micro- and macropores and therefore it can deal with drainages. A convection-dispersion-equation computes the pesticide transport in micropores, a more simple approach is applied to the macropores. Pesticide degradation is calculated with a first-order kinetic reaction for the four pools micro/macropores as well as soil/liquid phase. A Freundlich-isotherm describes sorption as equilibrium between liquid and solid phase (URL1, 12.07.2007).

The second soil water model is the PRZM_SW (Pesticide Root Zone Model).

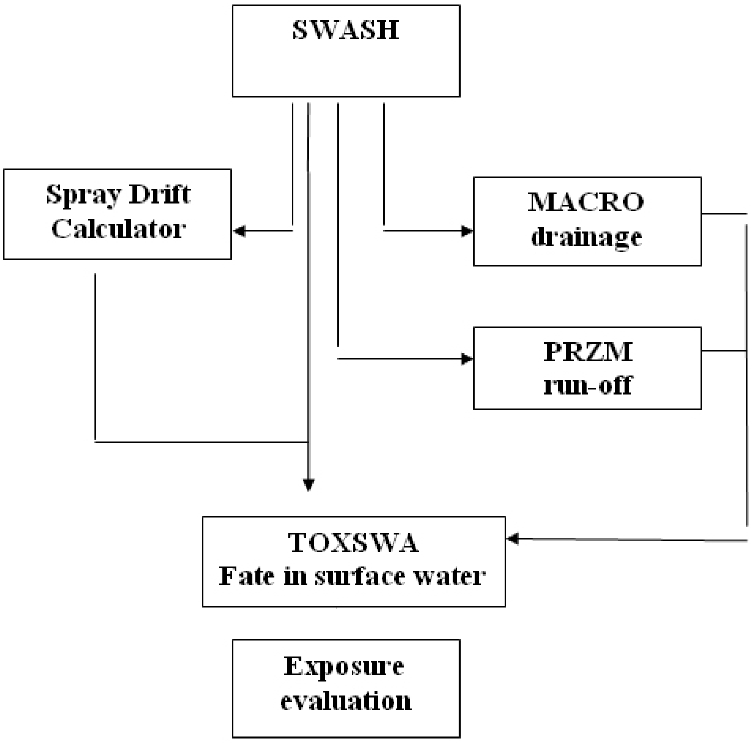

Figure 2.3.1.: The mesh of the FOCUS-models (URL1, 12.07.2007).

It is a one-dimensional non-deterministic model for prediction of the movement of chemicals in soils on a daily basis. For water movement in soils a Richard-equation is used and for chemical movement a convection-dispersion-equation. Overland flow is calculated with the SCS-CN-method. Plants are considered by adjusting the root zone and interception by the vegetation period. The erosion module is using the popular USLE (Universal Soil Loss Equation). Pesticide degradation is computed using a first order kinetic reaction, whereas soil temperature and moisture are considered and volatilisation of pesticides is integrated in the model. The sorption of the substances can be calculated with a linear or a Freundlich isotherm. A special feature of the model is that one can simulate up to two metabolites (URL1, 12.07.2007).

The FOCUS-model for behavior of pesticides in surface water is TOXSWA (TOXic substances in Surface WAters). The four in TOXSWA integrated processes are transport, metamorphosis, sorption and volatilisation of pesticides. The model has two layers: water and subjacent sediment. In the water layer pesticides move with advection and dispersion, while in the sediment diffusion is an additional process. Metamorphosis is a function of temperature and describes the processes hydrolysis, photolysis and biodegradation. Again, a Freundlich isotherm is responsible for sorption of pesticides to sediment particles. Sorption to macrophytes is using a linear isotherm. At the border between the layers pesticides are transported with diffusion and advection (URL1, 12.07.2007).

2.4. Discussion

To choose the best fitting model from the above explained, the model-requirements have to be clear. The requirements are defines in the classes pesticide module, hydrology, temporal as well as spatial resolution. The main points are:

- The pesticide module should be able to simulate pesticide degradation and sorption.
- The hydrology of the model should be process-orientated.
- The model should be distributed (in terms of runoff and therefore pesticide generation).
- The model should have a high temporal resolution (1-15 min).

The most detailed hydrology is included in the models DWSM and HSPF, whereas DWSM is mostly using physical and HSPF empirical equations. AnnAGNPS, SWAT and the FOCUS-models are using partly the SCS-CN-method and partly other hydrological equations like storages and the Darcy-equation for single processes. The SCS-CN-method is estimated critically for the calculation of overland flow, since precipitation intensity is not considered within calculation and all processes are expressed by one curve number. Hence the above mentioned models are rated lower in terms of hydrological representation. The AGNPS is focused completely on the SCS-CN-method and is therefore dropped back behind all other models in the hydrological evaluation.

Also in view of the pesticide modelling differences are shown. Thus the DWSM is here dropped back as it considers just sorption/desorption, but no degradation (Borah et al., 1999). AGNPS, AnnAGNPS, SWAT, HSPF as well as the FOCUS-models compute degradation with a first-order kinetic reaction, but just HSPF and the FOCUS-models permit a Freundlich-isotherm additionally, that is transformed to a linear isotherm with the exponent "1". The FOCUS-models even stand out of the others with estimating sorption to and from macrophytes as well as sediment separately.

The spatial resolution is important for the pesticide modelling of this thesis, as it should be possible to define accurately where the pesticides are put to the fields by the farmers.
The models DWSM, HSPF, SWAT as well as FOCUS are HRU-type models (Hydrological Response Unit). The basin is represented just semi-distributed, as it is separated into subbasins, within the subbasins by means of landuse and other hydrological parameters into HRUs. The models AGNPS as well as AnnAGNPS are distributed models in terms of runoff generation, with single parameters and input data for each cell. In terms of runoff concentration the models are non-distributed, too. AGNPS and AnnAGNPS are the only models with the possibility for a distributed pesticide input.

Since the Loechernbach catchment is very small (1,8 km^2) and with the anthropogenic deformation (drainages, road and path network) the reaction time of the basin to rainstorm events is very small. The duration of the events is just about an hour. As the pesticide output of the model should be a pesticide load curve, a model has to be found with output timesteps of a minimum of 15 minutes or less.
AGNPS is just able to give one output value for each event, AnnAGNPS, SWAT as well as FOCUS one per day. HSPF is used mostly in one-hour steps, but ought to be able to model less timesteps. Just DWSM is adequate to model small timesteps of one minute.

Table 2.4.1 shows a summary of the evaluation of the criteria important for model decision. Taking the above mentioned model-requirements into account, the following conclusion could be derived:
AGNPS as well as AnnAGNPS are indeed spatially but not temporally distributed. SWAT and the FOCUS-models are neither temporally nor spatially distributed. HSPF and DWSM are indeed temporally but not spatially distributed. In terms of pesticide and hydrological modelling just HSPF can insist. With being a HRU-type-model pesticides can not be modelled distributed with HSPF. Another disadvantage of the model is the enormous effort for the calibration process of the empirical equations. With no pesticide measurements in the Loechernbach catchments, the pesticide module can not be calibrated.

Table 2.4.1.: Usability estimation of the important components of the examined models.

Modell	AGNPS	DWSM	AnnAGNPs	HSPF	SWAT	FOCUS
spatial	**dist.**	HRU	**dist.**	HRU	HRU	HRU
temporal	one event	**min-h**	1d	1h	1d	1d
hydrology	-	+	o	+	o	o
pesticide module	o	-	o	+	o	+

dist.=distributed; HRU= HRU-type model; '-' = bad; 'o' = ok; '+' = good

2.5. Conclusion

There is no applicable model for the requirements of this thesis among the examined models. Either the temporal (AGNPS, AnnAGNPS, SWAT, FOCUS) or the spatial (DWSM, HSPF) resolution does not fit. Even if one settle with a lower spatial resolution, the bad pesticide module on DWSM and the elaborate calibration on HSPF would be KO-criteria.

The only way to model the pesticides with the above defined requirements anyway, is to develop new modules for this task.

3. Objectives and proceeding

The objectives of this thesis are a part of the the aims of the project ArtWET. The originally defined aims, the modelling of pesticide movement, can not be fit with the existing models as a high spatial and temporal resolution is required in the Loechernbach area.
To model the pesticides in the Loechernbach catchment anyway, the rainfall-runoff model ZIN, developed at the Institute for Hydrology of the University of Freiburg (Lange et al., 1999), should be expanded by an pesticide transport module. As some pesticides are strongly adsorbed to soil particles, it is existential to know the erosion and sediment transport in a catchment.
In a first step on the way to model pesticides, the erosion and sediment transport will be modelled in this thesis. Measurements of turbidity and suspended sediment concentrations will be the base for the model validation.

Figure 3.0.1 shows the proceeding of the thesis. The modelled hydrology and erosion/sediment transport should build a modelled suspended sediment concentration. The measurements of turbidity should provide measured concentrations as it is more easy to measure turbidity continuously than sediment concentration directly by samples. The measurements then should be able to validate the model results.
It is the aim to fit small and midrange events ($< 200\ \frac{l}{s}$) with the hydrological model, because the larger events are to large to run through the artificial wetland. As it is placed in a flood detention basin larger events are bypassed automatically or held back in the basin. So the test and the validation runs are only rated if they are in the specified runoff range.

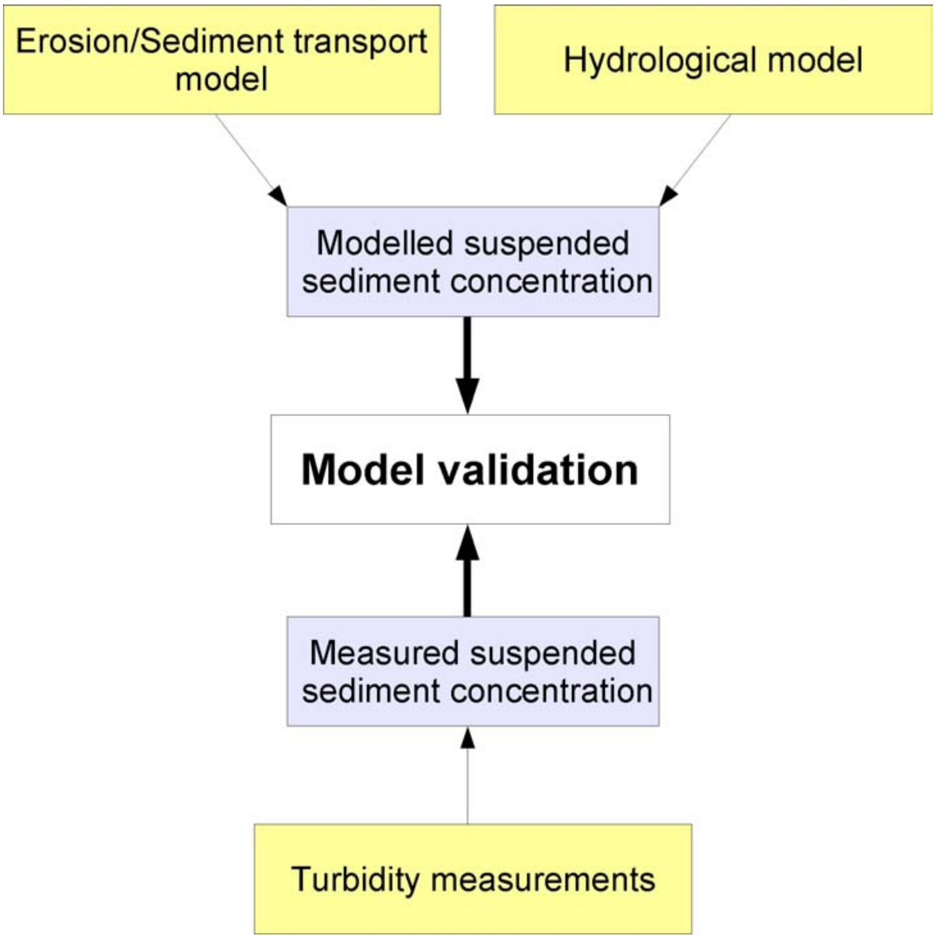

Figure 3.0.1.: Proceeding of the thesis.

4. Methods

This work combines measurements and data analysis with modelling. The base of the sediment modelling and sediment data analysis is explained here. However, hydrological modelling needs no further explanation as it is a usual tool for hydrologists.

4.1. Erosion by water

There are two main forms of erosion by water: sheet erosion and rill erosion. While sheet erosion happens mainly by the impact of raindrops on the soil, the rill erosion in all its forms (gully erosion, tunnel erosion) is caused by flowing water. For this work the sheet erosion is important and will be specified in this section.
Sheet erosion by water takes place in two different steps: detachment and transport, whereas both is possible with rainfall and runoff.
Detachment and transport by raindrops, called splash-effect, happens as follows (Auerswald, 1998):

- A Raindrop is falling to the ground with the kinetic energy $E = \frac{1}{2} \cdot m \cdot v^2$ (mass m, velocity v).
- If the ground is dry the falling raindrop is able to produce high air pressure in a soil units and can cause it to break.
- If the soil is already wet, the raindrop falls on the soft ground and creates a small crater while the soil-water mixture is thrown out of the crater by the kinetic energy of the raindrop.

So the soil particles are cracked, detached and transported by the impact of raindrops, that means the kinetic energy of the raindrops. After the detachment, the soil particles may be transported by flowing water, so the transport takes place not only by the splash effect but also by flowing water.
As mentioned above, the kinetic energy depends on the mass and the velocity of the raindrops. Brandt (1989) showed a power relationship between drop size diameter and rainfall intensity, that means between the mass of the raindrops and the rainfall intensity. Due to the impact of gravity on the falling raindrop in a non-vacuum

environment, the fall velocity gets larger with larger drop mass as it is shown in AUERSWALD (1998).
All in all, the kinetic energy of rainfall, that drives the erosion, can be written simplified as an equation depending on just the rainfall intensity (SALLES ET AL., 2002). On this knowledge, a relationship between rainfall intensity and sediment yield ($\frac{g}{m^2 min}$) will be searched for, to derive a simple measurement based sheet erosion model.

4.2. Sediment transport with water

There are three kinds of transported particles in water that build the total sediment load: solved load, suspended load and bedload. The solved load consists of solved material in water and differs from the other two, as it depends not that much on the kinetic energy of water. Bedload is that part of the total sediment load, that moves by rolling, sliding and/or hopping (saltation) along the streambed (SHEN and JULIEN, 1993). This load is to heavy to stay in suspension with water and sediments again after being lifted.
The most important type of sediment in water for this work is the suspended sediment load. With water movement and turbulences, forces drive sediment particles, that are light enough, to stay in suspension with water. It depends on the flow velocity of water which grain sizes are suspended sediments.

4.2.1. Dimensions

In literature there are two possibilities used to handle suspended sediment in water with respect to their dimensions. The sediment yield Q_s ($\frac{g}{s}$) is also called sediment discharge and declares how much sediment 'flows' through a cross section per timestep. In contrast, the sediment concentration C_s ($\frac{g}{l}$) shows the amount of sediment in respect to the amount of water. The transformation of the two dimensions goes with runoff Q:

$$Q_s = Q \cdot C_s \tag{4.2.1}$$

If it is spoken about sediment in this work, always suspended sediment it meant.

4.2.2. Sediment rating curves

It is a classical approach to compare suspended sediment concentrations C_s from measurements with runoff Q called 'Sediment Rating Curve'. Many studies showed more or less good relationships (Xu, 2002; Schmidt and Morche, 2006; Asselman, 2000; Khanchoul et al., 2007) and most of them were fitting power functions with two coefficients a and b:

$$C_s = a \cdot Q^b \tag{4.2.2}$$

The coefficients of determination derived in the studies were in a range of $r^2 = 0.06$ to 0.85. Some studies did not use single values to derive the relationship, but built classes or took averages. Khanchoul et al. (2007), for example, did not use a single relationship, but built runoff classes and calculated relationships for each class.
A single relationship of a sediment rating curve will be done in the Loechernbach catchment to compare it with the other technique used to derive suspended sediment concentrations by measurements in this work.

4.2.3. Suspended sediment concentrations by turbidity measurements

The main technique done in this study to derive suspended sediment concentrations is the measurement of turbidity. Turbidity was already shown in many studies to have a strong relationship to Q_s.
Ankcorn (2003) as well as Holliday et al. (2003) derived relationships between turbidity and suspended sediment concentration. The relationships derived by Ankcorn (2003) were made with field data taken in Georgia, USA and had coefficients of determination of $r^2 = 0.9752$ respectively $r^2 = 0.7465$.
The relationship by Holliday et al. (2003) was taken in the laboratory with soil samples from the catchment. Artificial concentrations were made and measured with a nephelometric turbidimeter. The relationships derived had r^2s of about 0.99, but just three sampling points per relationship were used. Both studies fitted power relationships of the form

$$turbidity = a \cdot {C_s}^b. \tag{4.2.3}$$

The range of the turbidity values was in the field study up to 1000 NTU and in the laboratory study up to 500 NTU.
Both, a relationship derived from field measurements and from laboratory measurements will be done here and compared to their usability.

4.3. Conclusion

The new erosion/sediment transport module of the ZIN model will be based upon the approach, that erosion takes place due to the amount of kinetic energy of a rainstorm. This kinetic energy was shown to depend mainly on rainfall intensities. Hence a relationship between rainfall intensity and amount of erosion may fit a measurement based erosion model. The form of erosion important in the test catchment is sheet erosion, as the bare surfaces are on the terraces and therefore are have no steep slopes.

The main technique used in this thesis to measure suspended sediment concentration is the calibration of turbidity measurements to sediment concentrations. For comparisons the classical approach of a sediment rating curve will be used as well.

5. Catchment description

The Loechernbach catchment, which is the test catchment for this thesis, is a small scale catchment located at the eastern edge of the Kaiserstuhl in south-west Germany. The area of the surface catchment is 1.61 km^2 and the area of the subsurface catchment 1.79 km^2. In this study, the subsurface catchment is shown in figures, whereas zones not contributing to overland flow were identified by Wagner (2002). There are two main tributaries in the catchment, the Loechernbach, that comes from north-west and the Biebenbach from west. Both start at artificial 'springs', that means the pipes draining the streets above are the springs.
The elevation of the catchment ranges from 213 m to 380 m over N.N. while the slope is mostly 1 - 7 % (82 % of the catchment, slopes of the terraces and the floodplain) or 90-100 % (11.9%, slope of the acclivity)(Demuth and Westphal, 1981).

5.1. Climate

The climatic exceptional position of the Kaiserstuhl is based upon its position between the Black Forest and the Vosges in the deep upper rhine valley. With an average of about 1700 hours of sunshine per year it belongs to the regions with the most sunshine in germany. Outstanding are the high afternoon and evening temperatures in the summer. The mean temperature of the adjacent weather station Lilienthal was 8.9°C for the period of 1965-1979 and the average yearly rainfall sum 846 mm for the same period. Figure 5.1.1 shows the climate chart of the station Lilienthal, which is located just a few kilometers south-west of the Loecherbach area and is lying in a comparable valley situation (Luft, 1980a).

The maximum rainfall sums are shown in august, june and may when the summer rainstorms take place. December to march and october show just small amounts of rainfall (up to 50 mm). Even in january, the average temperatures don't fall below 0°C, but reach nearly 20°C in august. The climate classification after Köppen results in a temperate climate with no dry season and warm summers (Cfb). If the average temperatures in august rise in the next decades by 1-2 K, as it was predicted by the climate change group KLIWA (Klämt, 2004), the classification may change to

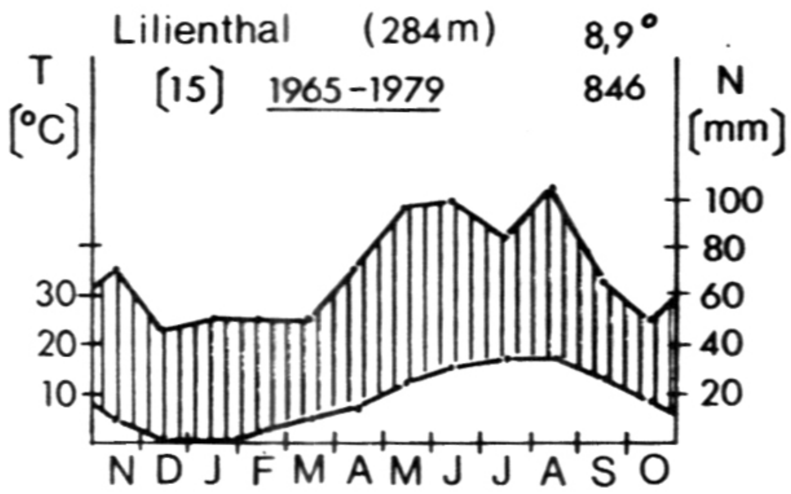

Figure 5.1.1.: Climate chart of the weather station Lilienthal for the period 1965-1979 (LUFT, 1980a).

a Cfs climate at the end of the 21st century. This will be the case when the august temperatures exceed 22°C.

5.2. Pedology and geology

The geologic development of the eastern Kaiserstuhl area took place in different steps (LUFT, 1980a):

- With the development of the upper rhine area, mesozoic and tertiary sediment layers were lifted at the end of the oligocene. This went along with faults and flexures.
- The oligocene layers were weathered intermediately.
- Multi-crater volcanic activities at the crossing of the two trenches 'Oberrhein-graben' and 'Bonndorfer Graben'.
- Since the upper miocene: constant weathering of the volcanic rocks and the 'Pechelbronner Schichten'. This is a tertiary stage with steep sloping in eastern and south-eastern directions.
- Mighty aeolic loess sedimentations developed during the cold phases on the lee side of the Kaiserstuhl.
- Climatic and tectonic erosion formed the larger valleys in the pleistocene.

- The small scale formation of the valleys is an enduring process driven by climatic conditions.

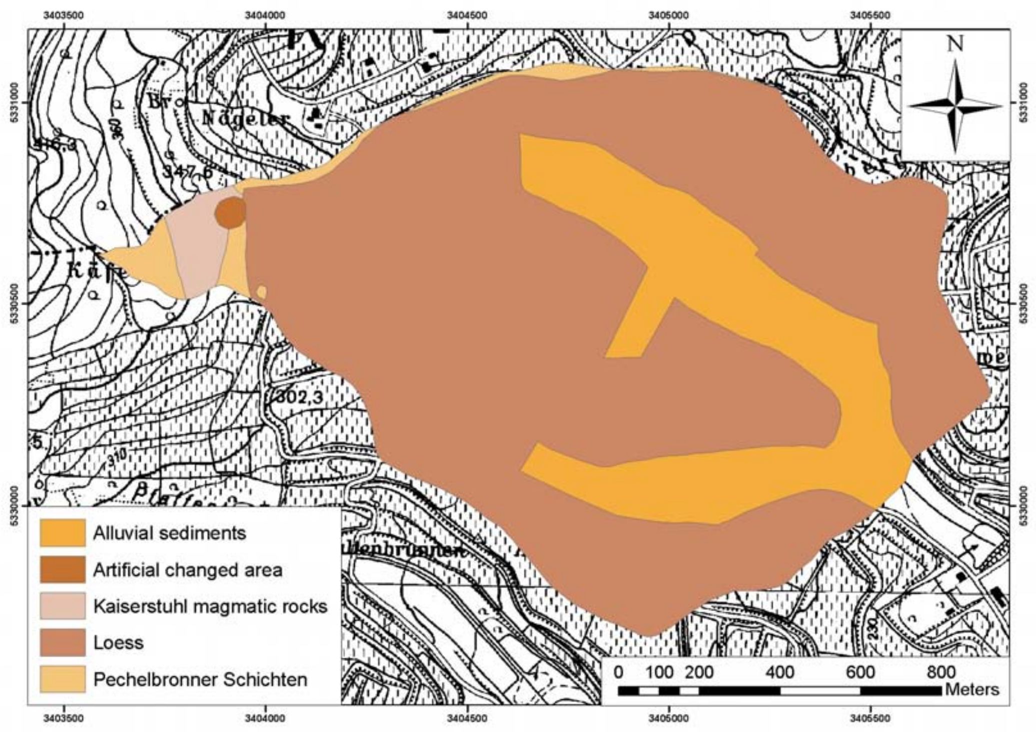

Figure 5.2.1.: Geology of the Loechernbach catchment (KRAEMER, 1999).

Figure 5.2.1 shows the geological situation in the Loechernbach area overtaken from KRAEMER (1999). In the upper part, the 'Pechelbronner Schichten' and magmatic rocks underly the catchment. A small part is marked as 'artificial changed area'. There is a playground located, but it is not known what this has to do with geology. The largest part are the large terraces consisting of loess. The floodplain is filled with eroded and sedimented loess from the terraces.
In a hydrogeologic view, there are two main aquifers at the Kaiserstuhl: The fissured rock aquifer consisting of the volcanic rocks and the pore aquifer in the loess sediments (UHLENBROOK, 1995). The more dynamic aquifer is the pore aquifer, that overlies the rock aquifer mostly.

As there is a wide spread of different geology, relief and time length of soil development, the soils at the Kaiserstuhl differ much. Three of the four main soil regions specified at the Kaiserstuhl by HÄDRICH and STAHR (2001) can be found in the Loechernbach area and are shown in figure 5.2.2:

- The crest region: Mostly vegetated by forest, the crest region differs the land-

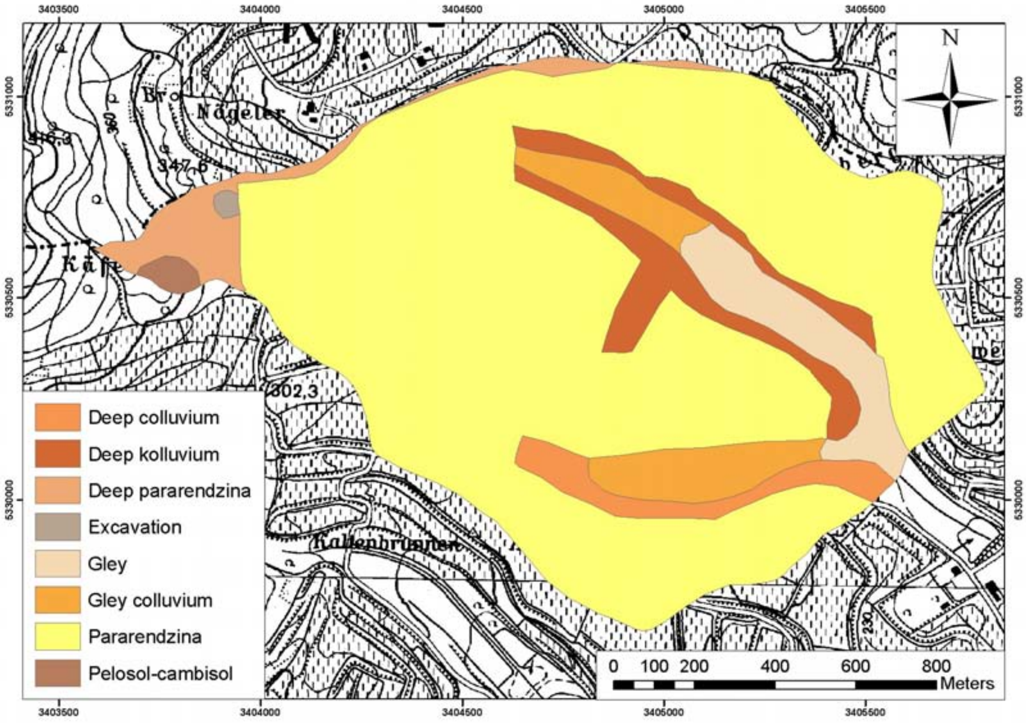

Figure 5.2.2.: Soils of the Loechernbach catchment KRAEMER (1999).

use by geological means. The soils found in the test catchment are pelosol-cambisols, originated by freeze weathering of the underlying rocks.

- The loess belt: The largest part of the catchment contains pararendzina, a not well developed soil from loess. Grain size analyses of SCHUMACHER (1981) showed about 70-80% silt and both 10% sand and clay. The pararendzina can have a depth of more than 50 meters at the acclivities of the large terraces and is characterized by a large field capacity of more than 200mm.

- The floodplain areas: Eroded loess material from the slopes sedimented in the floodplains and formed mainly three different soil types. The colluvisol is found at the foot of the terraces and is not influenced by waterlogging. The gley-colluvisol and the gley are waterlogging soils. Figure 5.2.3 shows a soil profile of the gley-colluvisol in the Loechernbach area. A small agricultural influenced A horizon is followed by a groundwater influenced oxidised Go horizon with a migration horizon M between them. The groundwater filled Gr horizon at the bottom is permanent under reductive terms. The groundwater lies in a depth of 40-120 cm.

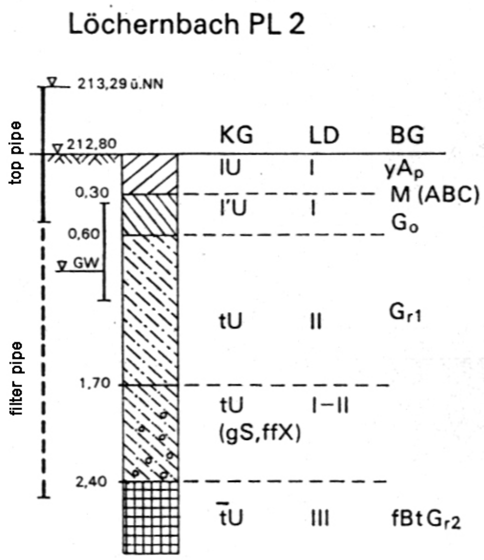

Figure 5.2.3.: Soil profile of the Loechernbach catchment near the catchment outlet (LUFT, 1980b).

5.3. Anthropogenic deformation

Between 1968 and 1980 the Kaisertuhl area experienced a large rearrangement. The vine growers were used to plant the vines on small terraces at the Kaiserstuhl since around 800 AD. Many of the small terraces were only accessible on foot and therefore could only be farmed without machines. To improve the economy of vine growing, the former small terraces were transformed to large terraces for a better cultivation at the beginning of the 20th century. The terraces have now a depth up to 120 meters and a height up to 50 meters and the acclivities have angles of about 45°. The terraces were inclined against the main slope with 2-4° to ensure a proper drainage. As loess is such a loose material, it is optimal for this purpose (WILMANNS ET AL., 1989).

This deformation in union with consolidation of farming was done in the Loechernbach catchment, too. In the curse of the reconfiguration, a dense asphalted street network was built and covers an area of 4.6% of the catchment. To drain this large area, a pipe network was constructed as shown in figure 5.3.1. Due to problems with waterlogging in the floodplain as well as at the terraces, a large drainage system was also built in the area. While the floodplain contains drainage pipes, the terraces were tried to drain with mole drainages (pipeless drainage) at a depth of 1.2 meters (figure 5.3.1).

However, the efficiency of the mole drainages is in question as they were built about 30 years ago. EGGELSMANN (1981) reported a maximum age of just 5-10 years for

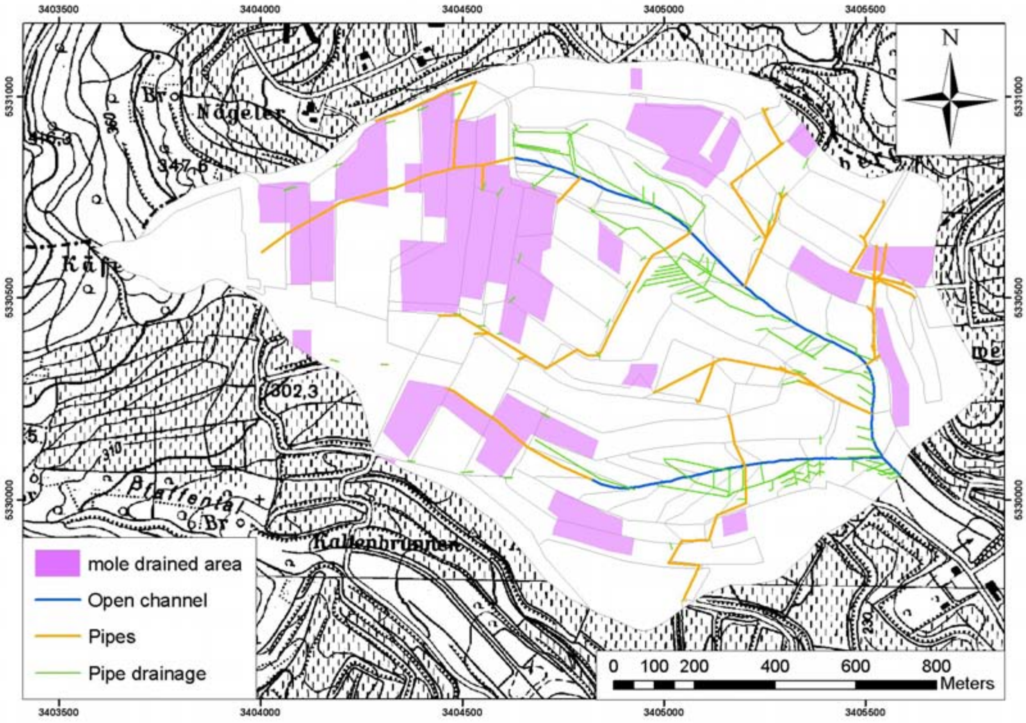

Figure 5.3.1.: Drainage system of the Loechernbach catchment (Wagner, 2002).

mole drainages, because of clogging by gravity with no supporting pipe. So it is possible that they deliver nearly no water now at all.

5.4. Landuse

The landuse of the Loechernbach catchment, shown in figure 5.4.1, is totally dominated by viniculture (61.2%) as it is the case in the whole Kaiserstuhl area. This is caused by the good water retention and ventilation of the loess. The steep acclivities (12.2%) are also a huge area and are not used by human activities. In the upper part the above mentioned forest begins and takes an area of 3.5%. The streets cover 4.6% of the catchment while the rest (18.5%) is used as agricultural area located in the floodplain.

5.5. Former research

In the two research catchments Rippach and Loechernbach many hydrological studies were done with the aim of comparing them. As the Rippach was not transformed from small to large terraces, the aim was to show the difference between small and large terraced catchments. The summaries in this section were restricted to the

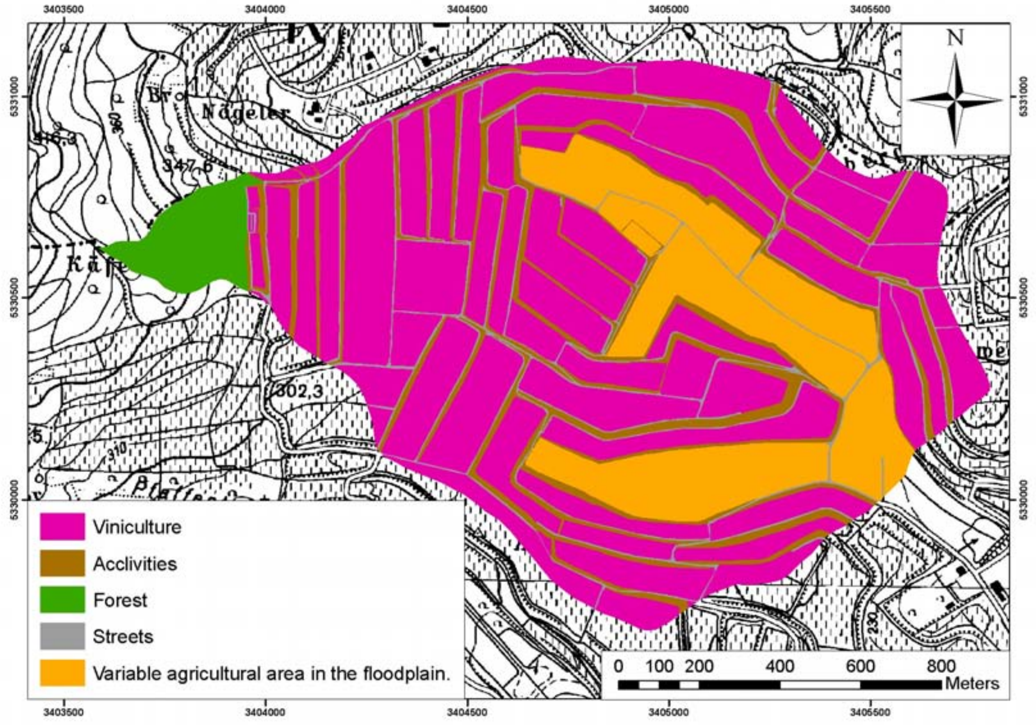

Figure 5.4.1.: Landuse of the Loechernbach catchment (NIPPGEN, 2007).

works used for this thesis.
The only research in terms of sediment in water was done by DEMUTH and WESTPHAL (1981). They measured suspended sediment in the Loechernbach catchment as well as in the Rippach catchment. Samples of different events were taken and analysed to suspended sediment yield, concentration, grain size distribution and to their relationship with runoff (sediment rating curve).
A first result was that the maximum sediment concentration comes along with the maximum runoff. With this result they tried to set the sediment concentration in a relationship with the runoff. The coefficients of determination were r^2=0.53 for the rising and r^2=0.58 for the falling limb. The grain size analysis brought mainly silt and clay, whereas in the Loechernbach catchment also coarse sand was found on high flow conditions.
A further result of the whole study was an assumption how the sediment reaches the stream:

- The sediment lying on the streets gets washed off with starting rainfall and reaches the stream.

- At the same time soil from the acclivities gets eroded and transported to the streets and stays there when rainfall stops.

- If rainfall starts again, the cycle closes.
- At low rainfall intensities just the streets deliver water to the channel, whereas at large rainfall intensities overland flow is also built at the soils and erosion by water occurs.

For setting up the hydrological model in this study, further studies were found important. First, SCHUMACHER (1981) did some measurements of soil-physical properties in a thesis with the aim of a comparison of soil moisture values in the Rippach and the Loechernbach. He derived saturated hydraulic conductivities by laboratory measurements with permeameters on soil samples, infiltration capacities with double ring infiltrometers, the effective pore volume and the grain size distribution.
Uranine tracer tests in the groundwater of the Loechernbach catchment were done by LUFT (1980b). He derived values for the saturated hydraulic conductivity of 0.61 $\frac{m}{d}$ and compared them to values earlier derived by a drill hole technique. The values were nearly the same.
BUCHER and DEMUTH (1985) did a comparative water balance of the two research catchments. They published values for the water balance from 1977-1980, including percentage values for the monthly evapotranspiration, that were used in this thesis. The conclusion of their article was, that the land consolidation in the Loechernbach catchment brought a large rise in runoff and a decline in evapotranspiration and catchment-storage.
With dye tracer tests in the unsaturated zone and in the overland flow, UHLENBROOK (1995) showed the fast reaction time of the catchment. Uranine was put on the streets and with a mean residence time of 20,6 minutes found at the outlet. A second tracer test was done in the unsaturated zone. At a drained field in the floodplain, a tracer was brought out on soil and a shower test was started. The mean residence time in the unsaturated zone was measured to 2.5 hours. Also a hydrograph separation by means of ^{18}O was done for two events. 55 respectively 72 % of the water were proven to be 'event water'. This showed a relatively large fraction of 'event water', but also a part of preevent water was found, what means that not just infiltration excess overland flow occurs in the Loechernbach catchment.
WAGNER (2002) applied an early version of the rainfall-runoff model ZIN (LANGE ET AL., 1999) in the Loechernbach catchment. For the runoff generation, runoff coefficients were used instead of infiltration values and the runoff concentration was done by Dirac impulses. The results were well indeed, but just with calibrated parameters. The runoff coefficients were set to values, that are not interpretable: the streets got 0.35 while the terraces 0.04 to 0.055. So the results of this work have to be used carefully.

6. Measurements

As input for the model, measurements of rainfall and for validation of the model, measurements of runoff and turbidity were taken. Three events were investigated with a sample collector for sediment concentration measurements, too. Precipitation and runoff data for testing the model was taken over from NIPPGEN (2007). The measuring network as it was installed in the Loechernbach catchment is shown in figure 6.0.1.

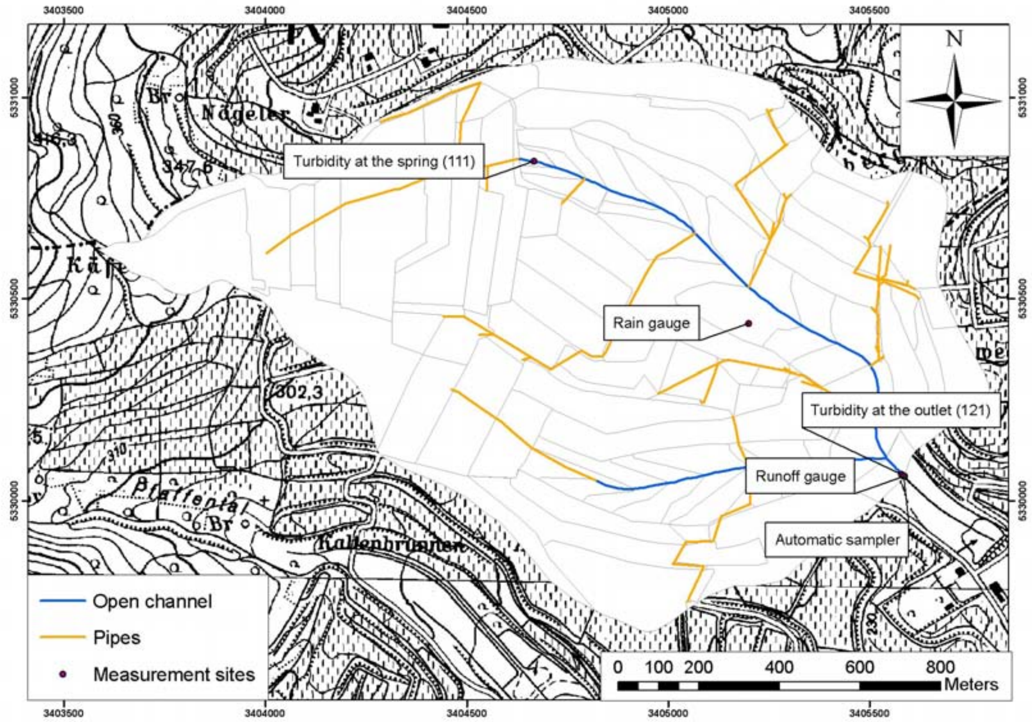

Figure 6.0.1.: Placement of the measuring instruments in the Loechernbach area.

6.1. Rainfall

Rainfall was measured by a raingauge of the company 'OTT Messsysteme' in the center of the catchment as shown in figure 6.0.1. The temporal resolution was two minutes. The measurement principle of the instrument is based upon weighing the

precipitation with a resolution of 0.01 mm/min and a maximum of 15 mm/min. The area where rainfall is collected is same as at the common Hellmann raingauge (200 cm^2) and the measuring height at 1 m above surface, too (NIPPGEN, 2007).
During the event at the 18.09.2007 the raingauge was broken and data from the municipality Eichstetten, recorded few hundred meters behind the catchment outlet, was taken. This data was recorded in an interval of five minutes. So it may be that rainfall intensities are not as big as at our recordings due to the larger timestep. It emerged, that this measurements could not be taken for model runs, as there were problems with measuring, too.

6.2. Runoff

The outlet of the Loechernbach catchment is prepared with a 4.5 ft H-flume runoff gauge with maximum water level of 4.5 ft (1.37 m). This maximum level is related to a runoff of 2.4 $\frac{m^3}{s}$. The connected data logger was read out once a week. The measured water level P can be converted to runoff Q with the following relationship (NIPPGEN, 2007):

$$Q = 10^{0.23377\cdot(lgP)^2+1.2843\cdot(lgP-0.4312)} \tag{6.2.1}$$

The special design of this gauge allows relatively good measurements of low flow conditions. Within 4 weeks the gauge had to be cleaned from sediment, that was lying with a height of about 1 cm.

6.3. Turbidity

Turbidity measurements are able to measure suspended sediment concentration in streams continuously (ANKCORN, 2003). The aim of the measurements of this thesis is a unique relationship between turbidity and sediment concentration as shown in ANKCORN (2003) or HOLLIDAY ET AL. (2003).
Measurements of turbidity were done with the online fluorometer 'GGun FL-30'. Usually it is taken for measuring the dye tracers uranine, sulphorhodamine and tinopal, but turbidity is also recorded for correction of data. The measurement principle is shown figure 6.3.1. Light sources send light of different wavelenghts through the water. In an angle of 90° the light is detected, in case of fluorescent tracers the fluorescent light, in case of turbidity the light scattered by the suspended sediment (SCHNEGG and FLYNN, 2002). The measuring units of the Fl-30 for turbidity are NTU (Nephelometric Turbidity Unit), which is a measure of light diffusion in a hydrazine sulfate and hexamethylemetetramine solution that forms a formazine

suspension (McCutcheon et al., 1993). Before measurements can be started, the instrument has to be calibrated. In this case the former calibration was checked and declared right for turbidity measurements.

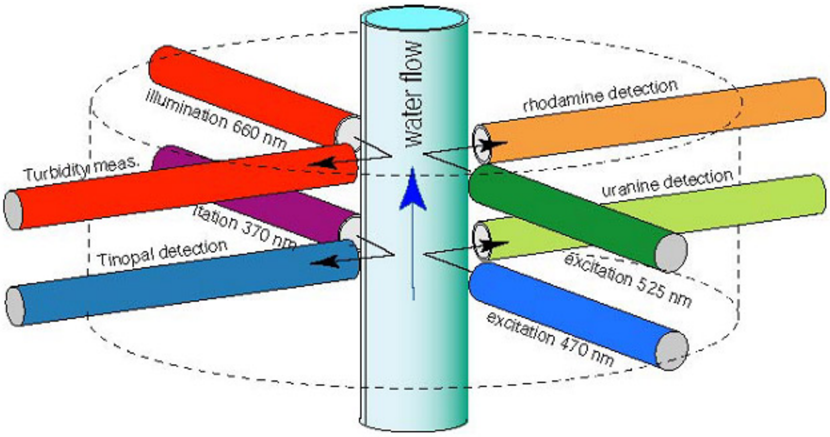

Figure 6.3.1.: Measuring principle of the GGun Fl-30 online Fluorometer. The different light sources are used for different tracers (Schnegg and Flynn, 2002).

6.3.1. Field measurements

The Fl-30 had been modified for long time use in the Loechernbach area. To avoid daylight disturbing the measurements, two metal pipes were placed at the front and the rear. For a more streamlined shape a sliced plastic bottle was put over the front pipe and finally, to prohibit obstruction with lager sediment particles, a perforated plastic pipe was put at the front of the front metal pipe. The setup is shown in figure A.5.1.
Two modified Fl-30 were brought out in the Loechernbach catchment from mid of august to the end of september. One instrument was placed at the spring (Turbidity 111) and one at the outlet (Turbidity 121) of the catchment as shown in figure 6.0.1. The measurement at the spring was taken to check the model results, the measurement at the outlet to derive the suspended sediment - turbidity relationship.

Ankcorn (2003) did some recommendations for the placement of the turbidity sensors for a proper measurement:

1. The placement should be representative for the whole cross-section and mixing of the stream should be well there.

2. The streamflow velocity should be big enough to flush the sonde.

3. The sonde should be protected against high flow conditions.

4. The sonde should be at a proper depth for accurate measurements at low flow conditions and far enough above the bottom to reduce negative effects of suspended bedload transport.

At such a small stream like the Loechernbach we can be sure that the mid of the stream represents the whole cross-section.
The second point is more difficult. Especially the Fl-30 at the spring needed extensive service as the flow was not so strong and therefore there were deposits in the instrument. So the Fl-30s were cleaned twice a week.
The protection against high flow conditions was done with anchoring the instruments in the river bed.
The last recommendation is also not facile. Low flow at the catchment outlet is mostly between 3-6 $\frac{l}{s}$ and therefore very low against the high flow of more than 1 $\frac{m^3}{s}$. So the sonde was brought out some centimeters above the river bed to be sure it is flushed at low flow conditions.

6.3.2. Laboratory measurements

A second measurement for the relationship between turbidity and suspended sediment concentration was done in the laboratory. The method was the other way around as the field measurement. An artificial suspended sediment concentration was produced and turbidity of it was measured.
First soil samples were taken from three different locations in the catchment. Then they were mixed up and dried at 105 °C. With a crucible the partly aggregated soil samples were disaggregated to primary granulation. So it was assured that the mixture of soil and water resulted exclusively in suspended sediment in the water.
The measurement instrument for turbidity was also the FL-30 Fluorometer, but with different setup. Other top parts, that avoid daylight, were screwed to both ends of the instrument. This parts were linked to tubes, through which water was pumped from a reservoir. The reservoir was mixed automatically and the soil samples of known weight were put to the water (compare figure A.5.4). So an artificial suspended sediment concentration was achieved and the turbidity of every concentration step was measured.

6.4. Sediment

Samples of stream water were taken by the automatic sampler APEG (Automatisches Proben Entnahme Gerät), which takes 42 samples in an interval of three minutes. Once started, the sampler takes all 42 samples. It was coupled to the runoff gauge and started taking samples at a water level of 11 cm. This was done to prohibit that very small events were sampled. Unfortunately there is a part of the rising limb missing at every sampled event.
Three events were sampled as shown in table 6.4.1 and therefore three events could be analysed for the suspended sediment concentration. The samples were analysed in

Table 6.4.1.: Sampled events with maximum runoff Q_{max}, maximum precipitation intensity PI_{max} and precipitation sum P.

event	date	time	$P(mm)$	$PI_{max}(mm/h)$	$Q_{max}(l/s)$
1	29.08.2007	4:35	5.38	30.9	47.38
2	03.09.2007	16:10	7.54	11.1	39.21
3	18.09.2007	1:04	28.00[1]	17.77[1]	82.6

[1]recordings taken from municipality Eichstetten.

the laboratory. First the sampling bottles were poured in glasses with known weight (m_{glass}). After that, the wet samples were weighted with a microgram scales (m_{wet}). Then they were evaporated two days at 105°C in a drying cupboard. The now dry samples were again weighted (m_{dry}). The suspended sediment concentrations (Q_s) were now derived by

$$Q_s = \frac{m_{dry} - m_{glass}}{m_{wet} - m_{dry}}. \tag{6.4.1}$$

6.5. Discussion

As discussed in Nippgen (2007) the error of the runoff measurements is high at low flow conditions (40 % at 4 cm) because of the resolution of 1 cm of the pressure sonde. With rising water level the relative error decreases.
Turbidity measurements with the Fl-30 Fluorometer have one big limitation: the measurement range has a maximum of 400 NTU which is not enough for big events in the catchment. The special equipment of the instrument is a new approach to measure turbidity. An earlier approach by Hugenschidt (2006) failed. They tried to pump water out of the channel and through the instrument. The main problem was that the inlet of the pumping tube was blocked by coarser sediment. The new

approach introduced in this thesis seems to work, but just when the instrument is cleaned extensively. A verification of the method in other catchments should be done in future.

7. Data Analysis

7.1. Turbidity measurements

Turbidity was measured for the events shown in table 7.1.1. At the most events the values had to be corrected as they showed a linear rise in baseflow despite the cleaning. To correct this measurement error, straight lines were fitted to each event and subtracted from the measured turbidity curves. Thus the baseflow showed no turbidity, which had been observed with freshly cleaned measurement instruments. At some events it was more difficult, especially the instrument at the spring, which was not well streamed by the water. There the background turbidity rose very high after events. This happened probably due to sediment particles that sedimented in the instrument. It was attempted to calculate this out, as good as possible.

Table 7.1.1 shows the measured turbidity events. It is noticeable that the turbidity

Table 7.1.1.: Turbidity events recorded at the spring (111) and the outlet (121) in the Loechernbach catchment.

date/time	max. turb. 111 (NTU)	max. turb. 121 (NTU)
[1]21.08.2007 08:06	11	43
[1]21.08.2007 16:33	294	234
29.08.2007 04:35	238	228
03.09.2007 16:10	70	60
11.09.2007 00:53	87	no data
18.09.2007 01:04	no data	124
18.09.2007 05:00	no data	30
18.09.2007 17:24	no data	>395
27.09.2007 13:32	21	21

[1]different instrument setup

at the spring was in general larger than turbidity at the outlet. There are two possibilities to explain this observation: First, the suspended particles sedimented in the channel between spring and outlet and the concentration decreased. The second possibility is, that water with less concentration was mixed with the original water and so the concentration was lowered. Observations in the catchment showed that there is no sediment in the channel, and so the lower turbidity values at the outlet have to come from dilution with lower concentrations.

In figure 7.1.1 the turbidity load curves of the spring and the outlet are shown.

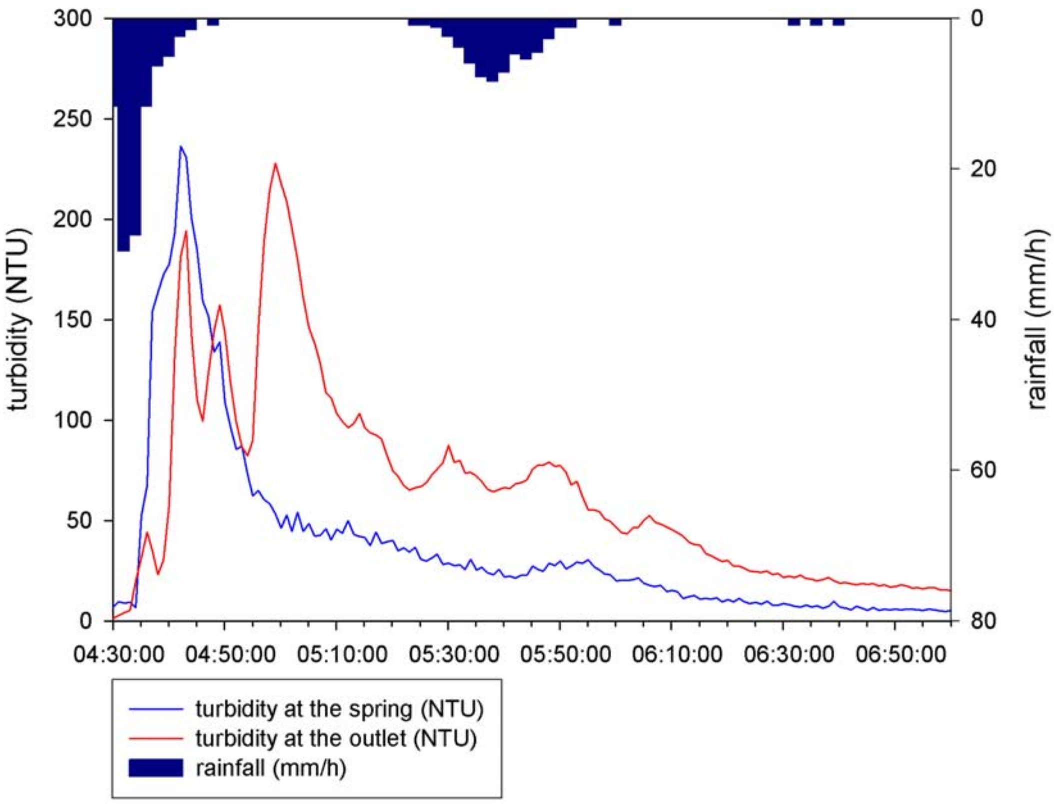

Figure 7.1.1.: Measured turbidity at the spring and the outlet of the Loechernbach catchment at the 29.08.07.

One can see the two main peaks of the curves, which are estimated to have the same origin. With this peaks and the distance between the spring and the outlet, it is possible to calculate the flow velocity of the water to $v = 78\ \frac{m}{min}$. If this result is compared to the values Nippgen (2007) derived by temperature measurements (45-60 $\frac{m}{min}$), it seems somewhat large, especially the peak runoff of 47 $\frac{l}{s}$ at the 29.08.07, which is less than the analysed events of Nippgen (2007), is taken into account. Other analysed turbidity events brought values in the range of 30-45 $\frac{m}{min}$.
One other thing in the sediment load curve of the outlet seemed to be interesting: before the main peak there were two lower peaks noticed. Nippgen (2007) got the same behaviour when he observed event temperature and electrical conductivity. After Nippgen (2007) this peaks came from the pipes discharging into the main channel of the Loechernbach and could be observed in the other turbidity events measured in this thesis, too. So it may be possible to use turbidity and so suspended

sediment concentration in this catchment as a natural tracer for event analysis, especially as there is no sedimentation in the channel and the pipes.

7.2. Sediment rating curve

The sediment rating curve is done here for comparative reasons. As already shown in table 6.4.1 three events were sampled with each 42 samples. Three samples had errors during the analysis and so 123 samples could be taken to derive the relationship.
As mostly done in the literature a power function was fitted to the measured values. Figure 7.2.1 shows runoff plotted against Q_s for the three sampled events. The plotted power-regression function $Q_s = 207.78 \cdot Q^{0.1109}$ has an r^2 of 0.03.
With an $r^2 = 0.03$ the regression brought bad results, which confirmed the simple

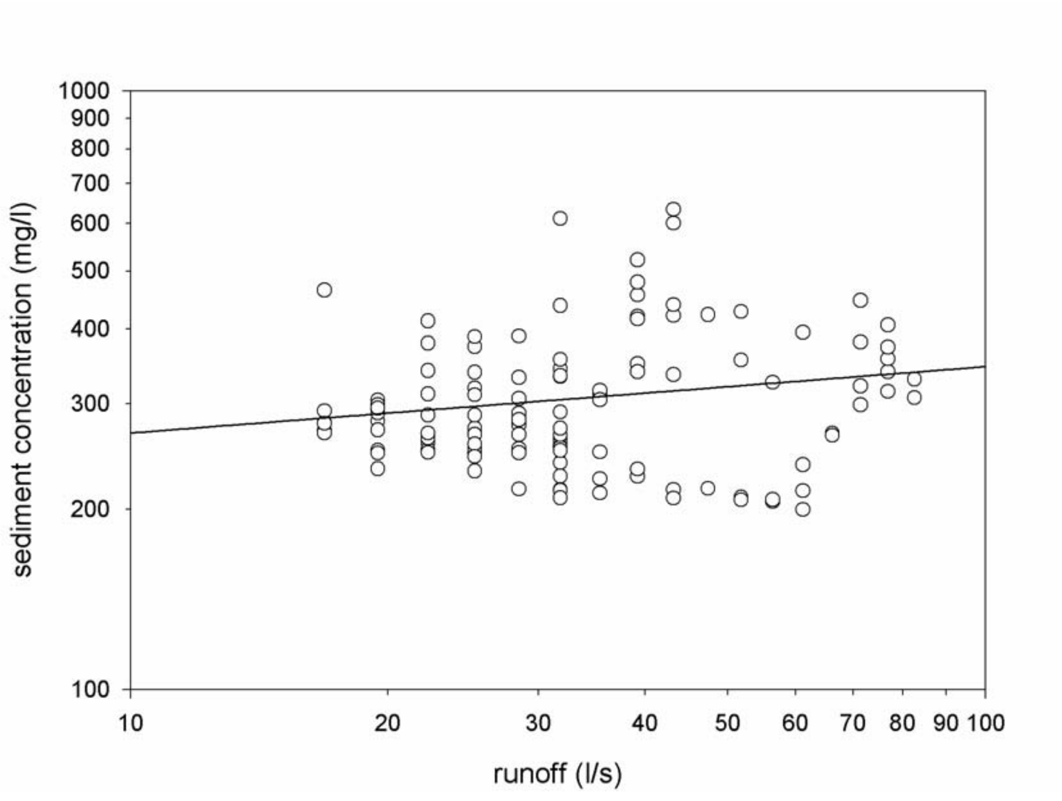

Figure 7.2.1.: Relationship between Runoff (l/s) and suspended sediment concentration (mg/l) derived by field measurements in the Loechernbach catchment.

view of the plot. It is also bad compared to rating curves found in literature, but it must be mentioned, that sometimes average values were taken and so a better relationship was derived than taking just the event samples. Nevertheless, the classical approach failed for the Loechernbach catchment and was rejected for this work

7.3. Suspended sediment - turbidity relationship

With the data measured in the Loechernbach catchment respectively in the laboratory with soils from the catchment, relationships as mentioned in section 6.4 will be calculated in this section.

7.3.1. Field relationship

The event water samples used to derive the sediment rating curve are also used to derive a field relationship between turbidity and suspended sediment concentration. The plot of turbidity (NTU) against suspended sediment concentration (Q_s) is shown in figure 7.3.1.
The power relationship derived by a regression is

$$NTU = 0.0078 \cdot Q_s^{1.5453}. \tag{7.3.1}$$

and has an r^2 of 0.42.
This relationship is not as strong as the relationships derived in the literature mentioned above. Partly it may be up to the number of sampling points. In this study the number of points was 123 while Ankcorn (2003) just used 16 samples. The natural diffusion make a larger cloud of sampling points. On the other hand this relationship had only turbidity values up to 228 NTU while Ankcorn (2003) was in a range up to 1000. The third thing to mention is that the literature relationship was derived by composite samples, thus an average of an unknown time, while this samples were taken in a few seconds.
Hence, the relationship derived in this work by field measurements is not that bad as it seemed at a first view. There are possibilities to strengthen it like a larger measurement range or average values.

7.3.2. Laboratory relationship

The laboratory measurements were done with nine different artificial concentrations, that cover the whole range as shown in figure 7.3.1. The power regression equation automatically derived by the program 'SigmaPlot' is:

$$NTU = 0.2584 \cdot Q_s^{0.9960}. \tag{7.3.2}$$

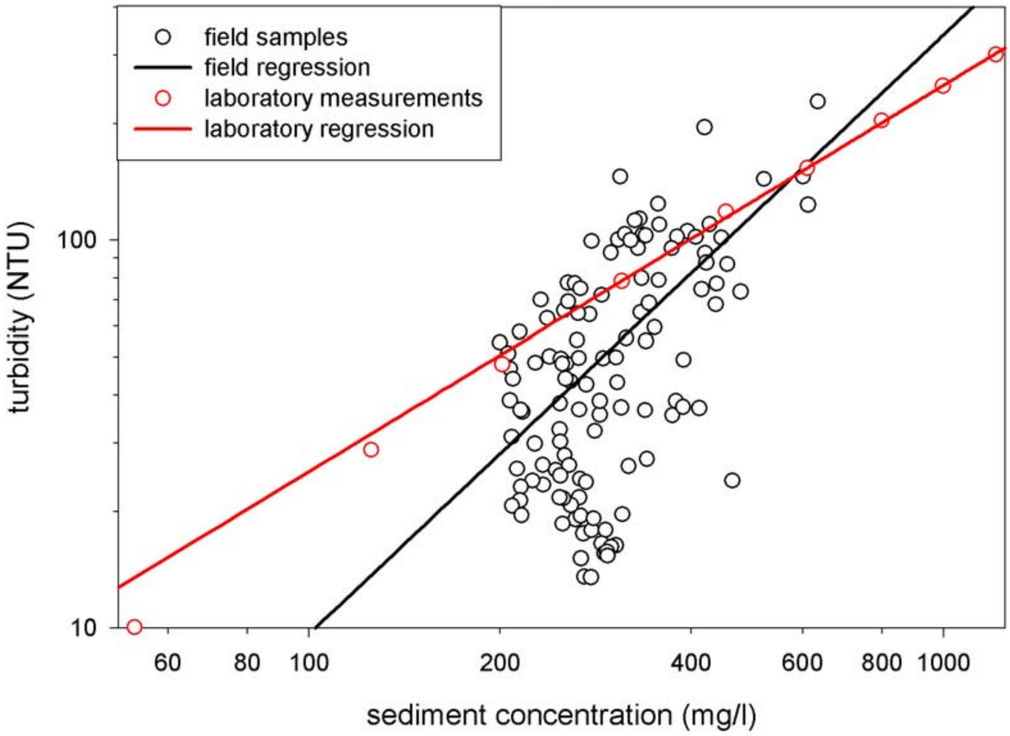

Figure 7.3.1.: Relationship between turbidity (NTU) and suspended sediment concentration (mg/l) derived by field measurements in the Loechernbach catchment and laboratory measurements.

The coefficient of determination is nearly one ($r^2 = 0.9998$) for this relationship. If it is compared to the laboratory relationships by HOLLIDAY ET AL. (2003), the regression is in the same range of accuracy, but calculated with more sampling points. The regression equation itself is comparable to the equations found by HOLLIDAY ET AL. (2003). Especially the exponent of 0.996 is nearly the same and so the equations showed almost a linear relationship between turbidity and suspended sediment concentration, too.

7.3.3. Comparison

The laboratory relationship showed, as it was expected, a much more unique relationship between suspended sediment concentration and turbidity than the relationship derived by field measurements. A Comparison between the different relationships can be done by calculating the sediment concentrations with the two equations and comparing the curves with the measured sediment values. In figure 7.3.2 the calculated suspended sediment concentrations (SSC) were plotted with the measured samples for the 29.08.07. (The other two events are shown in figure A.1.1 and A.1.2).

The comparison showed two estimations: first the laboratory as well as the field relationship underestimate the concentrations at low NTU values and overestimate them at large NTU values. Second, the laboratory relationship worked worse than the field relationship. So the field relationship was taken for this work to calculate the concentration values from the measured turbidity.

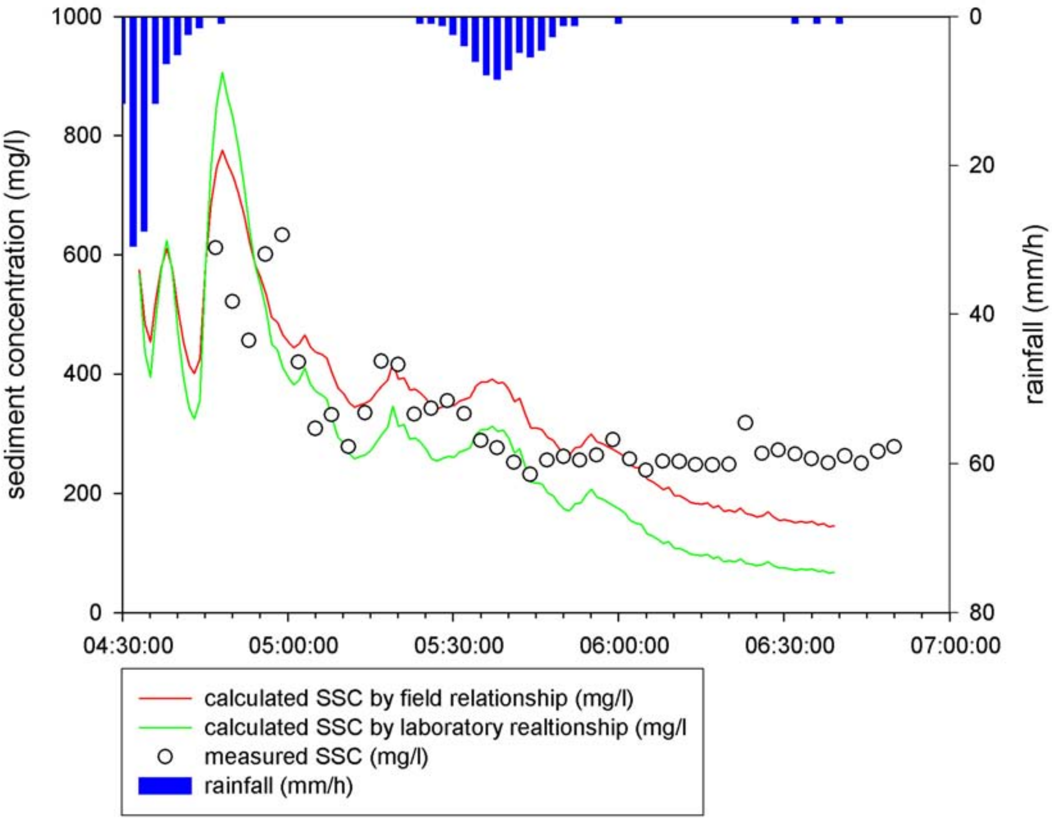

Figure 7.3.2.: Comparison of the turbidity-Q_s relationship derived in the field and the laboratory at the event on the 29.08.07.

7.4. Conclusion

The analysis of the measured turbidity values was complicated by the rising background turbidity and the so necessary correction of the values. Nevertheless there were eight events measured with useful data, five of them with data at both the spring and the outlet. In the sediment load curve at the outlet of the catchment, it is possible to see the different pipes, that discharge to the main channel, and therefore it may be possible to use turbidity as a natural tracer in the catchment.
As a classical approach, the relationship between suspended sediment and runoff

was plotted respectively the regression was made. The relationship proved not to be strong (r^2=0.03) and so the approach was rejected and not used for further calculations.
The relationship between turbidity and suspended sediment concentration derived by field measurements is not as strong as shown in literature. Partly this may be the case due to the large number of sampling points and the natural diffusion. But a more important point is, that the relationships showed in Ankcorn (2003) were derived by composite samples, which was not done in this work.
The laboratory relationship brought a very well coefficient of determination and the regression equation itself is similar to the relationships derived by Holliday et al. (2003). However, the comparison of the application of the two relationships showed, that the relationship derived in the field calculates better values than the laboratory equation.

8. Model description

As it will be used for the modelling part of the thesis the recent version of the hydrological model ZIN (Lange et al., 1999) is explained in this chapter. Also the constitution of the new parts developed within this work, baseflow and erosion/sediment transport, are presented.

The rainfall-runoff-model ZIN was originally developed by Lange et al. (1999) for large arid catchments to model single events. It is a conceptual based distributed model in terms of runoff generation and consists of the three classical parts of hydrological models:

- Runoff Generation
- Runoff Concentration
- Channel Routing

Recently the model was used for humid/semi-arid catchments, too (Wagner, 2002; Schütz, 2006; Fischer, 2007). Gunkel (2006) coupled the model TRAIN, a distributed model for calcultation of evapotranspiration, with the model ZIN. So the coupled TRAIN-ZIN model is able to do a continuous simulation.
Wagner (2002) used it in the same catchment as it is used in this work, but an early version with no evapotranspiration and runoff coefficients instead off infiltration values. Also it might have been a problem that in this early version no baseflow was calculated as there is no baseflow in arid regions and semi-arid regions with a dry and a wet period.

For a proper application of the hydrology of the rainfall-runoff model ZIN in the Loechernbach area, it has to be extended by a baseflow module, as there was baseflow observed the whole year.
The overall aim of this work is to simulate pesticide transport in surface water. As Pesticides are often strongly adsorbed to soil particles, there has to be an erosion- and sedimenttransport module in the model used for simulating pesticide transport. This module will be integrated in an conceptual and measurement-based way.

As there were no meteorological input data for the use of the model TRAIN, the simulation of this thesis was done without TRAIN. The evapotranspiration was taken from the literature.

8.1. Rainfall input

The distributed runoff generation module in ZIN allows radar rainfall input. So every cell in the catchment has its own rainfall input.
If there are no radar data available, the model can be run with raingauge precipitation. Then all cells have the same precipitation input as it was used in SCHÜTZ (2006).
HAGENLOCHER (2007) integrated two other precipitation methods. The first is the Thiessen-polygon-method, that becomes constant spatial rainfall when there is just one raingauge. The second method is the inverse distance weighting that is only applicable when there are at least two raingauges. Additional to the inverse distance weighting a precipitation gradient with height can be entered.
Train-ZIN is not able to handle frozen precipitation input.

8.2. Runoff generation

The runoff generation module of ZIN divides the precipitation falling on a cell in infiltrating water and infiltration excess overland flow after the interception storage is full. The infiltrating water fills the catchment storage (CaStor) and if the CaStor is full, saturation excess overland flow is built. At every timestep the deep infiltration, which is actually groundwater recharge, flows in dependence of the unsaturated hydraulic conductivity out of the CaStor. The unsaturated hydraulic conductivity $K(\theta)$ is calculated with the Mualem-Van Genuchten-equation (RAWS ET AL., 1993):

$$K(\theta) = K_f \cdot \left(\left(\frac{\theta - \theta_r}{\phi - \theta_r} \right)^{\frac{1}{2}} \cdot \left\{ 1 - \left[1 - \left(\frac{\theta - \theta_r}{\phi - \theta_r} \right)^{\frac{1}{m}} \right]^m \right\}^2 \right) \tag{8.2.1}$$

with

$$m = \left(\frac{\lambda}{\lambda + 1} \right) \tag{8.2.2}$$

K_f is the saturated hydraulic conductivity, θ the water content, θ_r the residual water content, ϕ the porosity and λ the Brooks-Corey grain size distribution index as defined in RAWS ET AL. (1993).

The deep infiltration flows out of the storage with the Buckingham-Darcy-equation

$$q = -K(\theta) \cdot \left[\frac{\partial h(\theta)}{\partial z} - 1 \right] \tag{8.2.3}$$

where there is q the water flow, θ the volumetric soil water content, $K(\theta)$ the unsaturated hydraulic conductivity, $h(\theta)$ the soil water matric potential head and z the soil depth. With no change in matric potential with depth, as it is used in the one-dimensional CaStor in ZIN, $\frac{\partial h(\theta)}{\partial z} = 0$ and the Buckingham-Darcy equation (8.2.3) becomes

$$q = K(\theta). \tag{8.2.4}$$

So the Mualem-Van Genuchten equation directly calculates the deep infiltration respectively groundwater recharge.

The second non-overland flow output is the evapotranspiration. Normally the model TRAIN calculates it, but it is also possible to switch TRAIN off and to take evapotranspiration (ET) data from literature.
Whatever method is taken, the input to the ZIN model are daily values, so the model has to calculate values for the ZIN timesteps. As radiation is the most important control on evapotranspiration (Shuttleworth, 1993), hourly values were taken in the model for distributing the daily ET values to the ZIN timesteps. So the ET-value is weighted by the radiation. This results in hourly ET values. Then it is divided by the timesteps with no rain of the actual hour. If there is rain the whole hour, the hour is excluded from the hourly weighting procedure. This is just a simple way of temporal distribution, but seems to work.
The ET first evaporates the interception storage. If it is empty the evapotranspiration goes out of the CaStor.

8.3. Runoff concentration

The runoff concentration is the transformation of the runoff built in the runoff generation to the runoff that enters the stream. In the ZIN model it is integrated as follows:
The mass of water built by the runoff generation and the baseflow module in a timestep is added up per subbasin and brought to the stream by a transformation function, a unit hydrograph. This unit hydrograph can be extracted from measurements or, as described in Hagenlocher (2007), by a parameterised Gumbel-

distribution, the Fisher-Tippet distribution. The Fisher-Tippet method takes also into account that large basins have broader transformation curves than small ones and steep basins a shorter concentration time than gentle.
The unit hydrograph is applied to every subbasin in every timestep. The water flowing to the channel in one timestep and subbasin is an addition of the fractions the unit hydrograph describes from this and the last timesteps.

8.4. Channel routing

'Flow Routing is a mathematical procedure for predicting the changing magnitude, speed and shape of a flood wave as a function of time at one or more points along a watercourse' (FREAD, 1993).
The channel routing method used in ZIN is the distributed storage based Muskingum-Cunge method as described in LEISTERT (2005) or LANGE ET AL. (1999). This method is a numerical solution of the kinematic wave approach, discretised by finite differences (SZEL and GASPAR, 2000).
For this method, the channel has to be divided first in channel segments, that represent each a storage. The movement of the flood wave is calculated for each segment j and each time i by

$$Q_{i+1}^{j+1} = C_1 \cdot Q_i^{j+1} + C_2 \cdot Q_i^j + C_3 \cdot Q_{i+1}^j \tag{8.4.1}$$

with

$$C_1 = \frac{\Delta t - 2KX}{2K(1-x) + \Delta t} \tag{8.4.2}$$

$$C_2 = \frac{\Delta t + 2KX}{2K(1-x) + \Delta t} \tag{8.4.3}$$

$$C_3 = \frac{2K(1-x) - \Delta t}{2K(1-x) + \Delta t}, \tag{8.4.4}$$

that $C_1 + C_2 + C_3 = 1$.

The values for the storage constant K and the weighting factor X are:

$$K = \frac{\Delta x}{v_k} \tag{8.4.5}$$

$$X = 0.5 \cdot \left(\frac{Q_{REF}}{B \cdot v_k \cdot S_0 \cdot \Delta x} \right). \tag{8.4.6}$$

Q_{REF} is an estimated reference discharge which is calculated as an arithmetic average of the known discharges from previous timesteps and/or segments:

$$Q_{REF} = \frac{Q_i^{j+1} + Q_i^j + Q_{i+1}^j}{3} \tag{8.4.7}$$

Δx is the length of the channel segment (m), v_k the kinematic wave celerity (m/s), B the with of the channel (m) and S_0 the energy slope.
After FREAD (1993) the kinematic wave celerity can be approximated for a wide rectangular channel by $v_k = 5/3 \cdot v$ with the water velocity v. The water velocities are computed for the open channels in the catchment with the Manning equation:

$$v = \frac{R_{hy}^{\frac{2}{3}} \cdot S_0^{\frac{1}{2}}}{n} \tag{8.4.8}$$

with
R_{hy} = hydraulic radius (m)
n = Manning roughness coefficient ($\frac{s}{m^{2/3}}$)

The Loechernbach catchment contains about 9 km pipes and just 2 km open channel, so the pipes should be considered when calculating flow velocity. Thus, pipe flow velocity is calculated by a combination of the Colebrook-White with the Darcy-Weisbach formula. The equation for full pipes is (CHADWICK and MORFETT, 1998):

$$v_{full} = -2 \cdot \sqrt{2gDS_f} \cdot \left(\frac{k_s}{3.7 \cdot D} + \frac{2.51 \cdot \nu}{D \cdot \sqrt{2gDS_f}} \right) \tag{8.4.9}$$

where g is the acceleration due to gravity in $\frac{m}{s^2}$, D the pipe diameter (m), S_f the hydraulic gradient, k_s the surface roughness length (m) and ν the kinematic viscosity ($\frac{m^2}{s}$).
If the pipe is not full, the velocity has to be calculated as friction $fric$ of the velocity of the full pipe as $v_{part} = fric \cdot v_{full}$. The friction is calculated with:

$$fric = \left(1 + \frac{log(R_p)}{log(D/k_s)} \right) \cdot R_p^{\frac{1}{2}} \tag{8.4.10}$$

with

$$R_p = \left(1 - \frac{sin\phi}{\phi} \right) \tag{8.4.11}$$

as shown in figure 8.4.1 The angle ϕ depending on the flow depth d can be calculated by trigonometry with:

$$\phi = 180 + 2 \cdot arcsin\left(\frac{2d}{D} - 1\right). \tag{8.4.12}$$

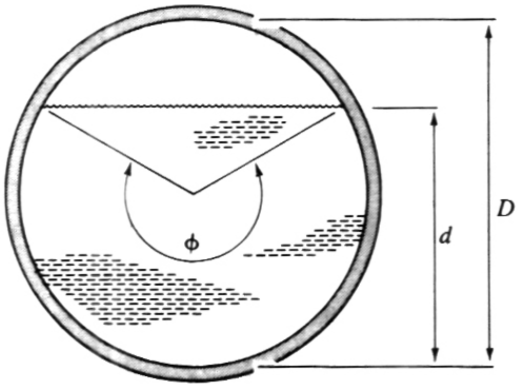

Figure 8.4.1.: Angle for calculating partially full pipes (CHADWICK and MORFETT, 1998).

The core of the Muskingum-Cunge routing procedure is the approximation of equations 8.4.1 and 8.4.7. In an iterative approach Q_{REF} is changed to fit Q calculated with the factors C_1, C_2 and C_3 that depend on Q_{REF}.
One problem already reported in LEISTERT (2005) is a very large decline of the hydrograph between two runoff peaks, when there are two ore more peaks in one event. This was caught by a condition: when the runoff of this timestep is larger than three times the last runoff or less than one third of the last runoff, the weighting factors are chosen one third each. The effect reached with this condition is a not so large decline before the next peak rising. The factor between this and the last runoff may have a large influence. Here it was chosen three respectively one third. Maybe in other catchments the factor has to be chosen higher or less. This maybe-improvement method is in doubt, but seems to work for this study and is therefore used for the modelling.

8.5. Groundwater recharge born baseflow module

As there is no groundwater module in TRAIN-ZIN it is difficult to derive baseflow. The only link to groundwater is the groundwater recharge. So the concept of the module is to catch the groundwater recharge and add it to the overland flow. The assumption that the long term average groundwater recharge equals the longterm

average baseflow was used by KILLE (1970). However, he handled with long time periods and not with short as this work does.
As the groundwater recharge is depending on the saturation of the soil, it will decrease when the filling of the CaStor decreases with outflow and evapotranspiration. Taking into account that not the whole basin produces baseflow, it is possible to define the area contributing to baseflow. If a cell is contributing to baseflow, the caught groundwater recharge is added to the built overland flow and is concentrated as described in section 8.3. So the same concentration time and the same subasins as for overland flow are used in the module for baseflow. Figure 8.5.1 shows the scheme of the new module.

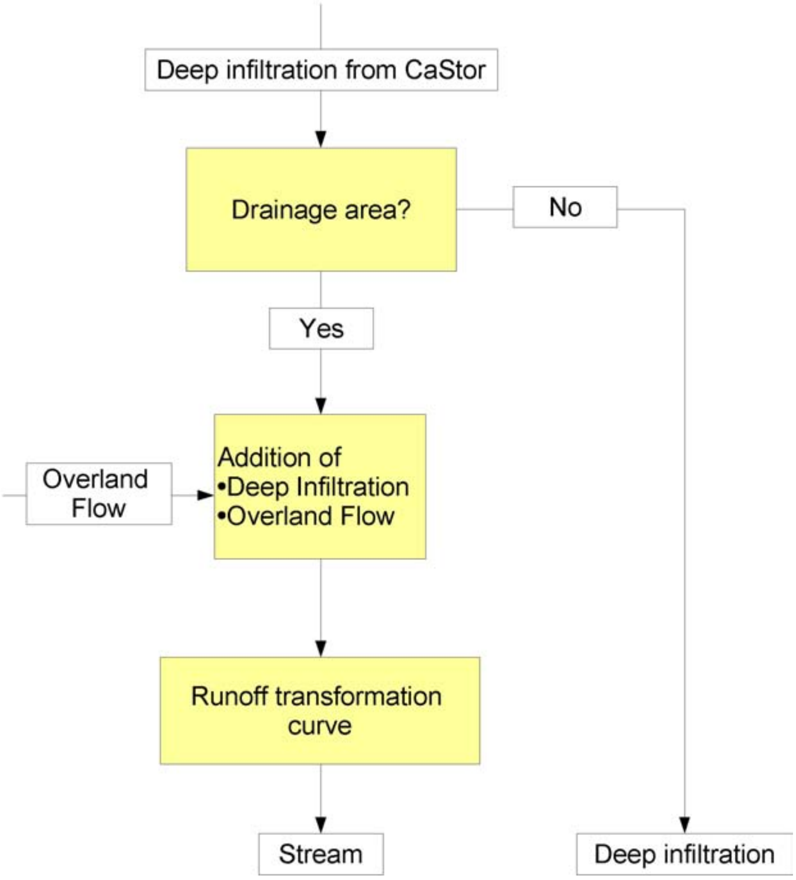

Figure 8.5.1.: Scheme of the Groundwater Recharge born Baseflow Module

8.6. Erosion- and sediment transport module

The erosion and sediment transport module is based upon the assumptions that the main variable factor influencing the erosion is the rainfall intensity and the only kind of erosion is sheet erosion. The module is divided in the same way as the hydrological part of the model:

- Sediment Generation
- Sediment Concentration
- Sediment Routing

The concept of the Sediment Generation module is shown in figure 8.6.1. First the rainfall intensity and the CaStor filling decide within the hydrological model if there is overland flow or not in a cell. With no overland flow, there is no erosion. Else a relationship between rainfall intensity and sediment yield in $\frac{g}{m^2 min}$ calculates in this cell the amount of sediment that enters the stream. This relationship should be derived by measurements or taken from measurements in the literature. There are three different equation types possible to be selected: a power equation ($y = a \cdot x^b$), a straight line ($y = a \cdot x + b$) or an exponential function ($y = a \cdot e^{b \cdot x}$). A relationship can be specified for every runoff generation zone already identified in the hydrological module.
After the generation, a mass of sediment per subbasin and timestep is brought to the stream with the same transformation function as the water.

The sediment routing had to be modified compared to runoff routing as the

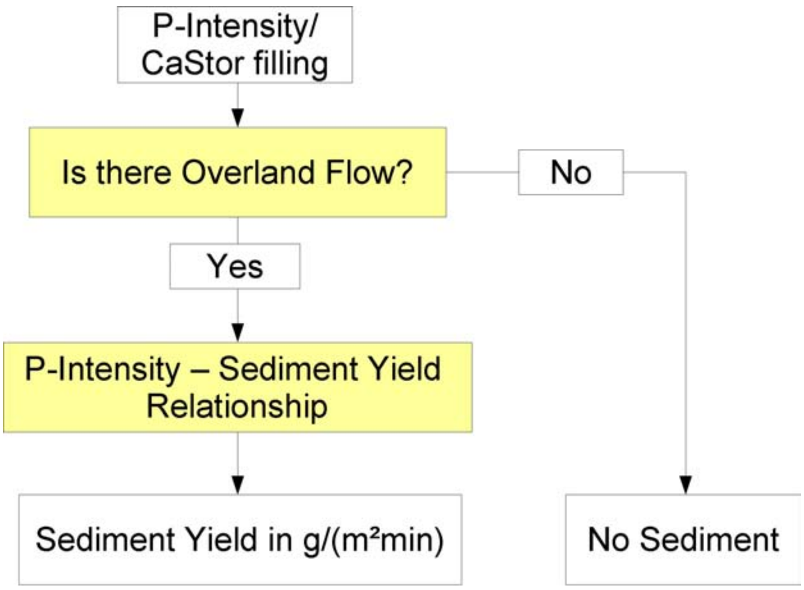

Figure 8.6.1.: Scheme of the Sediment Generation Module.

Muskingum-Cunge routing calculates the flow velocity by the mass of water respectively sediment. If the masses are not the same the smaller mass will be slower.

So the velocities calculated in the water routing are stored and taken for the sediment routing, too. With this approach it is ensured that the waves have the same travel time as it was observed by measurements in the catchment.

8.7. Discussion

The rainfall-runoff model ZIN was modified several times since LANGE ET AL. (1999) developed the first version. Every newly developed version was tested by the developer and seemed to work for their purpose. The new baseflow and erosion-sediment transport modules have to be discussed for their weakness and their strength.
The scheme of the baseflow module is very simple and so there are conceptual errors. The first known error is, that the subcatchments for the runoff concentration of baseflow are thought to be the same as for overland flow. This is not the case in the Löchernbach catchment. While the surface of the terraces is often inclined to the slope and therefore overland flow is running this direction, the infiltrated water is running with the main slope anyway. So surface and subsurface catchments are not the same. This conceptual error could be corrected in following works with the model.
A second error is the concentration time. As the module is implemented here the concentration time for both, overland flow and subsurface runoff, is the same. It is surely known that subsurface flow is slow flow and so the concentration time is larger than for overland flow. Also an individual baseflow concentration module with an own concentration time may be implemented later.
The third thing to be discussed is the concept to catch groundwater recharge to model baseflow. It is known that for long time intervalls ($>$ 1 year) the amount of groundwater recharge may be the same as the amount of baseflow (KILLE, 1970). But for event based modelling this assumption is not generally legal. Furthermore it may be a kind of black box modelling, if a soil storage outflow is taken to model baseflow event based.
The erosion/sediment transport module is also based upon a very simple scheme. The chosen concept is only able to take sheet erosion into account. Rill erosion with flowing water can not be modelled and will probably be underestimated. Due to the large terraces in the Loechernbach catchment the concept may suit as no rill erosion is expected here. Test runs will have to show the usability of the module.

9. Model setup

The first step to run a model is preparing the input timeseries and finding parameters. Then they have to be edited to fit as model input, that means they have to be in the right units and timesteps. In the following the input timeseries and parameters are described as they were used for a first uncalibrated model run.

9.1. Input timeseries

9.1.1. Rainfall

Rainfall has been recorded as described in section 6.1 by a Hellmann raingauge in a two minute timestep. There was no correction necessary. Rainfall could be put into the model as rainfall intensities ($\frac{mm}{h}$) in this timestep.

9.1.2. Evapotranspiration

With no meteorological data available to run TRAIN, the evapotranspiration had to be taken from literature. In the 'Water and Soil Atlas Baden-Württemberg' (Landesanstalt für Umwelt, 2004), a yearly actual evapotranspiration of 600-650 mm was calculated by a modified TRAIN model, the GWN_BW (Armbruster, 2002). The value of 625 mm as a mid-value of the class had been taken. To be used in ZIN it had to be scaled down in a temporary meaning.

The first step was to derive monthly values. Bucher and Demuth (1985) distributed it by a method of Liebscher (1979) and derived percentage values of the yearly sum for every month. Table 9.1.1 shows the monthly distribution of the yearly evapotranspiration sum of 625 mm.

The second step was to compute daily values. For that purpose, first a mean monthly value was calculated and assigned to the day in the mid of a month. Then straight lines were derived from mid-month-point to mid-month-point and the value of every day was calculated with that straight lines.

With this method a daily distribution with no step transitions from month to month

Table 9.1.1.: Monthly actual evapotranspiration (ETA) of the Loechernbach catchment, derived from the yearly value of the WaBoA and the fractions by Bucher and Demuth (1985).

Month	Jan	Feb	Mar	Apr	May	Jun	Jul	Aug	Sep	Oct	Nov	Dec
Fraction (%)	1	2	5	8	16	17	17	15	11	5	2	1
ETA (mm)	6.3	12.5	31.3	50.0	100.0	106.3	106.3	93.8	68.8	31.3	12.5	6.3
ETA_d (mm)	7.2	13.8	32.1	54.0	95.9	104.7	104.9	91.9	66.1	33.1	13.6	7.0
Error (mm)	0.9	1.3	0.8	4.0	-4.1	-1.6	-1.4	-1.9	-2.7	1.8	1.1	0.7

ETA = monthly ETA sum from Bucher and Demuth (1985)
ETA_d = monthly sum after daily distribution
Error = difference of ETA_d and ETA

was achieved. The monthly sums showed little errors due to the distribution, as it is shown in table 9.1.1. These error can be accepted as the yearly sum is 624.42 mm after distribution and therefore the absolute error is just 0.38 mm which is in the range of rounding errors. Figure 9.1.1 shows the daily evaportranspiration values after daily distribution.

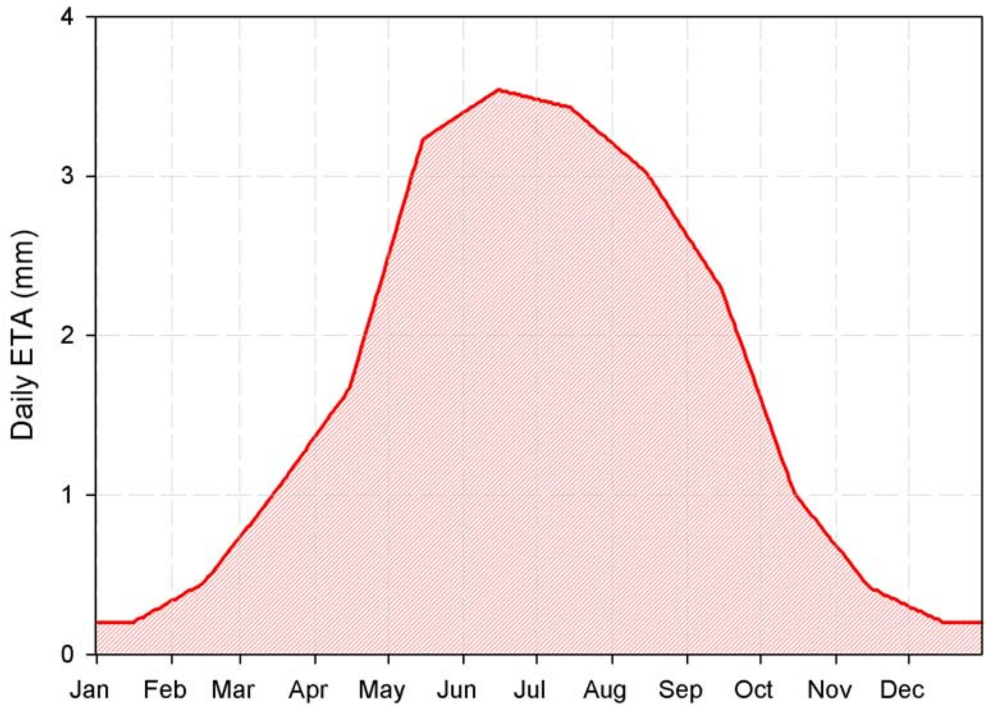

Figure 9.1.1.: Daily evapotranspiration (ETA) values for the Loechernbach catchment as used as model input.

9.1.3. Radiation

Hourly radiation values are used in the model for distribution of the daily evapotranspiration in hourly values by weighting the daily value with the radiation. Unfortunately there were no radiation values for the Loechernbach catchment for the observed period.
To derive a somewhat better hourly distribution of the daily evapotranspiration than just dividing by the sunshine hours of a day, hourly global radiation values for a perfect radiation day were calculated by the equations of Bird and Hulstrom (1991). The input parameters were the coordinates (48.1°N, 7.72°E), the elevation (240 m), the barometric pressure derived with the barometric height formula (984,75 hPa) and some standard values for ozone thickness of the atmosphere, water vapor thickness of the atmosphere, aerosol optical depth, forward scattering of incoming radiation and albedo were taken.

9.2. Parametrization

The ZIN model is originally an uncalibrated model, that means it should run just with measured or calculated values. In a first step the model will be run this way. The values were mostly taken from literature.

9.2.1. Runoff generation

The distributed Runoff Generation module in ZIN needs several input parameters as soilphysical parameters, initial loss and, as the most important for runoff generation, infiltration rates. The soilphysical parameters are mostly used for the generation of saturation excess overland flow and deep infiltration, that means in this case baseflow generation.

Spatial disaggregation

The Loechernbach catchment was divided in eight zones with same properties for runoff generation. This was done by a combination of soils and landuse as it is shown in table 9.2.1 and figure 9.2.1.
With no runoff expected by the forest in the higher part of the catchment the forest with all soils is the first zone. The second zone are the streets, again on all soils, because soils play no role when runoff is generated on streets. The largest zone is the third with vine on pararendzina (44.2%). The mole drained zones (zone eight)

Table 9.2.1.: Runoff generation zones of the Loechernbach catchment.

No	soil	landuse	area (m^2)	%
1	all	forest	63379	3.5
2	all	streets	83469	4.6
3	(deep) pararendzina	vine	795406	44.2
4	all/most pararendzina	acclivity	184716	10.3
5	deep colluvium	all	144634	8.0
6	gley colluvium	all	98104	5.4
7	gley	all	88694	4.9
8	pararendzina	mole drainage	342657	19.0

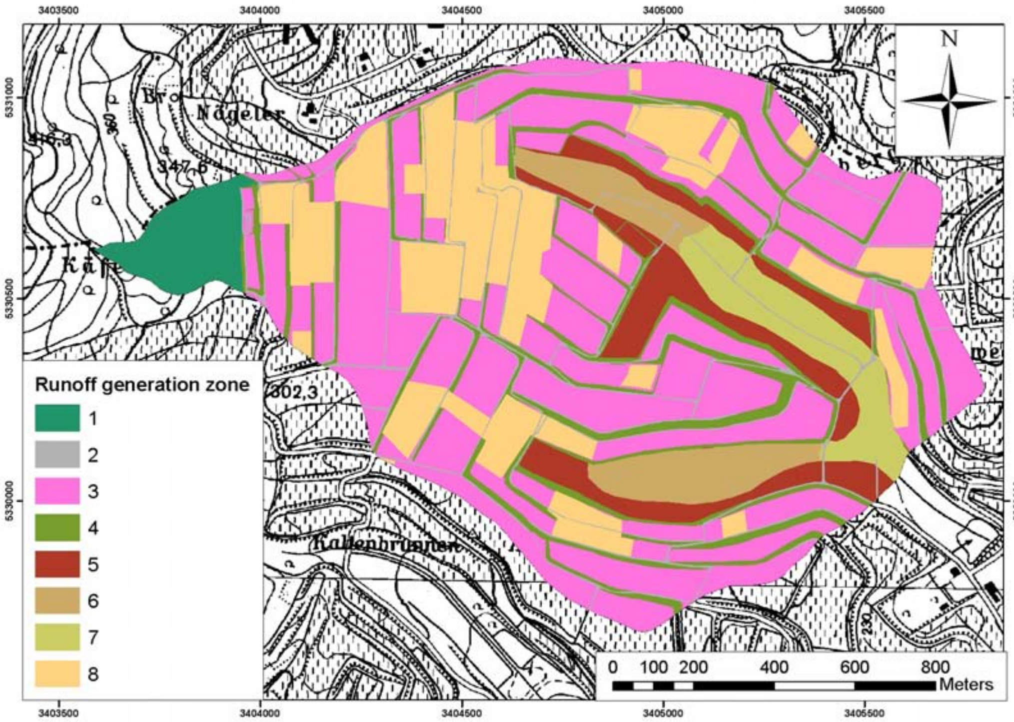

Figure 9.2.1.: Runoff generation zones of the Loechernbach catchment (compare table 9.2.1).

in the terraces (19.0 %) were identified as special runoff generating zone and cover large parts of viniculture and acclivity. Acclivities in the catchment cover also a large part (10.3%). It is thought that the slope of them (most approximately 45°) is more important than the underlying soil, so it is taken as the forth runoff generation zone. Deep colluvium, gley colluvium and gley are the soils of the floodplain of the Loechernbach catchment. As there are mixed and rapidly changing landuses in the floodplain the soils are responsible for dividing the zones five, six and seven.

Soilphysical parameters

The soilphysical input parameters for runoff generation are infiltration capacity ($\frac{mm}{h}$), initial loss (mm), soil depth (m), effective porosity (fraction), permanent wilting point (fraction), field capacity (fraction), the saturated hydraulic conductivity and the coefficient λ as it is used in the Mualem-Van Genuchten equation.
SCHUMACHER (1981) measured some of the parameters in the Loechernbach catchment as it is shown in table 9.2.2. So there are some values for the saturated

Table 9.2.2.: Soilphysical values of the Loechernbach catchment derived by SCHUMACHER (1981).

site	soil	I (mm/h)	K_f (cm/h)	P_{eff}	C (%)	U (%)	S (%)
Löcherntal	deep colluvium	37	0.46	0.41	8.7	81.9	9.4
Pegel-Löcherntal	gley	77	0.08	-	-	-	-
Buckacker-Roh	pararendzina	-	0.79	0.44	7.1	80.9	12
Buckacker-Lehm	pararendzina	-	0.38	0.42	8.9	80.6	10.5
Bütze	pararendzina	-	0.13	0.41	11.7	72.7	15.6
Gutensberg	pararendzina	60	1.04	0.45	8.8	81.8	9.4
Kähnental	pararendzina	64	0.13	0.39	10.5	78	11.4
Mittlingen	pararendzina	-	0.33	0.42	9.1	76.2	14.7
Mittlingen-Ab	pararendzina	-	1.33	0.41	9.4	79.9	10.7
Reblinstal	pararendzina	-	0.08	0.42	13.8	74.6	11.6

I=infiltration capacity, K_f=saturated hydraulic conductivity, P_{eff}=effective porosity
C, U, S=fraction of clay, silt, sand

hydraulic conductivity measured in the laboratory with stationary permeameter on soil samples. Also the effective pore volume for pararendzina, gley and deep colluvium were found there. If there were more than one value, an arithmetic mean had been taken. The values for gley were also used for gley colluvium as we have no other values.
LUFT (1980b) did some measurements of the saturated hydraulic conductivity with uranine tracer tests in the groundwater of the Loechernbach catchment. The test was done in the floodplain near the runoff gauge in the gley soil. He a derived value of K_f =2.54 $\frac{cm}{h}$. Tracer tests in the field are more reliable in deriving the saturated hydraulic conductivity than laboratory measurements, because the soil is not disturbed and it is not as punctual as soil sample tests. On the other hand, this test was done in the aquifer and not in the unsaturated zone, so it was not used for the CaStor. It was used later for the calculation of the drainage catchments in the floodplain.
The missing parameters permanent wilting point and field capacity were calculated with the Soil-Water-Characteristics-Analysis-Tool by SAXTON and RAWLS (2006) as it was also done for deriving input parameters by SCHÜTZ (2006). The fractions

of sand and clay were taken to consider a soil type. With no measured values of organic matter and gravel fraction, they are both considered to be 1 Vol-%. Then the compaction of the soil was adjusted until the computed saturated hydraulic conductivity suited the measured by SCHUMACHER (1981). The so derived values for the permanent wilting point and the field capacity were taken as input for the model as shown in table 9.2.3. The values for deep colluvium were taken as values for all soils in the floodplain.

The parameter λ of the Mualem-Van Genuchten equation was calculated by the empirical Brooks-Corey pore-size distribution as found in RAWS ET AL. (1993):

$$\begin{aligned}\lambda = exp[&-0.7842831 + 0.01775444 \cdot S - 1.062498 \cdot \phi - 0.00005304 \cdot S^2 \\ &- 0.00273493 \cdot C^2 + 1.11134946 \cdot \phi^2 - 0.03088295 \cdot S \cdot \phi \\ &+ 0.00026587 \cdot S^2 \cdot \phi^2 - 0.00610522 \cdot C^2 \cdot \phi^2 \\ &- 0.00000235 \cdot S^2 \cdot C + 0.00798746 \cdot C^2 \cdot \phi - 0.00674491 \cdot \phi^2 \cdot C]\end{aligned} \tag{9.2.1}$$

Here S is the percent of sand ($5 < \% < 70$), C the percent of clay ($5 < \% < 60$) and ϕ the porosity as a volume fraction.
With formula 9.2.1 values of $\lambda = 0.355$ for the deep colluvium and a mean of $\lambda = 0.353$ for pararendzina was determined. The value for the deep colluvium was also taken for gley colluvium and gley.
The infiltration capacities in table 9.2.2 were measured with a double ring infiltrometer by SCHUMACHER (1981). Multiple measurements were taken for each site and an average was calculated per site. These values were the only infiltration measurements made in the Loechernbach catchment, so they were taken as model-input. Measurements for gley were also used for clay colluvium (table 9.2.3).
As there was no runoff expected from the forest, a large infiltration rate of 200 $\frac{mm}{h}$ was set for this zone, while the streets, as a sealed area, were thought to have no infiltration.

Initial loss and soil depth

Initial loss is the amount of water to fill the interception storage and depressions before water is running to the channel. So vegetation and slopes play an important role in considering initial loss values.
The initial loss values are not easy to find in literature. MANIAK (2005) specified some values for streets (0.7 - 0.9 mm), forest (3 - 8 mm), pasturage (3 - 8 mm) and loamy sand with 45% grass cover (4.5 mm) for slopes of 0 - 1%.
So an initial loss for streets was taken with 0.8 mm, for forest 6 mm. For the acclivity, that is mostly covered with grass and brush, a low value of 2 mm had been

chosen because of the steep slope. The zones five to seven are located in the floodplain and therefore have very gentle slopes. They are covered with fruits, pasturage, vegetables and so a value of 4.5 mm, which matches the 45% grass cover is taken. The largest fraction in the catchment, vine on pararendzina, has somewhat steeper slopes (2 - 10 %) and so a value of 3.5 mm for initial loss had been taken. As the mole drained areas are mostly in the viniculture, an initial loss of 3.5 mm was taken, too.

Soil depth rules with porosity the storage volume of the unsaturated soil. Groundwater or more precisely capillary fringe is the bottom limit and therefore the soil depth. Observations at the Loechernbach Pegel site from 15.08.07 - 05.10.07 gave a weighted mean of 1.1 m for groundwater depth. With no other observation wells in the catchment, this value was taken as soil depth for the soils in the floodplain. As the mole drainages are known to lie in a depth of 1.2 m, this value was taken as input there. The forest soils are expected to be larger, and so a value of 2 m was taken. The vine growing areas are on very large and high terraces. Groundwater under terraces has to stay more or less in a line along the main slope. If it rises into higher regions within the terraces, water fills the pores and destabilizes the soil and the terraces will slip with gravity. So the unsaturated zone has to be mighty with terraces of 50 m height in the catchment. As a mid-value we take 5 m for the terraces and the acclivity.

Table 9.2.3.: Input parameters for the Runoff Generation module of ZIN for the Loechernbach catchment.

No	I (mm/h)	IL (mm)	depth (m)	P_{eff}	PWP	K_f (cm/h)	λ	FC
1	200	6.0	2.0	0.42	0.07	0.53	0.350	0.28
2	0	0.8	1.1	0.42	0.07	0.53	0.350	0.28
3	62	3.5	5.0	0.42	0.07	0.53	0.353	0.28
4	62	2	5.0	0.42	0.07	0.53	0.353	0.28
5	37	4.5	1.1	0.41	0.07	0.46	0.355	0.29
6	77	4.5	1.1	0.41	0.07	0.08	0.355	0.29
7	77	4.5	1.1	0.41	0.07	0.08	0.355	0.29
8	62	3.5	1.2	0.42	0.07	0.53	0.353	0.28

IL=Initial Loss, depth=soil depth,
PWP=Permanent Wilting Point (fraction), FC=Field Capacity(fraction)

9.2.2. Runoff Concentration

For runoff concentration, the catchment was divided into subcatchments as shown in figure 9.2.2. In contrast to WAGNER (2002) the generated water was not sent to the channel by a Dirac impulse but by a unit hydrograph.
The unit hydrograph was calculated with the Fisher-Tippet distribution introduced by HAGENLOCHER (2007). The parameters chosen are the concentration time a_{fish} = 5 and the width parameter b_{fish} = 15. As explained above the average slope and the area of every subbasin influences the runoff transformation curve and was calculated as an input for the runoff generation module, too. The dependence of the runoff transformation curve on the slope and the area of the subcatchments can be influenced with the parameters *slopeDep* and *areaDep* (%). As there were no experience values for the parameters, they were chosen *slopeDep* = 20% and *areaDep* = 20%. This resulted in a concentration time between 3.5 and 6 minutes, which is in an arguable range. The *areaDep* paramter influences the peak delivery of the unit hydrograph. Related to a timestep lenght of one minute, the peak deliveries ranged from 2 to 4 $\frac{\%}{min}$, which is comparable to the values LANGE ET AL. (1999) measured.

9.2.3. Channel routing

The most parameters for channel routing can be measured. The channel network has to be divided in channel segments with measured length, width and slope as it is shown in figure 9.2.2. The floodwave is routed from segment to segment. Additional channel properties are needed. By means of this properties the segments were gathered into five groups of channel segments. The Manning n values were derived from SHEN and JULIEN (1993) and fitted to observations in the catchment. The roughness needed for calculating the pipe flow is the roughness length. WONG and PARKER (2006) showed an improved relationship between the Manning n value and the roughness length k_s, which is used in the model to calculate the roughness length:

$$n = \frac{(\frac{k_s}{2})^{\frac{1}{6}}}{26} \tag{9.2.2}$$

The parameter $frac\_chan$ is the fraction of the inner channel compared to the whole channel. It was set 0.999, because the whole water flows within the inner channel. The parameter $depth\_full$ is the water depth when the inner channel is full. This values were measured in the Loechernbach channel, too. Table 9.2.4 shows the channel properties for the five channel types.

To obtain the routing timestep of the model, the maximum flow velocities v and

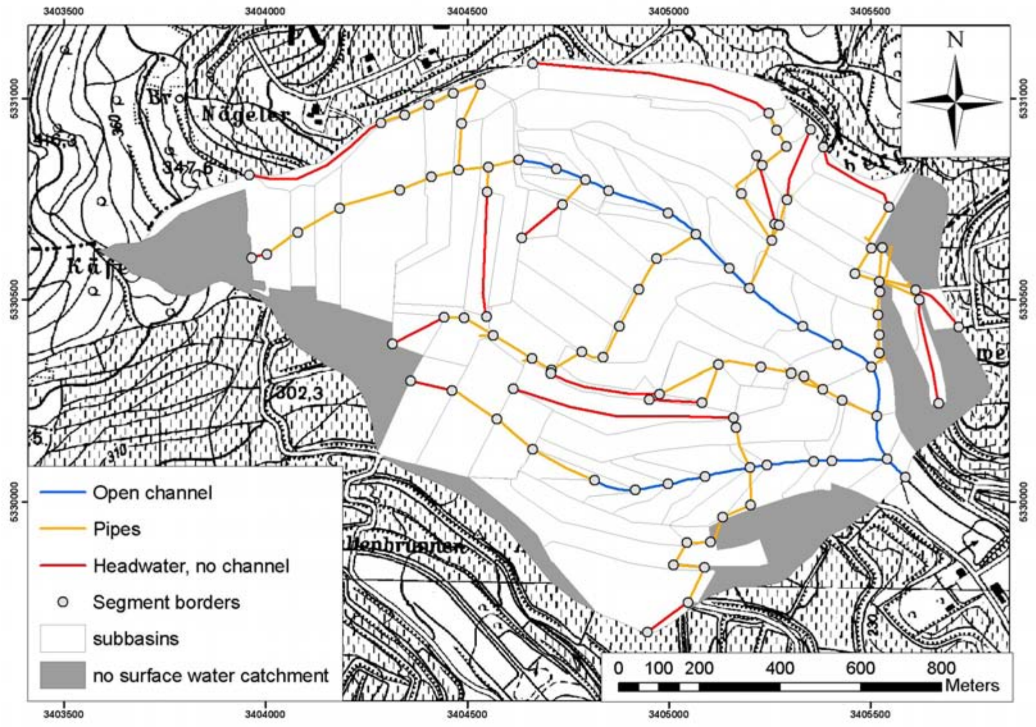

Figure 9.2.2.: Segments and subbasins of the Loechernbach catchments as divided for the model setup.

Table 9.2.4.: Channel properties of the Loechernbach catchment.

No	description	Manning n	frac_chan	depth_full (m)
1	pipes	0.02	0.999	0.6
2	upper	0.035	0.999	1
3	mid	0.035	0.999	1.5
4	mid	0.03	0.999	2
5	lower	0.035	0.999	3

frac_chan=fraction of inner channel
depth_full=water depth when inner channel is full

the routing segment length x had to be considered. Lange et al. (1999) stated the following formula for choosing the routing timestep t:

$$t < \frac{x}{v} \tag{9.2.3}$$

Test runs showed maximum velocities of about 10 $\frac{m}{s}$ in a segment with the length of x=26. So a timestep of 2.6 seconds had to be chosen. As it is special in the model that the timestep of the routing has to be a multiple of the runoff generation timestep (which was chosen 2 minutes according to the rainfall input data), the routing timestep was chosen 3 seconds.

9.2.4. Baseflow module

The baseflow module needs not much special input, just the zones where the baseflow comes from. In the Loechernbach catchment, the baseflow was expected to come from drained zones. The first zone is the mole drained area in the viniculture, whose extend is known. The second baseflow part comes from the drainage pipes in the floodplain, what was proved by Nippgen (2007) with measurements of electrical conductivity before and after the confluence of the drainage pipes.
The draining areas around the drainage pipes in the floodplain is not known. But there are methods to calculate the distance between drainage pipes for planning purposes, so a zone of the half calculated distance around the pipes was taken as drainage catchments. The distance a between the drainage pipes in groundwater soils can be calculated using a formula found in Eggelsmann (1981):

$$a = \sqrt{4 \cdot h \cdot K_f \cdot \frac{2 \cdot d + h}{s}} \tag{9.2.4}$$

Here h is the allowed height of groundwater over the drainage pipe, K_f the saturated hydraulic conductivity, d a factor depending on the distance D between the drainage pipe and the aquitard. s is the maximum rainfall depth per day ($\frac{m}{d}$), the drainage has to discharge.
The factors d respectively a can be calculated in an iterative process using formula 9.2.4 or by a nomogram found in Eggelsmann (1981). The easier way is the nomogram and so it was used here. For the nomogram K_f, h, s and D were needed. The saturated hydraulic conductivity was taken from the tracer experiment by Luft (1980b) as K_f =2.54 $\frac{cm}{h}$ and the allowed groundwater height over the drainage pipe h =0.3 m. The depth to the aquifer bottom was easily calculated with the soil profile in figure 5.2.3 and the drainage depth of 1.2 m as D=1.2 m. Not so easy is the calculation of the maximum rainfall depth per day, that can be discharged by the pipes. In the precipitation time series of this study, the maximum daily sum is 32.76 mm at the 21.06.2007. By considering a runoff coefficient of 0.15 (Pilgram and Cordery, 1993), a soil storage of 40% and an evapotranspiration of 3 $\frac{mm}{d}$ a value of $s = 0.015\frac{m}{d}$ was found. So this was taken as the input value as no other value was available. With the above described input value a drainage distance of a = 10 m was derived from the nomogram and so a drainage catchment of 5 m around the pipes.
The mole drained area as well as the drainage pipes with their catchments were

taken as input for the baseflow module.

9.2.5. Sediment module

The input for the sediment generation module are the rainfall intensity, which was already provided for the hydrological modules and the relationship between rainfall intensity and sediment release ($\frac{g}{m^2 \cdot min}$) for every runoff generation zone. This relationship was derived from studies found in the literature.
The best suiting literature was RÖMKENS ET AL. (2001). A Grenada loess soil was placed in a 3.7 x 0.61 m bed with a depth of 0.23 m. Then rainfall simulator test were undertaken. The grain-size distribution of the Grenada loess is 18% clay, 80% silt and 2% sand, which is comparable to the pararendzina in the Loechernbach catchment. There was no vegetation at the surface which was charaterised as smooth (elevation variation of less than 1 mm). The slope steepness was 2% which fits the Loechernbach catchment because of the large terraces. Sprinkler tests with different rainfall intensities (PI) brought different soil loss (SL). The relationship was derived from eight measurement points, each of them was an average of many samples. A power function was successfully fitted as shown in figure 9.2.3. The regression function used as model input is

$$SL = 0.0007335 \cdot PI^{2.2242560}. \tag{9.2.5}$$

All soils in the catchment are loess soils and so this equation was taken for all runoff generation zones but the forest.

As it is the theory in the catchment that the sediment comes from the streets, and there from the bare borders of the streets, the relationship was divided by ten for zone two. So it was considered, that 10% of the streets deliver sediment to the channel.
To derive a value for the vegetated areas in the catchment, the erosion value derived by equation 9.2.5 was multiplied with the C-factor of the Universal Soil Loss Equation (USLE). This factor is the ratio of erosion from the considered surface to erosion from a bare surface (WISCHMEIER and SMITH, 1978). The values were taken from the 'Soil-Erosion Atlas Baden Württemberg' (GÜNDRA ET AL., 1995) and are shown in table 9.2.5 for each runoff - generating zone. No values for forest were entered as no overland flow was expected for this zone.

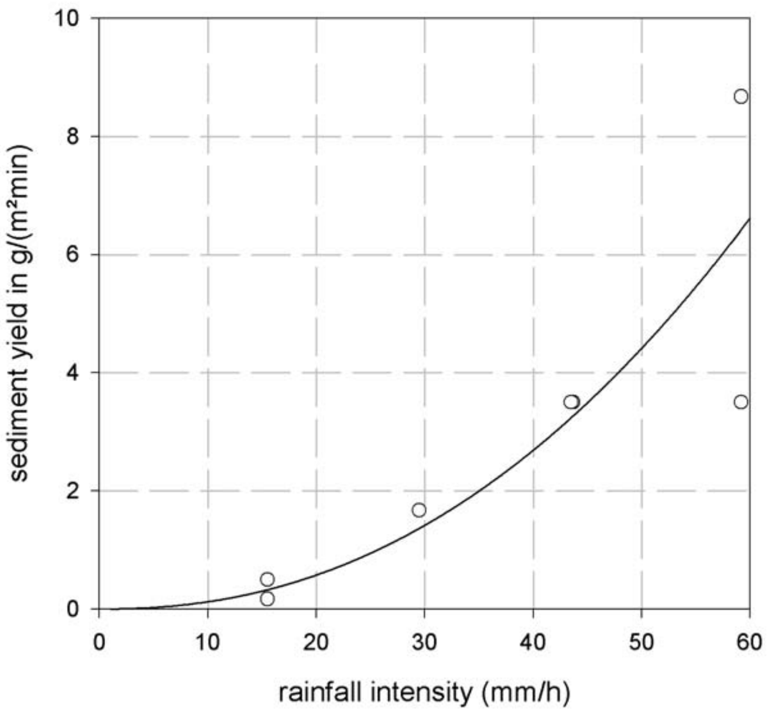

Figure 9.2.3.: Relationship between rainfall intensity ($\frac{mm}{h}$) and sediment yield ($\frac{g}{m^2 \cdot min}$) (data from Römkens et al. (2001)).

Table 9.2.5.: C-factors of the USLE and overall relationships between Soil Loss SL ($\frac{g}{m^2 min}$) and rainfall intensities PI ($\frac{mm}{h}$) as used in the erosion-sediment transport module in the loechernbach catchment for each runoff-generation zone.

Zone	Description	Landuse	C-factor	Overall relationship
1	forest	forest	0.0	0
2	streets	streets	1.0	$SL = 7.335 \cdot 10^{-5} \cdot PI^{2.2242560}$
3	vine	vine	1	[1] $SL = 7.335 \cdot 10^{-5} \cdot PI^{2.2242560}$
4	acclivity	grass	0.004	$SL = 2.934 \cdot 10^{-7} \cdot PI^{2.2242560}$
5	floodplain 1	grain	0.1	$SL = 7.335 \cdot 10^{-5} \cdot PI^{2.2242560}$
6	floodplain 2	grain	0.1	$SL = 7.335 \cdot 10^{-5} \cdot PI^{2.2242560}$
7	floodplain 3	grain	0.1	$SL = 7.335 \cdot 10^{-5} \cdot PI^{2.2242560}$
8	mole drainage	vine	0.1	$SL = 7.335 \cdot 10^{-5} \cdot PI^{2.2242560}$

[1] multiplied by 0.1 as the coverage is just 10%

9.3. Conclusion

The input timeseries of the model were partly measured (precipitation) and partly calculated with values found in the literature (evapotranspiration, radiation).
The catchment was divided in 83 subbasins by means of a digital elevation model.

However the division could not be made automatically by a GIS as it is a strongly man-made catchment, and the terraces slope contrary to the main slope. The standard algorithms could not handle this.
Some of the channel routing parameters were measured in the Loechernbach channel (width, depth) and other were derived by literature (roughness). Some of the parameters for the runoff generation were taken from earlier studies in the catchment, the rest were calculated. The parameters were distributed to the catchment area by means of the soils and the landuse of the catchment.
The new baseflow module as well as the new erosion/sediment transport module were totally set up with values taken from the literature. The baseflow generation zones were thought to be the drained zones in catchment. The input relationship for the erosion calculation was derived by sprinkler tests found in Römkens et al. (2001). To take the vegetation into account, the relationships were multiplied by the C-factor of the Universal Soil Loss Equation.
Test runs will show the applicability of the parameters.

10. Module test

The newly developed baseflow and erosion-sediment transport modules will be tested for usability in this chapter, that means if they behave as they are expected and if the derived values are in the right dimensions.

10.1. Baseflow module

The ability to simulate baseflow with this module was proved by test runs. To start the simulation not with dry soils, an initial moisture value can be set at the beginning. Then all soils have the same start moisture. The sensibility of the model to the set initial moisture was tested using different initial moisture values. The start values for the baseflow as reaction to the initial moisture for the setup in the Loechernbach catchment are shown in figure 10.1.1. It is as expected, the baseflow rises to a power relationship with rising initial moisture.

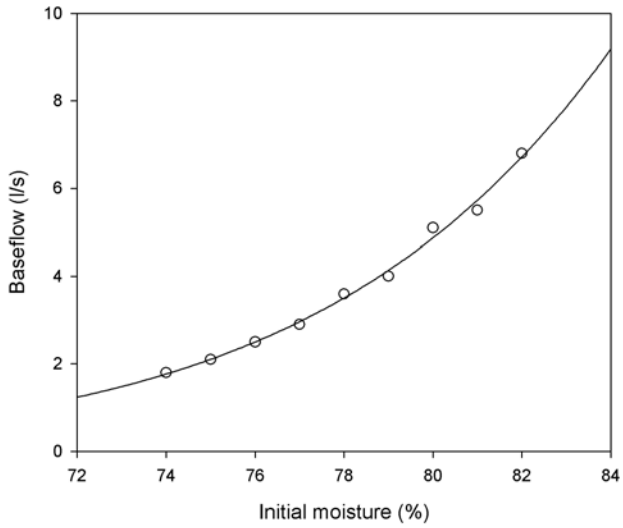

Figure 10.1.1.: Sensibility of the baseflow module to the initial moisture for the setup in the Loechernbach catchment.

Figure 10.1.2 shows an example of a test run with and without baseflow at the

27.06.07. To point out the baseflow, the runoff was plotted on a logarithmical axis. It is obvious that the module is able to simulate baseflow event based, but not able to simulate the large rise after the event. Indeed the baseflow is larger after the event, but not that much as it was measured. This may be an effect of the parametrization, especially the extend of the zones where the baseflow comes from.
A second thing is shown at the start of the simulation in figure 10.1.2, that has to be considered, when the baseflow module is used event based: At the beginning of a modelling period, the baseflow 'wave' needs time until it reaches the outlet of a catchment. So if one needs the baseflow from midnight on, the day before should be modelled as well.
The soil storage outflow proved to be very lazy to rainfall input. This depends hard

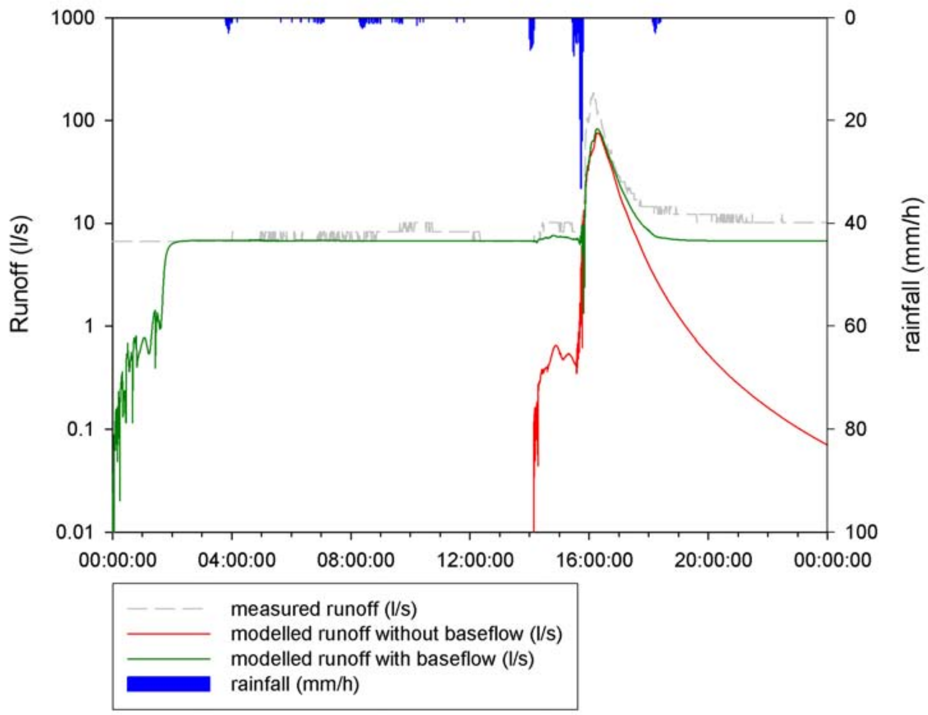

Figure 10.1.2.: Example of the effect of the baseflow module in the Loechernbach catchment at the 27.07.07.

on the soil depth. With just one soil storage the saturation of a soil is the amount of water (volume) in the storage divided by porosity and soil depth (that means the volume). So with a larger soil depth, the saturation changes less to the same water input. If there is rainfall input on the mighty Loechernbach pararendzina soils, the saturation and the outflow change therefore just little.
A test run with a start saturation of the field capacity showed, that one month in summer was not able to fill the storage of a soil with a depth of five meter in a degree,

that it was able to deliver baseflow for several days. This was surely not only an effect of soil depth, but depended on the evapotranspiration, which was about 3.5 mm per day, too. A test run over a winter season could bring further information about the soilstorage and baseflow behavior, but there where no data available for a winter season.

To test the long term dynamic of the module, a simulation over the whole observed period (26.05.07 - 03.09.07) was done. The hydrograph is shown in figure 10.1.3. As the baseflow module depends very hard on the filling of the soil storage, thus the soil moisture, the initial moisture value was chosen to fit the observed baseflow.

In the first weeks, the baseflow module seemed to work properly with filling of

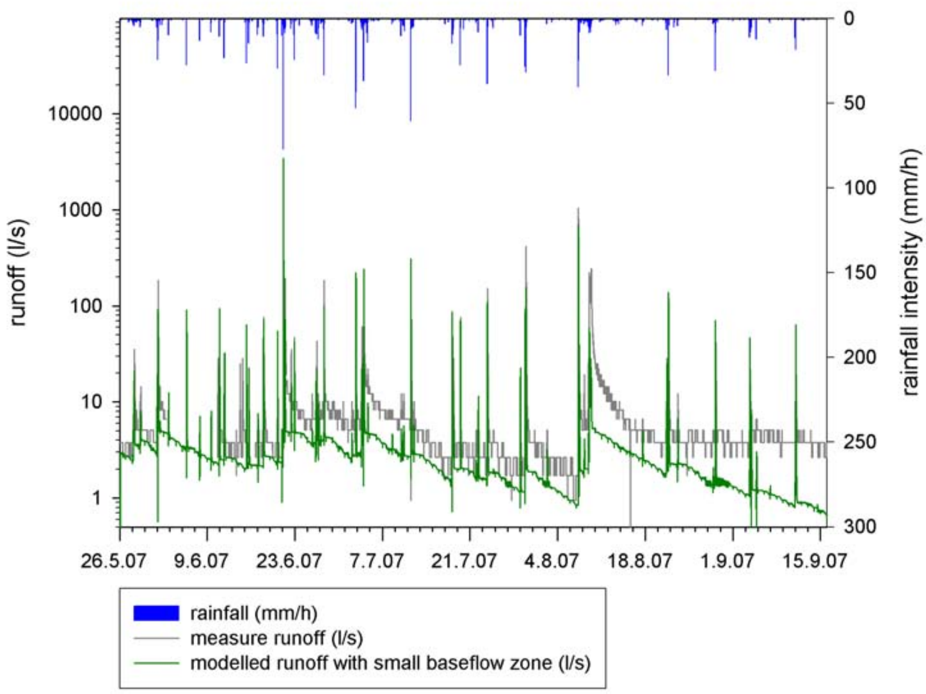

Figure 10.1.3.: Long term test of the baseflow module.

the storage by events and so a larger baseflow after events. But when larger events happened, the storage was filled more in nature than predicted by the model. Especially after a series of large events at the 07.08.07-09.08.07 the baseflow storage seemed to be filled up enormously as the baseflow stayed at a high level (10-20 $\frac{l}{s}$) for several days. The test run pointed out the problem that the storage is filled to low by the model. In contrast, the dynamic of the modelled baseflow seemed to fit the measured well, that means that the decline of the modelled baseflow hydrograph is as strong as the measured.

10.2. Sediment module

The sediment module was tested to dynamic, peak yield and total sediment amount of an event. Test runs of the model with enabled sediment module showed the following results:

- sediment is delivered by the module and increases with increasing rainfall intensity.
- a sediment wave runs through the channel (figure 10.2.1)
- the sediment yield at the outlet is in the right dimension.

With this results the measurement based conceptual erosion-sediment-transport module seemed to work properly and was therefore used for modelling sediment yield.

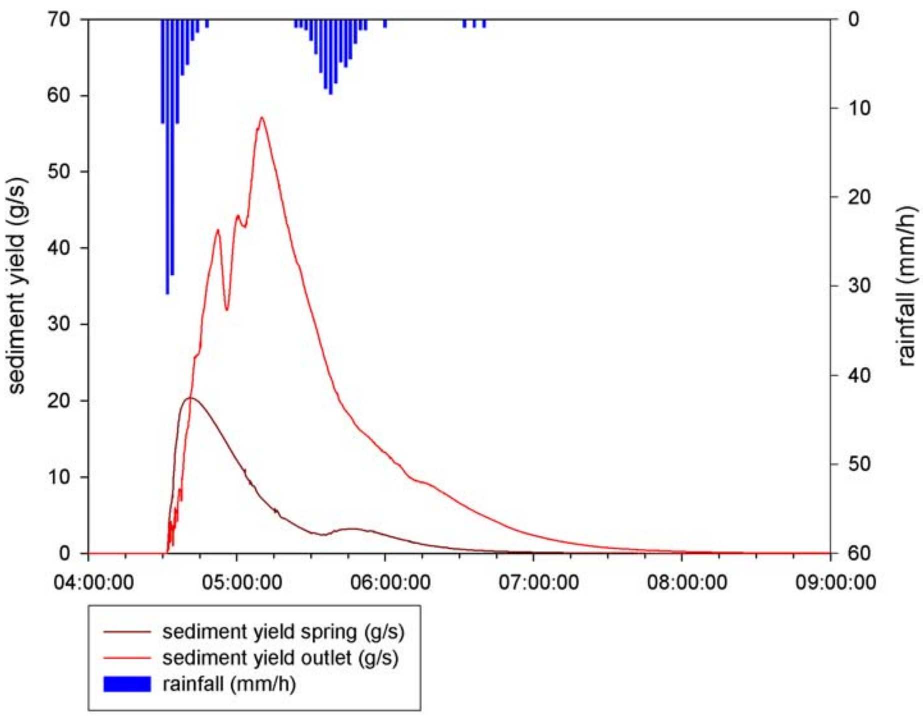

Figure 10.2.1.: Test of the sediment module at the 29.08.07. The 'Sediment Wave' runs from the spring to the outlet of the Loechernbach catchment.

10.3. Conclusion

The baseflow module worked well on an event based approach, but the rise in the baseflow as answer to a rainfall event is not as large as measured. This became clearly when the long term modelling was considered.
The sediment module was tested and found working, too. With larger rainfall intensity, the sediment yield got larger and a 'sediment wave' was observed running through the channel.
Both new modules were tested and found working whereas the baseflow module has to be tested with other parameters.

11. Parameter improvement

As some uncalibrated model test runs showed common errors in the modelling results, several input parameters will be modified in this chapter for better model results. This will not happen as a black-box model calibration, but as an improvement of the parameters for reasons.

11.1. Hydrological model

The quality of a rainfall-runoff model result compared to measurements can be calculated using the Nash-Sutcliffe efficiency (NASH and SUTCLIFFE, 1970) R_{eff} as it is given by formula 11.1.1.

$$R_{eff} = 1 - \frac{\sum(Q_{obs} - Q_{sim})^2}{\sum(Q_{obs} - \bar{Q}_{obs})^2} \tag{11.1.1}$$

The sum of the squared difference between the observed runoff Q_{obs} and the simulated runoff Q_{sim} is divided by the sum of the squared differences between the observed runoff and the average observed runoff $\bar{Q}_{obs}$. This fraction is subtracted from 1. So the range of the efficiency values is from $-\infty$ to 1. If the efficiency is 1, an optimal fit was done by the model. A Zero value means that the model prediction fits the measured curves as well as the arithmetic mean of the measured values. This formula was used to rate the model results and decide if they are able or not to represent the respective processes.

11.1.1. Event flow

Some model test-runs for the hydrological part during events showed two main errors: the small events were overestimated and the large events underestimated. So it was tried to improve the model parameters for reasons.
For testing the model the input timeseries, that reaches from 18.05.2007 to 15.09.2007 was divided in two parts. The period from 18.05.07 - 15.07.07 was taken for the test runs and the parameter improvement. The second period was then taken for a model validation.

With the setup shown in table 9.2.3 at nearly all events just the roads showed overland flow. For small events the mass of water built on the streets is to large to fit the observed runoff. So if it was taken into account, that water built on the streets was able to re-infiltrate at the borders of the roads, the small events fitted better. The test runs for the small events (peak $< 40\ \frac{l}{s}$) showed, that a value of 2 $\frac{mm}{h}$ fitted best and is in an arguable range.
The values for the infiltration rates found in literature and taken as model input are in doubt. Schumacher (1981) measured this values with a double ring infiltrometer. Such infiltrometers are known to overestimate infiltration compared to rainfall simulators as shown in Sidiras and Roth (1989) or Merzougui and Gifford (1987). There were overestimation ratios from 1.6 to 2.7 (Merzougui and Gifford, 1987) and 7.7 to 12 (Sidiras and Roth, 1989) reported. Rainfall simulator tests fit the natural circumstances better than double ring infiltrometers as there is unsaturated flow in the soil and the influence of raindrops falling on the soil (splash-effect) happens. The overestimations reported in the literature were taken for an improvement of the modelling. The values found in Sidiras and Roth (1989) were thought too high for our purpose, because the largest infiltration rate would be at about 10 mm/h, which is definitively too low. So an overestimation ratio of 2 for correcting the infiltration values was taken. Just the value for zone 5 seemed to low after this improvement. As it is located in the floodplain, too, the same value as for zone 6 and 7 was chosen. The improved infiltration rates as well as the other soil properties needed by the model are collected in table 11.1.1. To test the new

Table 11.1.1.: Improved input parameters for the Runoff Generation module of ZIN for the Loechernbach catchment.

No	I (mm/h)	IL (mm)	depth (m)	P_{eff}	PWP	kf (cm/h)	λ	FC
1	200	6.0	2.0	0.42	0.07	0.53	0.350	0.28
2	2	0.8	1.1	0.42	0.07	0.53	0.350	0.28
3	31	3.5	5.0	0.42	0.07	0.53	0.353	0.28
4	31	2	5.0	0.42	0.07	0.53	0.353	0.28
5	38.5	4.5	1.1	0.41	0.07	0.46	0.355	0.29
6	38.5	4.5	1.1	0.41	0.07	0.08	0.355	0.29
7	38.5	4.5	1.1	0.41	0.07	0.08	0.355	0.29
8	31	3.5	1.2	0.42	0.07	0.53	0.353	0.28

IL=Initial Loss, depth=soil depth,
PWP=Permanent Wilting Point (fraction), FC=Field Capacity(fraction)

infiltration values, test runs with three events of the calibration period with different runoff peaks were done. The Nash-Sutcliffe efficiencies (table 11.1.2) as well as a view of the hydrographs (figures 11.1.1, A.2.1 and A.2.2) showed better results with the new model setup. Especially the small events (29.05.07) and the large one (02.07.07) were improved much with the street re-infiltration.

The mid-range event at the 26.06.07 was somewhat underestimated by the new

Table 11.1.2.: Nash-Sutcliffe efficiencies of original and the improved model setup for three modelled days.

date	R_{eff} of the original setup	R_{eff} of the improved setup	$Q_{max} \frac{l}{s}$
29.05.2007	-3.11	0.38	14.4
26.06.2007	0.76	0.79	42.2
02.07.2007	0.87	0.95	224

infiltration values. But this was a special situation noticed in other test runs in the calibration period, too, when looking at the second peak of the 26.06.07. If there are two or more runoff events in short sequence, the first peak is modelled well, but the second peak is underestimated by the model. If the precipitation is taken into account, one can see that the second peak, that is larger than the first, was caused by rainfall with nearly the same intensities. Sometimes the intensity was watched to be even less at the second runoff peak, that was larger (compare figure 12.1.2).
There may be several possibilities to explain this behavior of the catchment. First, the infiltration rates decrease with increasing time of the infiltration event due to splash effects and with this clogging of the soil pores. If two events follow in short sequence, it will have the same effect as it were one long event and with the less infiltration rates the runoff coefficient gets larger.
A second possibility is that the soils stay saturated or nearly saturated after the first event. When the second rainfall event arrives, the nearly saturated soil parts get saturated and subsurface flow like a piston flow effect starts. This assumption is supported by the relatively large pre-event water concentrations Uhlenbrook (1995) found with a hydrograph separation done by ^{18}O.
This two attempts of explaining the larger peak due to less rainfall intensities have one in common: the processes are not integrated in the rainfall-runoff model ZIN and so the model is not able to simulate this behavior properly.
All in all the test runs showed that the model results are better with the new setup and so the new infiltration rates were taken for further model runs.

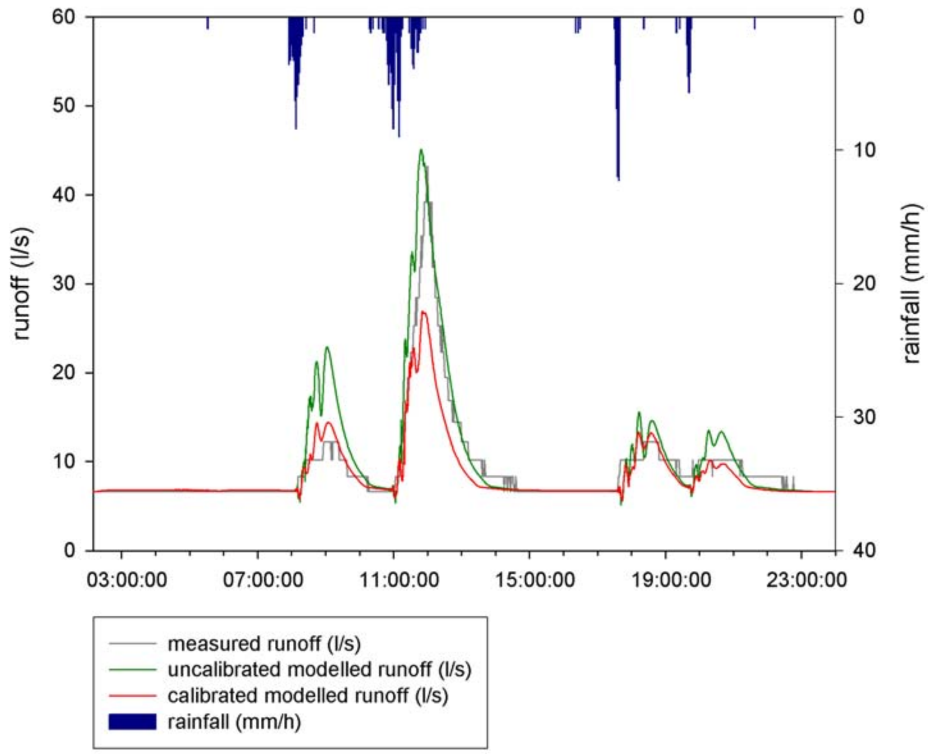

Figure 11.1.1.: Events at the 26.06.07 before and after improvement of the infitration rates.

11.1.2. Baseflow

As it is the only possibility to influence the baseflow module, the baseflow generating zones were changed. Instead of the drained zones, the whole subsurface catchment was taken as area contributing to baseflow.

The result was generally a baseflow of a higher level (compare figure 11.1.2). The dynamic was found not as heavy as with the old setup and fitted better before. This can be explained by a less filling of the soil storage needed to produce the same amount of baseflow than with a smaller area. As the Mualem-Van Genuchten relationship gets steeper with larger soil moisture, a change in a low moisture range changes the unsaturated hydraulic conductivity not as much as in a high moisture range and the outflow dynamic is more gentle.

To express the results of the long term modelling with the larger zone compared to the modelling with the smaller zone in numbers, the Nash-Sutcliffe efficiencies of the calibration period were calculated. As low flow takes the most time in the catchment, it has a large influence on the efficiencies. Table 11.1.3 contains the values for two different runoff ranges. The efficiencies were provided for the runoff up to 200 $\frac{l}{s}$ as it were defined important for this study and for the low runoff values below 20 $\frac{l}{s}$

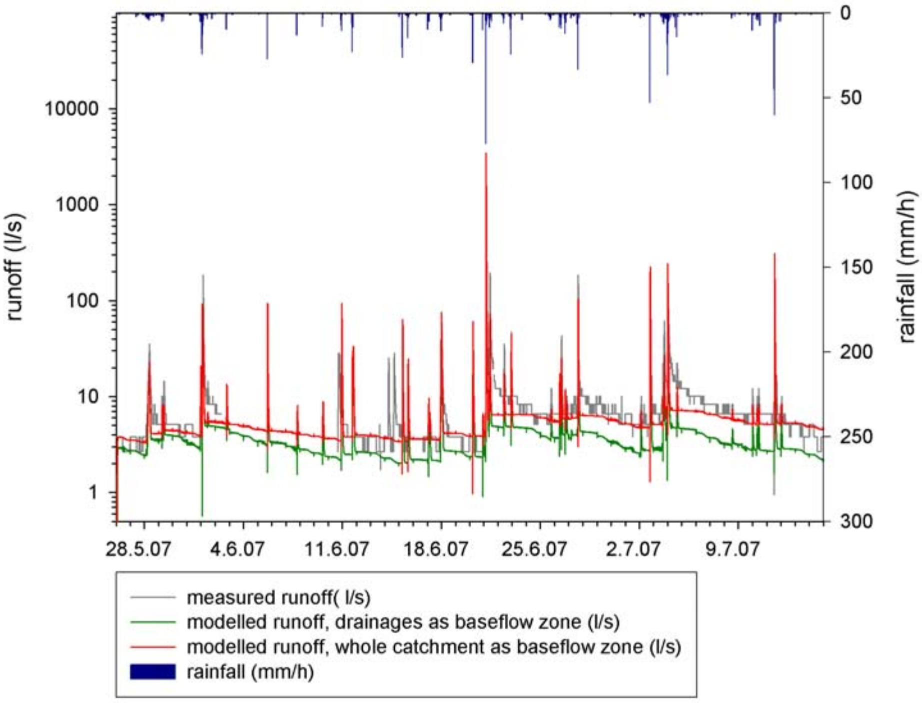

Figure 11.1.2.: Long term modelling for the calibration period with the old and the new setup of the area contributing to baseflow.

to compare low flow conditions. The values for the wide range showed a smooth improvement when the whole catchment area is taken as runoff generating zone, whereas the values for the low flow were improved much. The absolute efficiencies of the baseflow were not well, but it has to be noticed that a difference of just 1 $\frac{l}{s}$ in the low flow has a large influence on the efficiency. As Nippgen (2007) reported large relative errors while measuring low flow, the efficiencies should only be interpreted qualitatively.

With the better fitting of the modelled hydrograph to the measured, the whole

Table 11.1.3.: Nash-Sutcliffe efficiencies of the calibration period for the original baseflow generating zone and the whole catchment as baseflow contributing area. Values were calculated for different runoff ranges.

start	end	baseflow area	runoff range ($\frac{l}{s}$)	R_{eff}
26.05.2007	15.07.2007	drainages	up to 200	0.42
26.05.2007	15.07.2007	whole catchment	up to 200	0.49
26.05.2007	15.07.2007	drainages	up to 20	-1.47
26.05.2007	15.07.2007	whole catchment	up to 20	-0.66

catchment area should be taken as baseflow generating zone instead of just the drained zones. This could be argued by the fact, that the drainage pipes in the floodplain are known to be clogged and the mole drainages in the vine growing area are known to have low usability after about 30 years.

11.2. Sediment model

To test the setup of the sediment module, test runs with three events at the 29.08.07 and the 03.09.07 as shown in table 6.4.1 and at the 11.07.07 with data from NIPPGEN (2007) were done. As it was the aim of this thesis to model small to mid-range events properly, the three events were chosen to cover the whole range with the maximum runoff at the 11.07.07. (205 $\frac{l}{s}$).
The two calibration possibilities were the percentage value of the street-borders, that show bare soil and the C-factor used for the influence of vegetation on erosion. The calibration was done by sight and by comparing the peak yields. Then the amounts of sediment were compared for the uncalibrated and calibrated model.

The sediment model calculates a sediment yield in $\frac{g}{s}$. To compare the model results with the measurements, the measured concentrations were converted to sediment yield with measured runoff.
As erosion is calculated with rainfall intensity in the model, three events with different maximum rainfall intensities were taken to check the model parameters as shown in table 11.2.2.
If the maximum rainfall intensities and the infiltration rates are taken into account, one can see that at the two smallest events just the streets delivered overland flow (and so sediment). Only at the largest event, the whole area brought both water and sediment.

By comparing the modelled with the measured sediment peaks (table 11.2.1) as a first step, an overestimation by 129.7% at the 11.07.07 and 111.1% at the 29.07.07 was noticed. The smallest event fitted well with this setup (underestimation by 1 $\frac{g}{s}$). Unfortunately the two small events had the same origin region of sediment. So the good fit of the smallest event would become worse if the mid-event gets fitted. However, as the mid-event fit was that bad, the fit was done. As the sediment comes just from the streets, the area of the streets delivering sediment was changed from 10% to 7%.
To fit the large event, the C-factor of the USLE had to be changed. Taking a closer look at the USLE, it turned out that the C-factor depends on the vegetation and on the management of the soil like plowing and the crop rotation (WISCHMEIER and

Smith, 1978). As the USLE calculates erosion values of a whole year, the C-factor is calculated by multiplying a management or crop rotation factor with a coverage factor. The simulated period of this thesis was just in the vegetation period, so the crop rotation factor had to be taken out. That means the erosion per timestep was less than compared with the erosion of the whole year. A value of 0.4 fitted best with the peak sediment yields. If it was taken into account that vine plants have leaves about a halve year, the value is in an arguable range. So the equations 3 and 5-8 shown in table 9.2.5 were multiplied by 0.4 to eliminate the crop rotation factor. Table 11.2.1 shows a much better fit for the peak values of the two largest events after the parameter adjusting, while the smallest event became worse as it was expected. A comparison of the curves by sight (figures 11.2.1, A.1.3, A.1.4) showed a better fit to the measured values for the two larger events, and a worse fit for the smaller event, too.

The second step was to compare the measured amounts of sediment to the

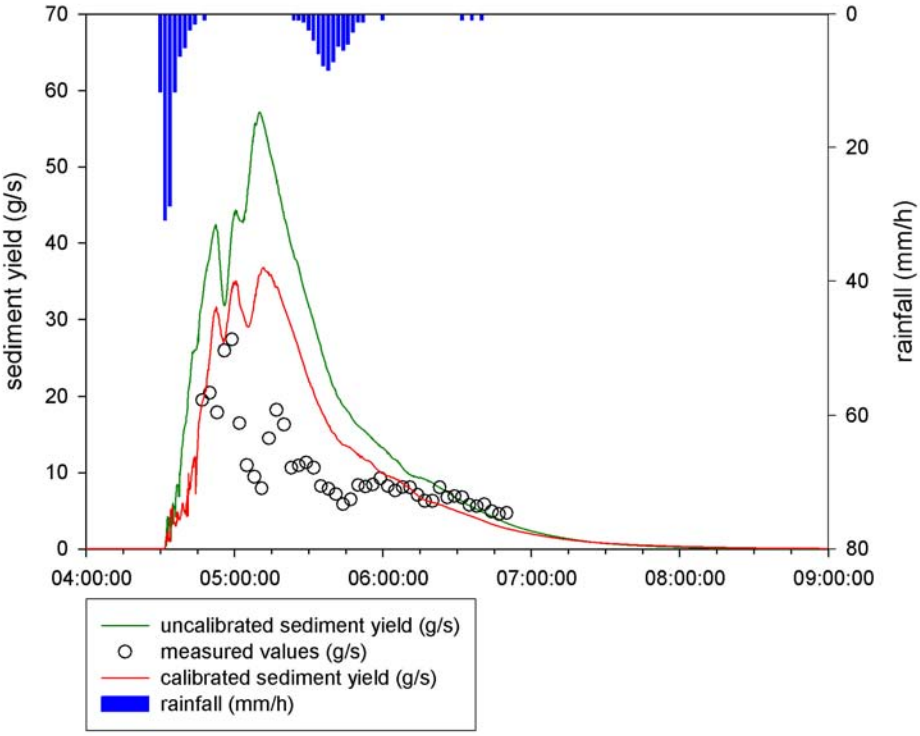

Figure 11.2.1.: Sediment load curve before and after calibration procedure and measured sediment yield at the 29.08.07.

modelled. This was not facile as the measuring started with a certain water level, took 42 samples and stopped. So not the whole sediment event was sampled. The comparison was done for the timespan the automatic sampler took samples. Thus an error was produced just when the measured and the modelled event arrived not

Table 11.2.1.: Uncalibrated and calibrated peak sediment yields.

event date	PI_{max} (mm/h)	Q_{max} (l/s)	measured sed. peak yield (g/s)	modelled sed. peak yield (g/s)	absolute error (g/s)	relative error (%)
uncalibrated						
11.07.2007	60.3	205	444	1020	576	129.7
29.08.2007	30.9	47	27	57	30	111.1
03.09.2007	11.1	39	14	13	-1	-7.1
calibrated						
11.07.2007	60.3	205	444	493	49	11.0
29.08.2007	30.9	47	27	37	10	37.0
03.09.2007	11.1	39	14	9	-5	-35.7

PI_{max} = maximum rainfall intensity
Q_{max} = maximum runoff

Table 11.2.2.: Uncalibrated and calibrated sediment amounts.

event date	measured sed. amount (kg)	modelled sed. amount (kg)	absolute error (kg)	relative error (%)
uncalibrated				
11.07.2007	493	2291	1798	364.7
29.08.2007	77	170	93	120.8
03.09.2007	53	46	-7	-13.2
calibrated				
11.07.2007	493	1092	599	121.5
29.08.2007	77	121	44	57.1
03.09.2007	53	33	-20	-37.7

at the same time.
Table 11.2.2 shows the amounts of sediment before and after parameter adjustment. The calibration had the same effect on the amounts of sediment as on the peaks of sediment yield. The two larger events got better, while the small got worse.

11.3. Conclusion

The parameters used for runoff generation were improved by reasons, that means the infiltration capacities derived by double ring infiltrometers were lowered by factors found in literature. With this improvement the hydrological model worked better in the Loechernbach catchment.

The output of the baseflow module could be improved by changing the zone, that contributes to baseflow. If not only the drained zones, but the whole catchment was taken, the baseflow fitted the measures values better. This was proved by sight and by Nash-Sutcliffe efficiencies. Anyway it has to be mentioned that the dynamic of the module seemed to fit better with the less zone as input area.

The sediment module parameters were first fitted to the peak sediment yields. It was reached that the results were in an arguable range for all events tested after parameter adjustment. The same was found for the amounts, but with larger errors. This may be due to the technique used for calculating the amounts, as not the whole events could be used but the timespan when samples were taken.
When the model should be used for a continuously simulation of the erosion, a timeseries of the C-factor, that represents the vegetation period, should be included in the model. This makes sure, that the actual management or crop rotation is considered when erosion values are calculated.
The underestimation for low events as well as the overestimation for the large events may origin in the power relationship ($y = a \cdot x^b$) used for the calculation of sediment yield from rainfall intensity. If a relationship with a larger multiplication factor a and a less exponent b would be used, better results could be received.
To test, if the model works well with this parameter setup in fact, a model validation has to be done.

12. Model validation

It is the aim of this work to model small and medium range events with the hydrological and the sediment model. Hence, events of this range were taken to show the ability of the model to calculate a timeseries not used until now properly, called the model validation. This method ensures the independence of the model results to the calibration. In this study the period from the 16.07.07 to the 15.09.07 was taken for the validation of the model.

12.1. Hydrological model

For the validation of the hydrological model, long term validation runs for the validation period as well as for the whole period were done in addition to single event validation runs. The techniques used for the validation were testing the agreement of the model results with the measured values by sight and by Nash-Sutcliffe efficiencies.

12.1.1. Baseflow

To validate the baseflow, long term runs for the validation period as well as for the whole period were done. As baseflow generating area, the whole basin was taken as it fitted the calibration period better. The long term hydrograph for the validation period is shown in figure 12.1.1. To evaluate the baseflow at the whole measurement period, a long term modelling was done for this purpose, too. The result is shown in figure A.2.5. In the validation period as well as the whole period the modelled baseflow hydrograph seemed to fit the measured all in all well. The dynamic was again not modelled well in both periods. The calculated efficiencies were $R_{eff} = 0.52$ for the validation period and $R_{eff} = 0.12$ for the whole period (compare table 12.1.1). The values are better than the values derived in the calibration period, but this could be an effect of the number of events. As there were not so many events, it happened not so often that the rise in baseflow after events was not predicted well. Therefore the sum of the differences between measured and predicted values was not

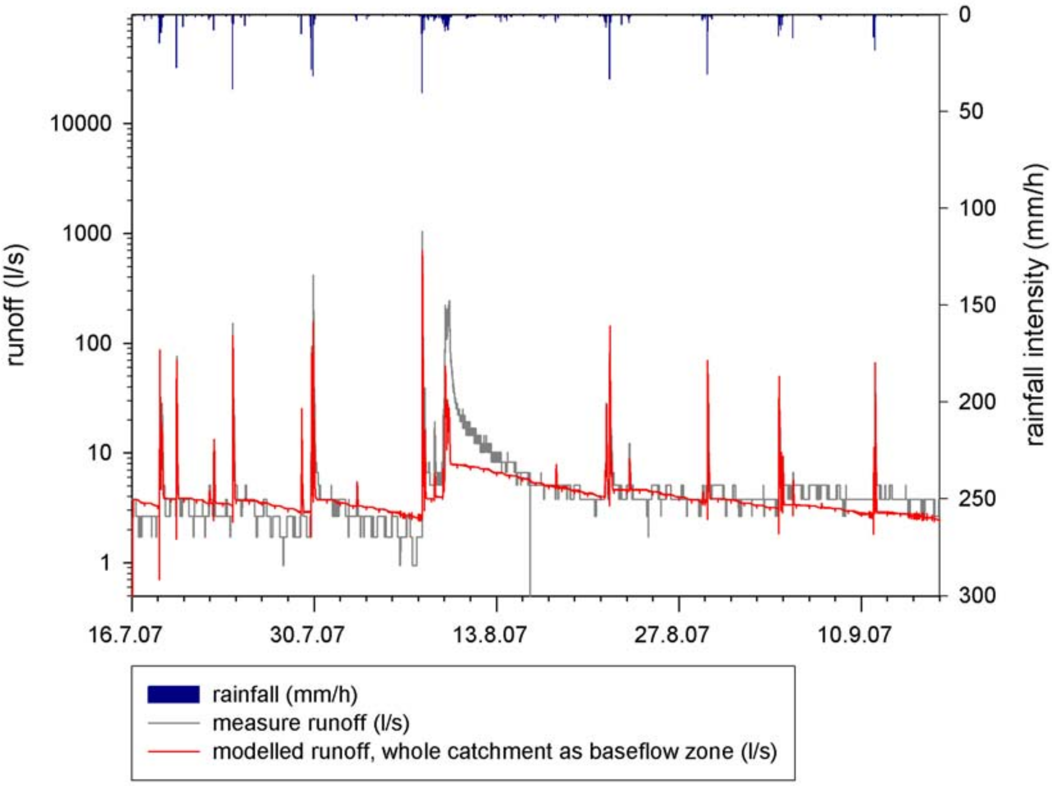

Figure 12.1.1.: Longterm validation period run plotted with respect to baseflow.

so large. The result is a better Nash-Sutcliffe efficiency (compare equation 11.1.1).

12.1.2. Event flow

Three days were modelled for validating single event flow as shown in the upper table 12.1.1. Figure 12.1.2 shows the contributing event hydrograph at the 18.07.07. The modelled hydrograph fitted the measured hydrograph very well. The corresponding Nash-Sutcliff efficiency for this event was found 0.92. However, the third peak in figure 12.1.2, that followed close to the second, was underestimated again as a second peak in short sequence.

The other two events brought similar results with a good fitting hydrograph (figures A.2.3 and A.2.4) and a large efficiency (table 12.1.1). The single event modelling was therefore found validated.

Long term efficiencies for event flow up to 200 $\frac{l}{s}$ in the validation as well as the whole observed period were calculated, too. The values found were not as well as for the single event modelling, within the validation period even worse than for base-

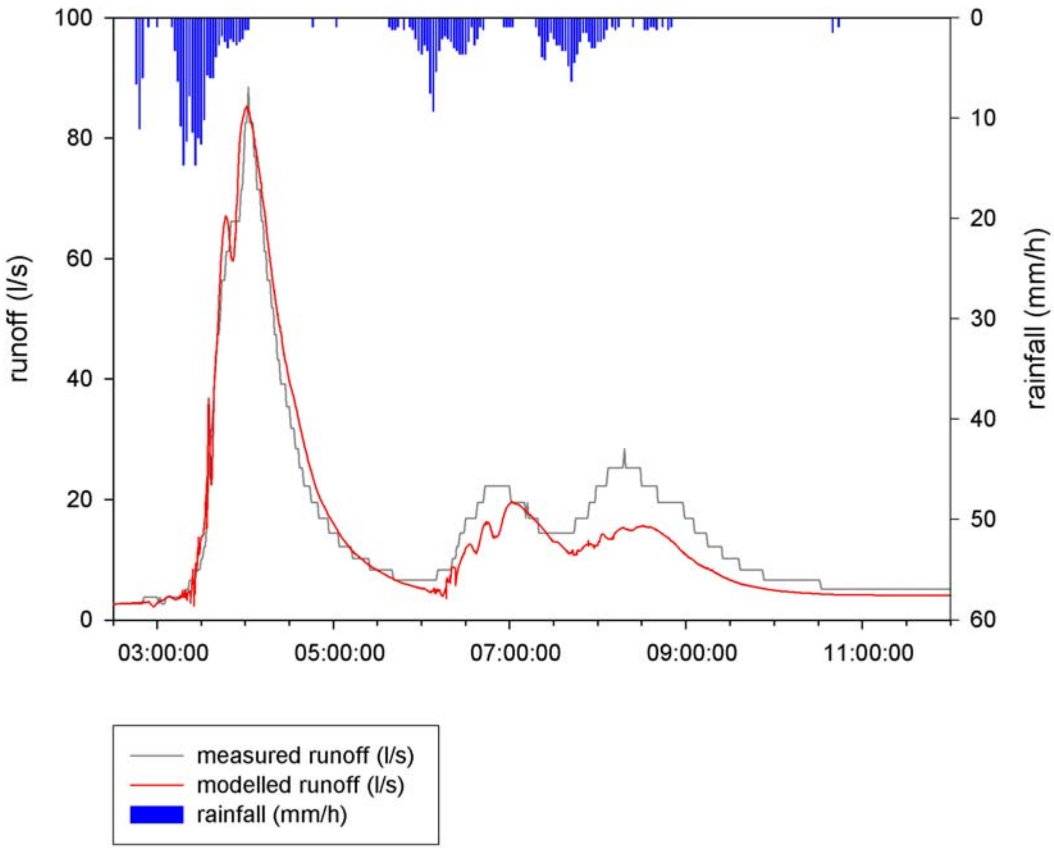

Figure 12.1.2.: Validation model run for the event on the 18.07.07.

Table 12.1.1.: Nash-Sutcliffe efficiencies of the validation and the whole period for baseflow (up to 20 $\frac{l}{s}$) and the whole range (up to 200 $\frac{l}{s}$).

start	end	note	runoff range ($\frac{l}{s}$)	R_{eff}
18.07.2007 03:00	18.07.2007 01:00	three events	up to 200	0.92
23.07.2007 17:00	23.07.2007 23:30	single event	up to 200	0.91
21.08.2007 06:00	21.08.2007 23:00	two events	up to 200	0.84
16.07.2007 00:00	15.09.2007 23:59	validation period	up to 200	0.35
16.07.2007 00:00	15.09.2007 23:59	validation period	up to 20	0.52
26.05.2007 00:00	15.09.2007 23:59	whole period	up to 200	0.42
26.05.2007 00:00	15.09.2007 23:59	whole period	up to 20	0.12

flow. But for the whole period, the longterm event flow brought better results than just the baseflow.

12.2. Sediment model

To validate the sediment model, test runs were conducted and compared to measurements of suspended sediment yield measured by Nippgen (2007). The evaluation was not done with the Nash-Sutcliffe efficiency as measuring and modelling erosion and sediment transport is much more difficult than doing the same with water. It would be a success if the results are in the right dimensions.
Two events sampled at the 18.07.07 and the 23.07.07 were taken to compare the model results with directly measured events at the outlet of the catchment. The results shown in figure 12.2.1 and A.1.5 were both not as good as the calibration. The model underestimated the peak sediment yields about three times for both events. The peaks arrived at the right time and small peaks before the main peak were shown in the model as well. So the dynamic was scored well, just the amount failed. The sediment model could therefore not be found validated by the event water samples offhand, and the results had to be discussed.

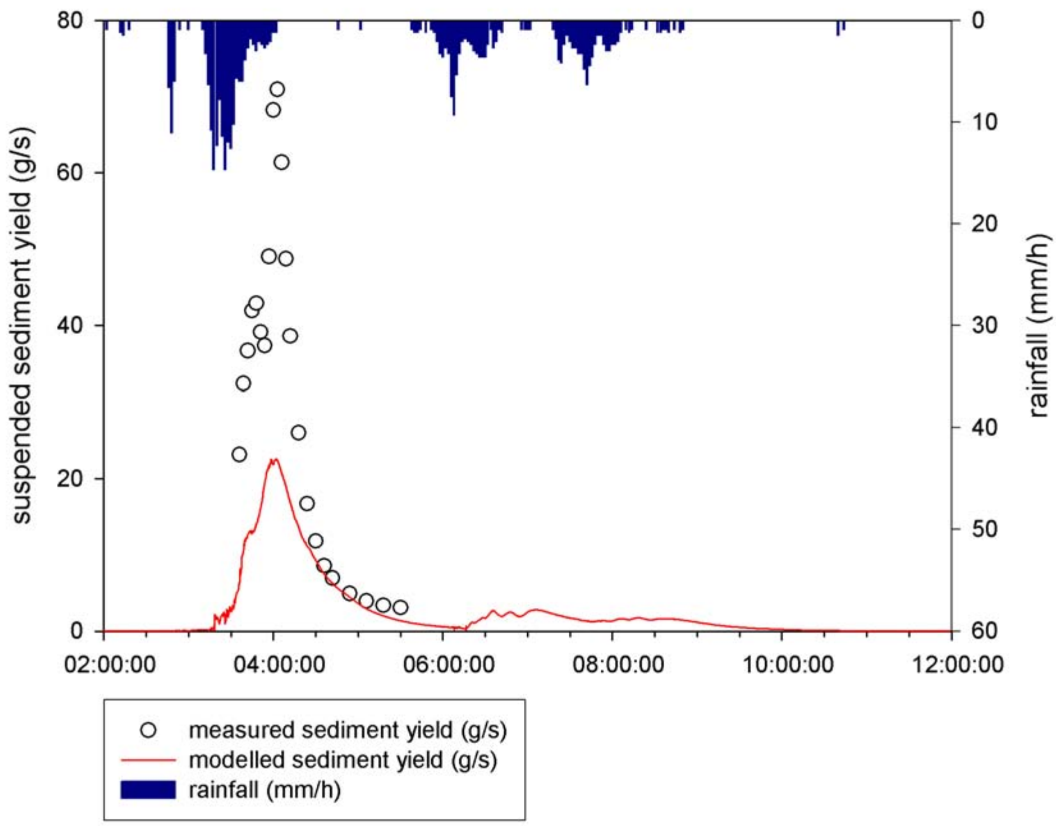

Figure 12.2.1.: Validation model run for the event on the 18.07.07.

12.3. Cross validation: model vs. turbidity

The two objectives of the thesis were the measuring of suspended sediment concentrations by means of turbidity measurements and modelling of erosion and suspended sediment transport. Each aim proved more or less well, at which the modelling was more in question than the measurement results. In this section an overall validation of the aims of the thesis was done by comparing the model results with the sediment concentrations derived by the turbidity measurements. For this purpose the sediment yield output of the model was transformed to sediment concentrations by the modelled runoff at both the spring and the outlet of the catchment. This method constituted a check of the hydrological and the sediment part of the model both and in union.

The validation was neither checked with Nash-Sutcliffe efficiencies nor with accurate peak concentrations. Again, it was rated as a success if the two curves showed to be similar by sight.

Three events were taken to do this check: The first event at the 21.08. (figures 12.3.1

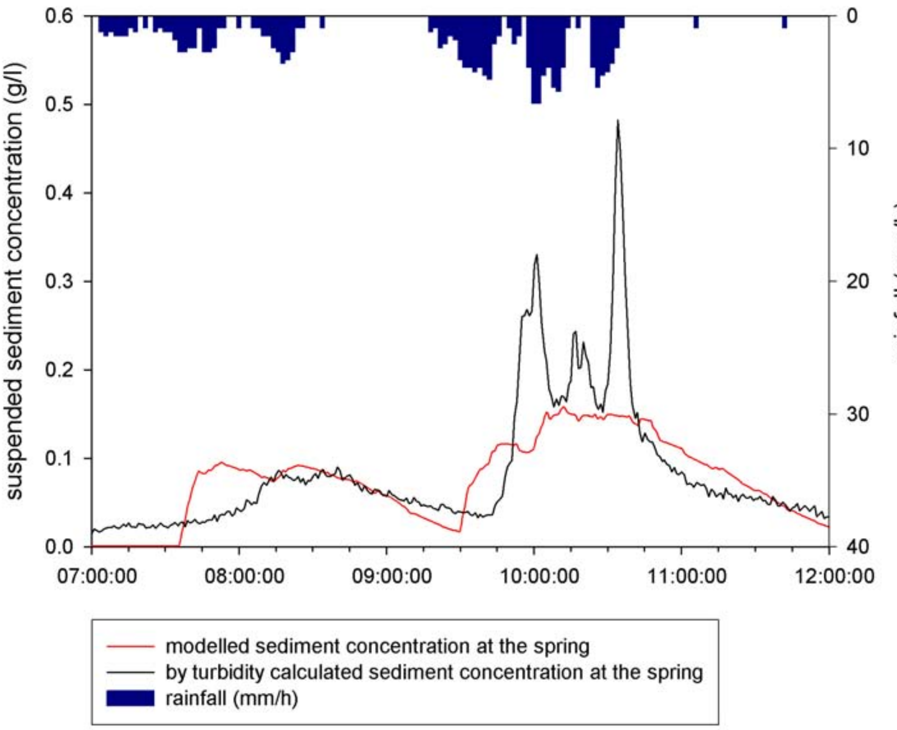

Figure 12.3.1.: Double validation: modelled sediment concentration compared to concentration derived by turbidity at the 21.08.07 at the spring of the Loechernbach catchment.

and 12.3.2) and the events at the 29.08.07 (figures A.1.7 and A.1.8) and 11.09.07

(figure A.1.6). For the event at the 11.07.07 unfortunately just data for the spring were available, the other ones had both, spring and outlet data. The data from the outlet of the event at the 29.08.07 were already used for the model calibration, so this was a check first, if the model simulates the water and the sediment well both and second, if the concentration was well calculated at the spring, when the outlet data were simulated well.

The first look at the 29.08.07 (figure A.1.7) showed a good agreement of the two

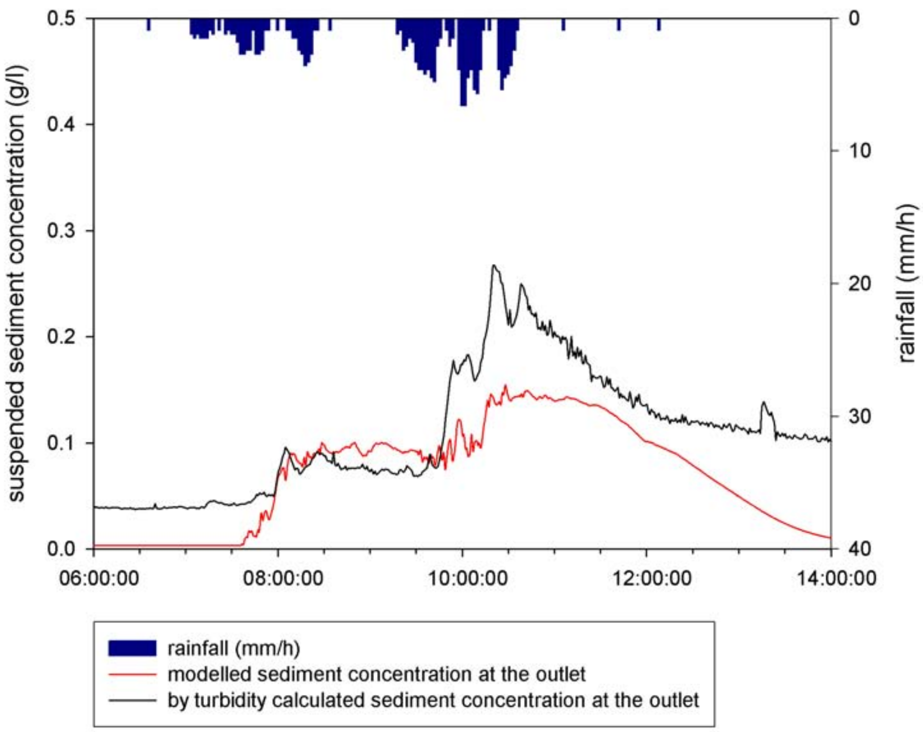

Figure 12.3.2.: Double validation: modelled sediment concentration compared to concentration derived by turbidity at the 21.08.07 at the outlet of the Loechernbach catchment.

curves at the outlet. Even the declining limb had a nice consistence. The result of a maximum rainfall intensity of about 30 $\frac{mm}{h}$ was a modelled peak of about 1 $\frac{g}{l}$ whereas the measured peak was later and had a maximum value of about 0.8 $\frac{g}{l}$. As the data were used for the calibration of the model, the modelling should work well and the concentrations derived by turbidity were in the same dimensions and emphasised this statement.

Going up the stream to the spring showed again a good fit. The modelled peak values were somewhat less than the measured and the peak was much wider.

The spring-curves for the 11.07.07 (figure A.1.6) demonstrated also a result with the same dimensions of the two ways to derive the sediment concentrations. The peak

concentrations to a maximum rainfall intensity of about 18 $\frac{mm}{h}$ were modelled with 0.3 $\frac{g}{l}$ and measured by turbidity with 0.4 $\frac{g}{l}$. Again, the modelled peak is not as narrow as the turbidity peak.
The event at the 21.08.07 was the smallest in rainfall intensity, with a maximum of about 8 $\frac{mm}{h}$. The overall result of the model was - again - well for both the spring and the outlet. The measurements at the spring showed some small peaks, that were not met by the model, but apart from the peaks the model worked well. At the outlet, the first rise due to the first rainfall was modelled very well, but the second rise was underestimated by about 0.1 $\frac{g}{l}$. This seems not much, but relative to the measured peak, the modelled was just a fraction of 0.6.

12.4. Discussion

The hydrological model was validated on a single event based approach with very nice results. The coefficients of determination were close to one. But one problem stayed nevertheless: If there is more than one peak in a short sequence, the second peak is underestimated. This is clearly a result of a runoff generation process, that is not integrated in the model.

The groundwater recharge born baseflow module is able to simulate baseflow on longterm periods, but not able to simulate the short term dynamic of baseflow. That means the rise of baseflow as answer to a rainfall event is not as large as it was measured. This may be due to a wrong parametrisation (the k_f-values for zones 6 and 7 seemed very low) or a conceptual error.
According to the tests of this thesis, the baseflow module may be useful either to simulate baseflow on long terms, that means for water resources modelling, or as an aid until a real baseflow module with an own storage is built.

The sediment concentration curves derived by turbidity measurements and the relationship 7.3.1 were compared to the modelled concentrations, that were computed by dividing the modelled sediment yield ($\frac{g}{s}$) with the modelled runoff $\frac{l}{s}$. The results fitted well, that means, were in the right dimensions, while the peaks did not differ more than 0.2 $\frac{g}{l}$. Just the event at the 21.08.07 at the spring of the Loechernbach catchment showed larger differences between the measured and the modelled curve. There the narrow peaks of the measurements could not be met by the model.
All in all the model is able to simulate erosion and sediment transport, compared to the measurements of the suspended sediment concentrations by turbidity measurements.

13. Conclusion and outlook

The aims of the thesis were defined as the measuring of turbidity and deriving the suspended sediment concentration from it and the modelling of erosion and suspended sediment yield. The final discussion will show the strength and the limitations of this approach.

The measured sediment concentration values did not match the measured turbidity values in a unique relationship, as it is usual in natural systems. But the regression relationship brought satisfactory results. The regression calculation of the values derived by laboratory measurements showed a nice fit and had a similar equation to the ones found in Holliday et al. (2003). However, a comparison of the two equations calculated in this work showed a better usability of the field relationship.
All in all the approach to use turbidity as a measuring device for suspended sediment succeeded for the Loechernbach catchment. The setup of the measuring device used in this work should be tested in other catchments to ensure the usability there, too. It may be, that there are more problems in catchments with a larger sand fraction in runoff, that may either clog the device or simply flow around it, as it does not fit the perforation of the water inlet.

As there was no fitting model found in literature, the rainfall runoff model ZIN (Lange et al., 1999), originally derived for arid catchments, was extended by a groundwater recharge based baseflow module and an erosion/sediment transport module as a first step on the way to model pesticide movement.

The concept of the baseflow module was chosen very simple. Just the outflow of the soil storage of prior determined areas contributing to baseflow was caught and added to the overland flow. So there are known conceptual errors in the module: the concentration time of groundwater born runoff is surely not the same as for overland flow and the subsurface subbasins are surely not the same as the surface subbasins. Despite this two known errors, the module was used as a simple approach to simulate baseflow as there was no possibility to compute baseflow in the model

before.
The application of the module in the Loechernbach area with the drainages as baseflow generating zones brought bad results. The storage was not filled enough by infiltration and therefore drained to zero on a long term run. Changing the baseflow generation zones to the whole catchment improved the modelling as the storage was not drained empty. But the dynamic was not suited well. After an event, the storage was again not filled as much as measured and the dynamic of the decline was not fitted. Partly this may have depended on wrong parameters (the k_f value for some zones seemed very low), but it rather seemed to be a conceptual problem.
So the baseflow module should only be used for water resources modelling as the concept that baseflow equals groundwater recharge was already proved for long time intervals larger than one year (KILLE, 1970). On event based model runs it may be an aid to take baseflow into account, but substitutes no real baseflow module with an own groundwater storage.
If the model ZIN is planned to be used in humid catchments frequently in future, a better groundwater storage based baseflow module should be included for a proper simulation of baseflow.

The event water simulation of events up to 200 $\frac{l}{s}$ was a full success after an improvement of the infiltration rates. The former measured double ring infiltrometer values were lowered as double ring infiltrometers are known to overestimate infiltration much. A factor 0.5 fitted the values found in literature and was applied to the infiltration rates.
One problem remained also after the parameter improvement: events in short sequence can produce larger peak runoff values to lower peak rainfall intensities. This may be due to runoff generation processes not considered in the model. UHLENBROOK (1995) estimated piston flow as runoff generation process in the Loechernbach catchment. This assumption is in good correlation with the observations of this study. If the soils are nearly saturated after an event and the next events starts close to the first, the nearly saturated zones may get saturated immediately and produce piston flow with a release of 'pre-event water'.
Before applying the model in humid regions in future, the runoff generation processes that take place in the catchment should be considered as ZIN is just able to model infiltration excess and saturation excess overland flow.

The amount of kinetic energy of a rainstorm specifies its ability to erosion. The new integrated erosion and sediment transport module was based upon the concept that a rise in kinetic energy can be expressed just by the rainfall intensity. So a

simple equation between rainfall intensity and erosion ($\frac{g}{m^2 s}$) had to be determined to make the model run. This relationship was derived from literature for a loess soil as found in the Loechernbach catchment. But the literature values were measured just for a bare surface and a method had to be found to correct the equation for vegetated surfaces. This method was found with the vegetation and crop rotation factor C of the USLE (Universal Soil Loss Equation). For the modelled period the crop rotation factor had to be removed as it was just in the vegetation period.
With this setup, the module brought satisfying results for the calibration events. However, the validation events were both underestimated three times. So the dimension is also right, but the values proved not as good as the calibration events. It has to be noticed, that they both were not measured by the author, but by a former thesis (Nippgen, 2007) and they both were measured at the end of july in close sequence. So differences in the measurement technique may be one possible explanation. The other one may be intensive farming with machines and therefore more soil may have been brought to the streets by the tyres. This anthropogenic process is very difficult, if not to say impossible, to be expressed by a hydrological/-geomorphological model.
A third this to be taken into account is the concept of the model. Just sheet erosion was attended in the module concept. It may be that rill erosion plays also a role under certain circumstances. This may be the best fitting explanation as large amounts of sediment were measured as answer to a relatively low rainfall intensities for the validation events.

A cross validation was done by comparing the results of the turbidity measurements with the modelled suspended sediment concentrations by sight. This validation could be rated, in contrast to the validation of the model with directly measured events, as a success. The difference was, that not the sediment yields were compared but the sediment concentrations. So the modelled erosion/sediment transport and the modelled water were used to derive the concentrations and therefore checked both. As the hydrological model showed a good validation at the outlet, the cross validation confirmed the quality of the sediment model there. At the spring no runoff was measured and so it is possible that both, sediment and water were not modelled well, but the ratio is right anyway.
As there was an error in transforming the turbidity measurements to suspended sediment concentrations and an error in modelling accepted, it is also possible that the cross validation just seems to be well. If both ways to derive the sediment concentrations produce errors in the same directions, the cross validation provides good results, but for the wrong reasons.

However, it is not likely that both ways produce the same errors and so the cross validation was rated as success anyway.

The results of this thesis make it now possible to model on the one hand water input to the artificial wetland in the detention pond near Eichstetten and so to calculate input data for the hydraulic model of the wetland. On the other hand it is possible to model erosion and sediment transport in the Loechernbach catchment as a first step to model pesticide movement from the application at the field to the artificial wetland at the outlet. Further studies may integrate two main things for the behavior of pesticides: the sorption to soil particles by means of a sorption isotherm and the decay of pesticides by kinetic reaction equations.

Bibliography

Adriaanse P., Allen R., Gouy V., Hollis J., Hosang J., Jarvis N., T.Jarvis, Klein M., Layton R., J.Linders, Schäfer H., Smeets L., Yon D. (1997). Surface Water Models and EU Registration of Plant Protection Products, http://viso.jrc.it/focus/.

Ankcorn P.D. (2003). Clarifying turbidity - The potenital and limitations of turbidity as a surrogate for water-quality monitoring, Proceedings of the 2003 Georgia Water Rescources Conference.

Armbruster V. (2002). Grundwasserneubildung in Baden-Württemberg, Freiburger schriften zur hydrologie, band 17, Albert-Ludwigs-Universität Freiburg i. Br., Institut für Hydrologie.

Asselman N. (2000). Fitting and interpretation of sediment rating curves., Journal of Hydrology, vol. 234, pp. 228–248.

Auerswald K. (1998). Bodenerosion - Analyse und Bilanz eines Umweltproblems, chap. 2, Wissenschaftliche Buchgesellschaft, ISBN 3-534-12574-6.

Bicknell B.R., Imhoff J.C., Kittle(Jr.) J.L., Jobes T.H., Donigian(Jr.) A.S. (2001). HYDROLOGICAL SIMULATION PROGRAM - FORTRAN, HSPF Version 12, User's Manual, EPA (Environmental Protection Agency) - March 2001.

Bird R.E., Hulstrom R.L. (1991). A Simplified Clear Sky model for Direct and Diffuse Insolation on Horizontal Surfaces, Tech. rep., Solar Energy Research Institute, Golden, CO, sERI Technical Report SERI/TR- 642-761, Feb 1991.

Borah D., Bera M. (2003). Watershed-Scale Hydrologic and Nonpoint-Source Pollution Models: Review of Mathematical Bases, Transactions of the ASAE, vol. 46(6), pp. 1553–1566.

Borah D., Bera M. (2004). Watershed-Scale Hydrologic and Nonpoint-Source Pollution Models: Review of Applications, Transactions of the ASAE, vol. 47(3), pp. 789–803.

Borah D.K., Bera M., Shaw S., Keefer L. (1999). Dynamic Modeling and Monitoring of Water, Sediment, Nutrients, and Pesticides in Agricultural Watersheds during Storm Events, Illinois State Water Survey, Watershed Science Section, Contract Report 655.

Brandt C. (1989). The size distribution of throughfall drops under vegetation canopies., Catena, vol. 16, pp. 507–524.

Bucher B., Demuth S. (1985). Vergleichende Wasserbilanz eines flurbereinigten und eines nicht flurbereinigten Einzugsgebietes im Ostkaiserstuhl für den Zeitraum 1977 - 1980, Deutsche Gewässerkundliche Mitteilungen, vol. 29(1), pp. 1–4.

Chadwick A., Morfett J. (eds.) (1998). HYDRAULICS IN CIVIL AND ENVIRONMENTAL ENGINEERING, chap. 4, E & FN Spon, ISBN 0-419-22580-3.

Demuth S., Westphal H.H. (1981). *Beitrag zum Vergleich der Schwebstoffführung zweier Bäche während unterschiedlich großer Niederschlagsereignisse in zwei verschiedenen Löss-Einzugsgebieten am Ostkaiserstuhl*, Diplomarbeit, Albert-Ludwigs-Universität Freiburg i. Br., Lehrstuhl für Geographie und Hydrologie.

Eggelsmann R. (ed.) (1981). Dränanleitung, Paul Parey, ISBN 3-490-15216-6.

Fischer C. (2007). *Hydrological Modeling of the Water Resources in the Nahal Harod, Israel.* , Diplomarbeit, Albert-Ludwigs-Universität Freiburg i. Br., Institut für Hydrologie.

Fread D. (1993). Handbook of Hydrology, chap. 10, McGraw Hill, ISBN 0-07-039732-5.

Gündra H., Jäger S., Schroeder M., Dikau R. (1995). Bodenerosionsatlas Baden-Württemberg, Ulmer, ISBN 3-8001-8684-5.

Gunkel A. (2006). *Kopplung der Modelle ZIN und TRAIN (Arbeitstitel)*, Dissertation, Albert-Ludwigs-Universität Freiburg i. Br., Institut für Hydrologie, unveröffentlicht.

Hagenlocher U. (2007). *Erweiterung des TRAIN-ZIN Modells und Anwendung im Dragonja Einzugsgebiet (Arbeitstitel)*, Diplomarbeit, Albert-Ludwigs-Universität Freiburg i. Br., Institut für Hydrologie, unveröffentlicht.

Hädrich F., Stahr K. (2001). Die Böden des Breisgaus und angrenzender Gebiete, Berichte der naturforschenden Gesellschaft zu Freiburg i. Br.

Holliday C.P., Rasmussen T.C., Miller W.P. (2003). Establishing the relationship between turbidity and total suspended sediment concentration., Proceedings of the 2003 Georgia Water Rescources Conference.

Hugenschidt C. (2006). *Kontinuierliche Tracer zur hydrologischen Prozessforschung in bewaldeten Einzugsgebieten.*, Diplomarbeit, Albert-Ludwigs-Universität Freiburg i. Br., Institut für Hydrologie.

Khanchoul K., Jansson M.B., Lange J. (2007). Comparison of suspended sediment yield in two catchments, northeast Algeria, Zeitschrift für Geomorphologie, vol. 51, pp. 63–94(32).

Kille K. (1970). Das Verfahren MoMNQ, ein Beitrag zur Berechung der mittleren langjährigen Grundwasserneubildung mit Hilfe der monatlichen Niedrigwasserabflüsse., Zeitschrift der deuschen Geologischen Gesellschaft, Sonderhaft Hydrogeologie/Hydrogeochemie, pp. 89–95.

Klämt A. (2004). Langzeitverhalten der Lufttemperatur in Baden-Württemberg und Bayern, Arbeitskreis KLIWA, ISBN 3-937911-17-0.

Kraemer A. (1999). *Anwendung des Wasserhaushalts- und Gewässergütemodells NSPM auf hydrologische Versuchsgebiete im Kaiserstuhl.*, Diplomarbeit, Albert-Ludwigs-Universität Freiburg i. Br., Institut für Hydrologie.

Landesanstalt für Umwelt M.u.N.B.W. (2004). Hydrologie und Wasserwirtschaft, LUBW, 2th edn., ISBN 3882512768.

Lange J., Leibundgut C., Greenbaum N., Schick A. (1999). A noncalibrated rainfall-runoff model for large, arid catchments., Water Resources Research, vol. 35, pp. 2161–2172.

Leistert H. (2005). *Modelling transmission losses; Applications in the Wadi Kuiseb and the Nahal Zin* , Diplomarbeit, Albert-Ludwigs-Universität Freiburg i. Br., Institut für Hydrologie.

Liebscher H. (1979). Verdunstung - Hydrologischer Atlas von Deutschland, Boppard.

Luft G. (1980a). Abfluss und Retention im Loess, Beiträge zur Hydrologie, Sonderheft 1.

Luft G. (1980b). Kennzeichnung der Fließrichtung und der hydraulischen Leitfähigkeit in schluffigen Aquiferen mittels Uranin-Markierungsversuchen - Teil II, Deutsche Gewässerkundliche Mitteilungen, vol. 24(2), pp. 124–132.

Maniak U. (2005). Hydrologie und Wasserwirtschaft, Springer, Berlin, Heidelberg, 5th edn., ISBN 3-540-20091-6.

McCutcheon S.C., Martin J.L., Thomas O. Barnwell J. (1993). Handbook of Hydrology, chap. 11, McGraw Hill, ISBN 0-07-039732-5.

Merzougui M., Gifford G.F. (1987). Spatial variability of infiltration rates on a semi-arid seeded rangeland., Hydrological Sciences Journal, vol. 32,2,6, pp. 243–250.

Nash J., Sutcliffe J. (1970). River flow forecasting through conceptual models part I - a discussion of principles., Journal of Hydrology, vol. 10, pp. 282–290.

Neitsch S., Arnold J., Kiniry J., Williams J. (2005). SWAT2005 Theoretical Documentation, Tech. rep., Grassland Soil & Water Research Laboratory USDA-ARS and BLACKLAND RESEARCH CENTER, http://www.brc.tamus.edu/swat/doc.html.

Nippgen F. (2007). *Abflussbildung im Löchernbach*, Diplomarbeit, Albert-Ludwigs-Universität Freiburg i. Br., Institut für Hydrologie.

Pilgram D.H., Cordery I. (1993). Handbook of Hydrology, chap. 9, McGraw Hill, ISBN 0-07-039732-5.

Raws W.J., Ahuja L.R., Brakensiek D.L., Shirmohammadi A. (1993). Handbook of Hydrology, chap. 5, McGraw Hill, ISBN 0-07-039732-5.

Römkens M., Helming K., Prasad S. (2001). Soil erosion under different rainfall intensities, surface roughness, and soil water regimes, Catena, vol. 46, pp. 103–123.

Salles C., Poesen J., Sempere-Torres D. (2002). Kinetic energy of rain and its functional relationship with intensity., Journal of Hydrology, vol. 257, pp. 256–270.

Saxton K.E., Rawls W. (2006). Soil Water Characteristic Estimates by Texture and Organic Matter for Hydrologic Solutions., Soil Sci Soc Am J, vol. 70, pp. 1569–1578.

Schmidt K.H., Morche D. (2006). Sediment yield estimation in small watersheds based on streamflow and suspended sediment discharge measurements., Geomorphology, vol. 80, pp. 131–145.

Schnegg P.A., Flynn R. (2002). Online field fluorometers for hydrogeological tracer tests., Wissenschaftliche Mitteilungen, Institut für Geologie, TU Bergakademie Freiberg.

Schütz T. (2006). *Prozessbasierte Niederschlag-Abflussmodellierung in einem mediterranen Kleineinzugsgebiet*, Diplomarbeit, Albert-Ludwigs-Universität Freiburg i. Br., Institut für Hydrologie.

Schulz R. (2007). Pesticide in Gewässern, Lecture at the hydrological colloquium of the Institute of Hydrology at the University of Freiburg i. Br.

Schumacher N. (1981). *Standortspezifischer Bodenwasserhaushalt im grossterrasiert umgestalteten Ostkaiserstuhl*, Diplomarbeit, Albert-Ludwigs-Universität Freiburg i. Br., Geographisches Institut I.

Shen H.W., Julien P.Y. (1993). Handbook of Hydrology, chap. 12, McGraw Hill, ISBN 0-07-039732-5.

Shoemaker L., Dai T., Koenig J., Hantush M. (2005). TMDL Model Evaluation and Research Needs, Publications of the National Risk Management Research Laboratory (EPA/600/R-05/149).

Shuttleworth W.J. (1993). Handbook of Hydrology, chap. 4, McGraw Hill, ISBN 0-07-039732-5.

Sidiras N., Roth C. (1989). Infiltration Measurements with Double-Ring Infiltrometers and a Rainfall Simulator under Different Surface Conditions on an Oxisol., Soil & Tillage Research, vol. 9, pp. 161–168.

Smith R., Parlange J. (1978). A parameter-efficient hydrologic infiltration model, Water Resources Research, vol. 14(3), pp. 533–538.

Szel S., Gaspar C. (2000). On the negative weighting factors in the Muskingum-Cunge scheme., Journal of hydraulic research, vol. 38(4), pp. 299–306.

Uhlenbrook S. (1995). *Untersuchung von schnellen Abflusskomponenten*, Diplomarbeit, Albert-Ludwigs-Universität Freiburg i. Br., Institut für physische Geographie.

URL1 (12.07.2007). http://viso.jrc.it/focus/.

Wagner A. (2002). *Anwendung eines nicht-kalibrierten Niederschlag-Abfluss-Modells in den hydrologischen Versuchsgebieten Ostkaiserstuhl*, Diplomarbeit, Albert-Ludwigs-Universität Freiburg i. Br., Institut für Hydrologie.

Wilmanns O., Wimmenauer W., Fuchs G. (1989). Der Kaiserstuhl - Gesteine und Pfanzenwelt, Ulmer, ISBN 3-8001-3310-5.

Wischmeier W.H., Smith D. (1978). Predicting rainfall erosion losses - A guide to conservation planning., USDA, Agric. Handbook No. 537.

Wong M., Parker G. (2006). Reanalysis and Correction of Bed-Load Relation of Meyer-Peter and Müller using Their Own Database., Journal of Hydraulic Engineering, vol. 132, pp. 1159–1168.

Xu J. (2002). Implication of relationships among suspended sediment size, water discharge and suspended sediment concentration: the Yellow River basin, China, Catena, vol. 49, pp. 289–307.

A. Appendix

A.1. Sedimentographs

A.1.1. Turbidity-concentration relationships

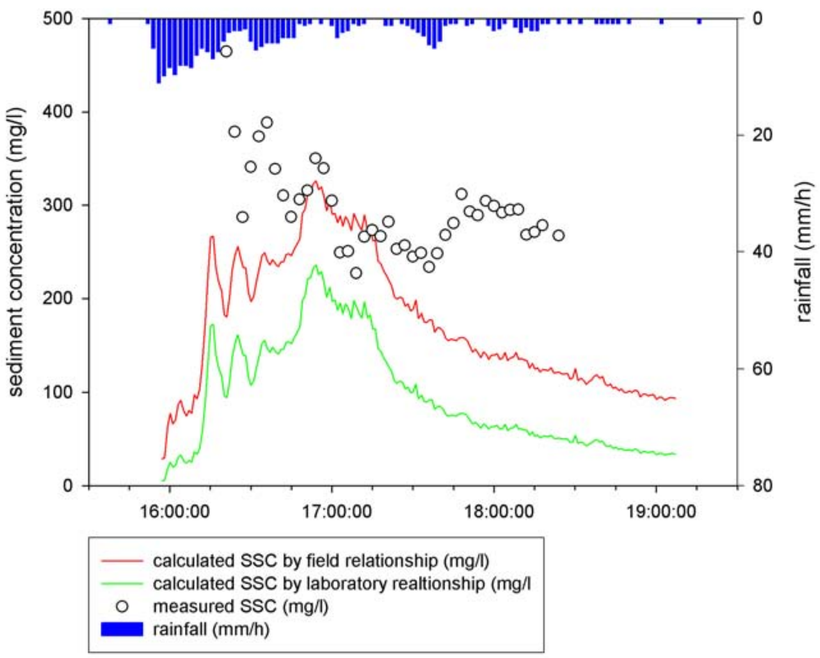

Figure A.1.1.: Comparison of the turbidity-SSC relationship derived in the field and the laboratory at the event at the 03.09.07.

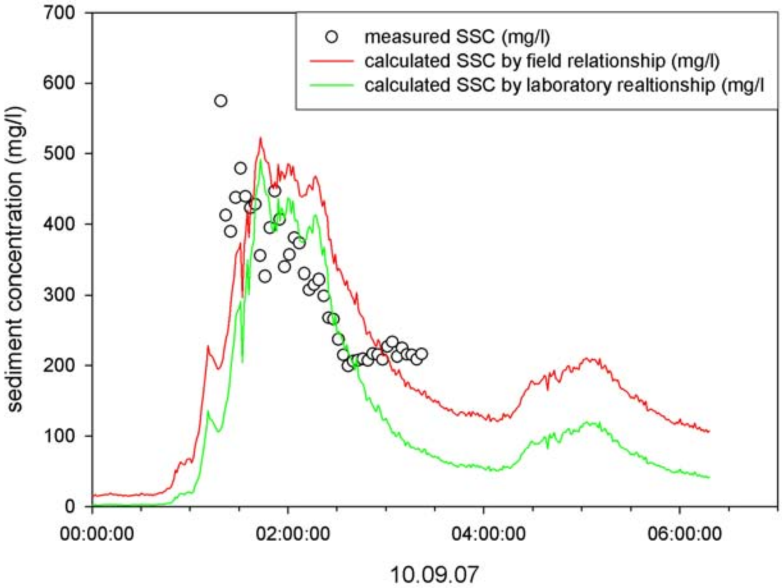

Figure A.1.2.: Comparison of the turbidity-SSC relationship derived in the field and the laboratory at the event at the 18.09.07. No rainfall data were available for this event.

A.1.2. Sediment module parameter improvement

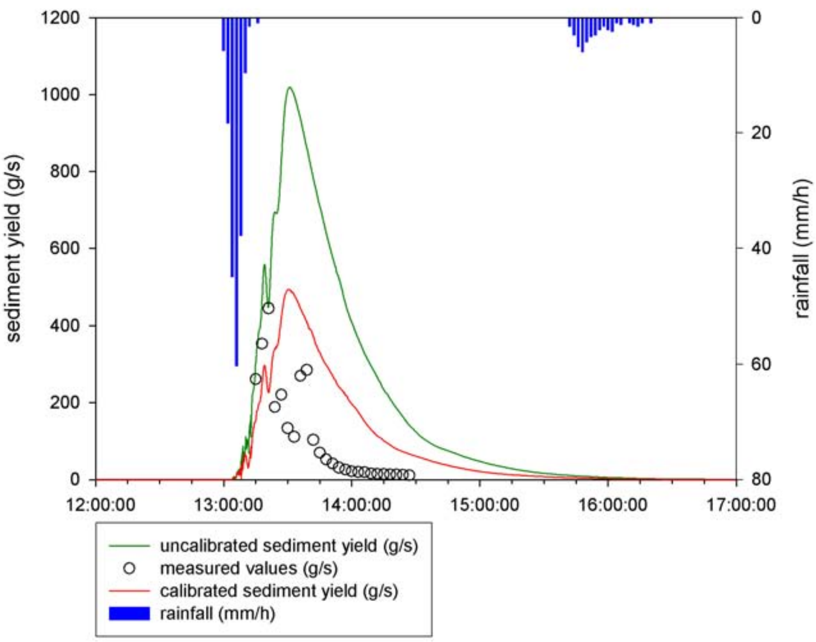

Figure A.1.3.: Sediment load curve before and after calibration procedure and measured sediment yield at the 11.07.07.

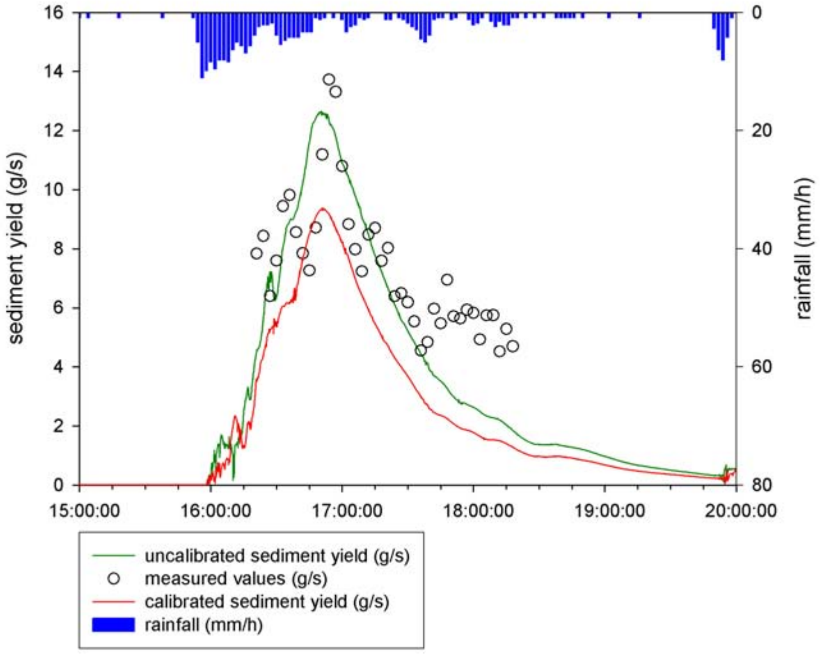

Figure A.1.4.: Sediment load curve before and after calibration procedure and measured sediment yield at the 03.09.07.

A.1.3. Sediment module validation

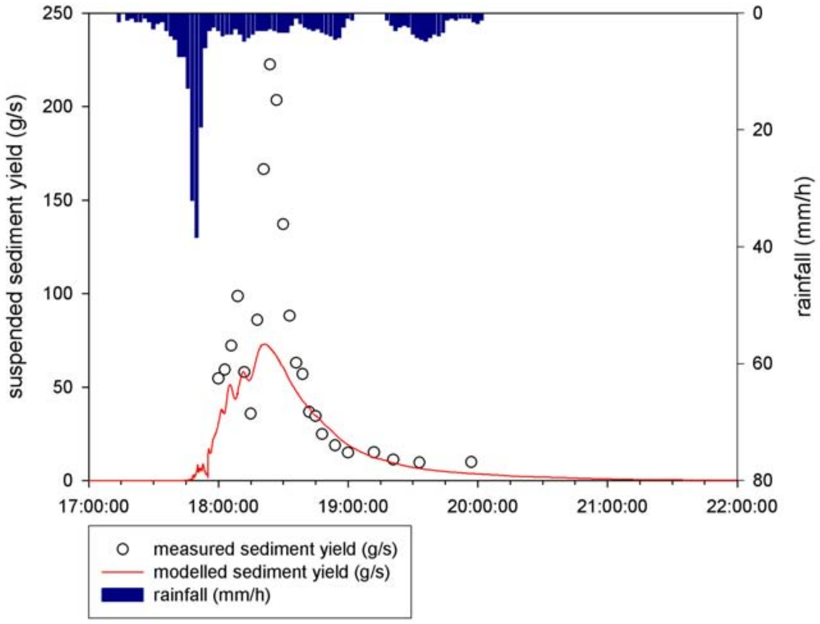

Figure A.1.5.: Validation model run for the event at the 23.07.07.

A.1.4. Overall validation

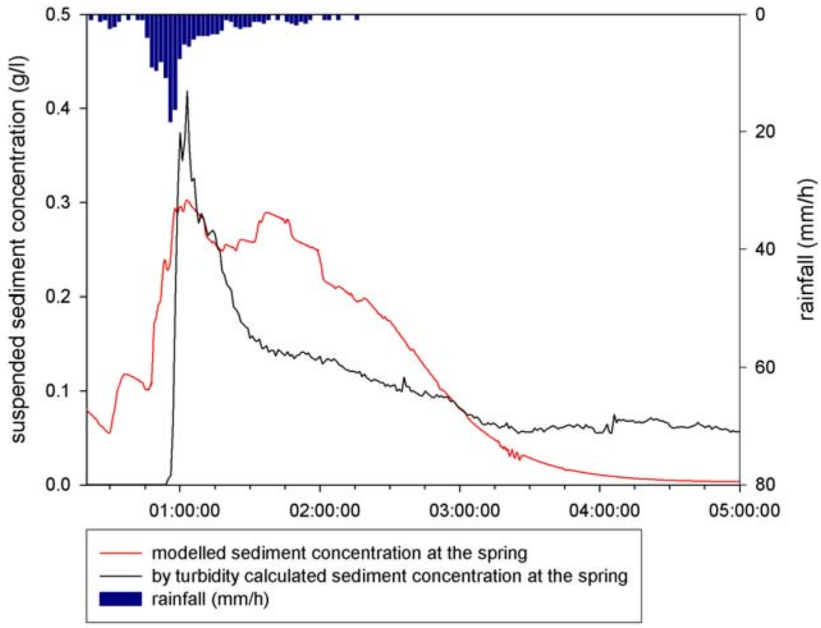

Figure A.1.6.: Double validation: modelled sediment concentration compared to concentration derived by turbidity at the 11.0.07 at the spring of the Loechernbach catchment.

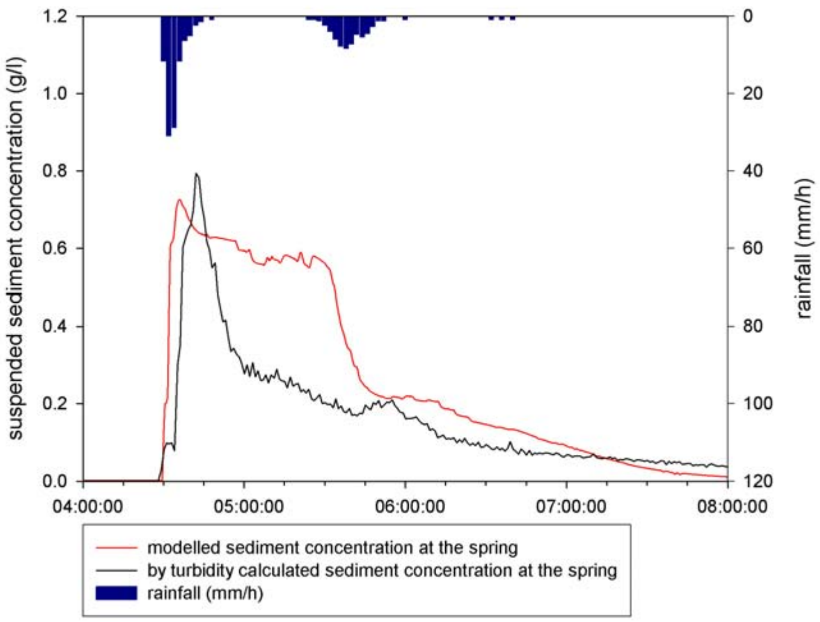

Figure A.1.7.: Double validation: modelled sediment concentration compared to concentration derived by turbidity at the 29.08.07 at the spring of the Loechernbach catchment.

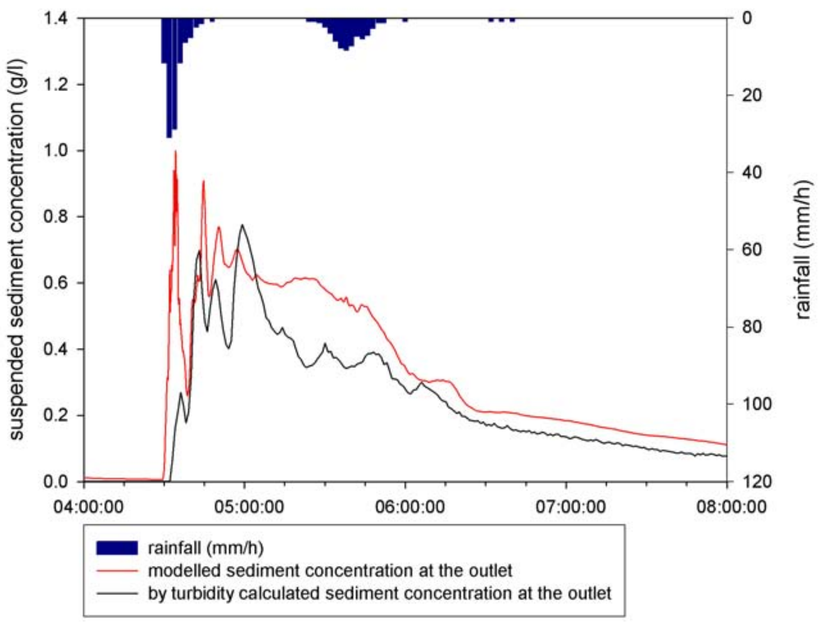

Figure A.1.8.: Double validation: modelled sediment concentration compared to concentration derived by turbidity at the 29.08.07 at the outlet of the Loechernbach catchment.

A.2. Hydrographs

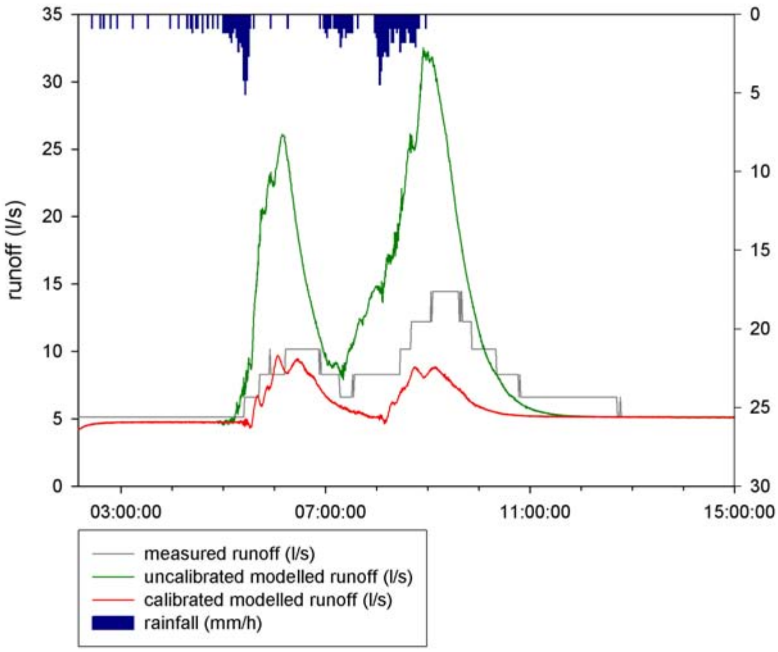

Figure A.2.1.: Events at the 29.05.07 before and after improvement of the infiltration rates.

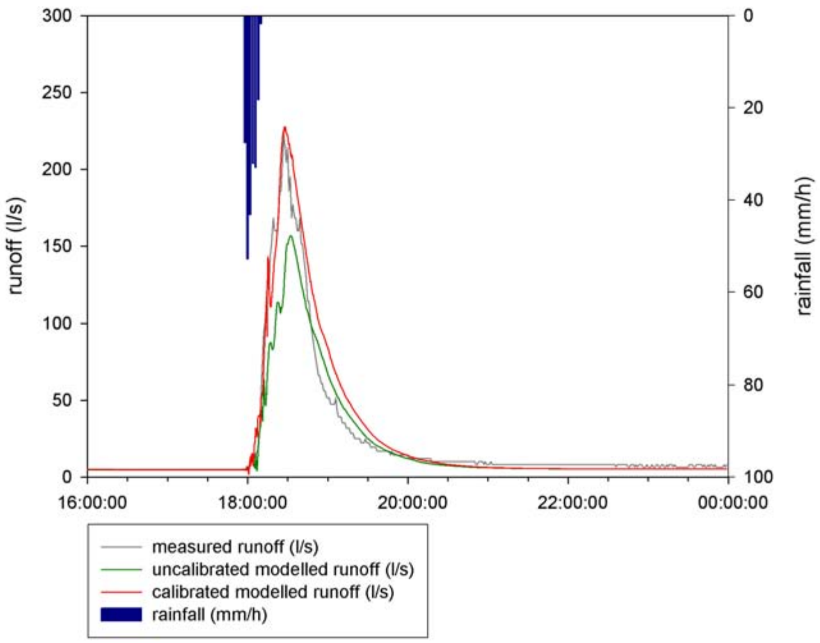

Figure A.2.2.: Events at the 02.07.07 before and after improvement of the infiltration rates.

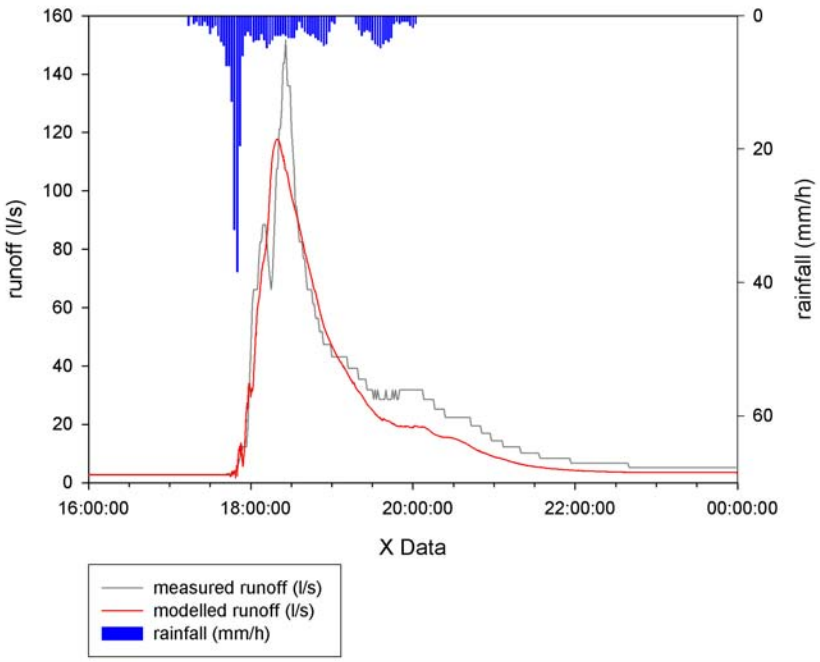

Figure A.2.3.: Validation model run for the event at the 23.07.07.

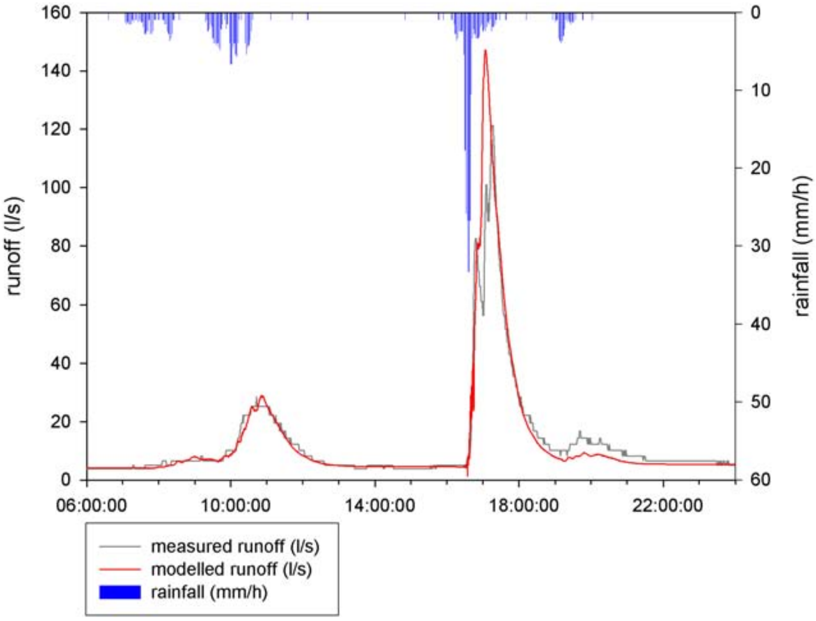

Figure A.2.4.: Validation model run for the event at the 21.08.07.

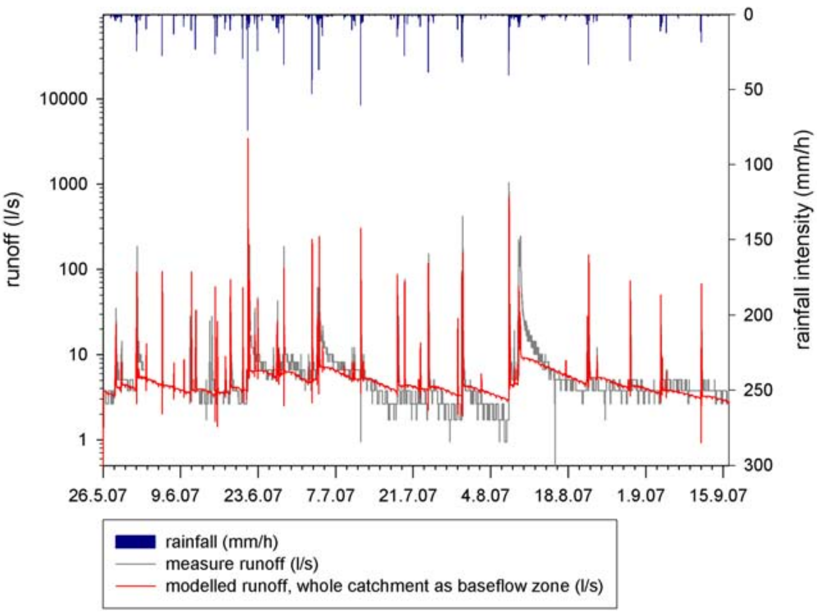

Figure A.2.5.: Longterm validation run for the whole period plotted with respect to baseflow.

A.3. Source code

The source code of the new developed modules is commented in this chapter.

A.3.1. Baseflow module

```
#include "stdafx.h"
#include "Baseflow.h"
#include <math.h>

Baseflow::Baseflow(SoilStorageVG * baseflowSoil, Runoff *
    baseflowRunoff, Controller * baseflowCont) //Constructor
{
        cout << "Baseflow" << endl;
        this->baseSoil = baseflowSoil;
        this->baseCont = baseflowCont;
        this->baseRunoff = baseflowRunoff;
        int min = baseRunoff->getMin();
        int max = baseRunoff->getMax();
        int xSize = this->baseCont->getInt("xSize");
        int ySize = this->baseCont->getInt("ySize");
        this->m2perCell          = baseCont->getInt("sqmPerCell");

        basesegGrid        = new Grid(this->baseCont->getPath("Subbas",
            true), 1, "int", this->baseCont); //subbasins were Baseflow
             is summarized
        baseGrid = new Grid("float", this->baseCont); //grid for
            storing Baseflow values
        baseArea = new Grid(this->baseCont->getPath("BaseArea", true),
            1, "int", this->baseCont); //grid where baseflow is
            generated
        baseZonalSum = new ZonalSum(basesegGrid, "float", min, max,
            this->baseCont);

        this->timeStepZin = this->baseCont->getFloat("ZinStep");//gets
            ZIN timestep in min
        this->numStepsZin = int (24 * 60 / timeStepZin); //total number
             of ZIN timesteps

        sumBase = new float* [this->numStepsZin + 1]; //creates pointer
             array
            for ( int i = 1; i <= this->numStepsZin; i++ ){
                    sumBase[i] = new float[max - min + 3];
```

```
                }
        for (int y=0; y < ySize; y++){
                for (int x=0; x < xSize; x++){
                        baseGrid->putFloatAt(x, y, 0);
                }
        }
        baseZonalSum->defArray(numStepsZin);
}

Baseflow::~Baseflow()
{
}

void Baseflow::baseflowGeneration(int x, int y){
//the deep infiltration is gotten from the soilstorage module and put
    to the baseflow grid
        float DeepInfxy = baseSoil->getDeepInf();
        baseGrid ->putFloatAt(x, y, DeepInfxy*this->m2perCell);
}

void Baseflow::baseflowZonalsum(int time){
//the generated baseflow is added up per subbasin
        baseZonalSum->calcSum(baseGrid, time, baseArea, 1);
}
```

A.3.2. Erosion/sediment transport module

```
#include "stdafx.h"
#include "SedGeneration.h"
#include <math.h>

SedGeneration::SedGeneration(SoilStorageVG * soil, Runoff * zone,
    Controller * sediCont) //Constructor
{
        cout << endl << "SedGeneration" << endl ;
        this->soiltype = soil;
        this->subbasins = zone;
        this->sedimentCont = sediCont;
        min = subbasins->getMin();
        max = subbasins->getMax();
        segGrid = new Grid(this->sedimentCont->getPath("Subbas", true),
            1, "int", this->sedimentCont); //subbasins grid
        sediGrid = new Grid("float",   this->sedimentCont); //grid for
            storing Sediment values
        sediGrid->setValueF(-9999);
        xSize = this->sedimentCont->getInt("xSize");
```

```
        ySize = this->sedimentCont->getInt("ySize");
        m2perCell = this->sedimentCont->getInt("sqmPerCell");
        this->timeStepZin = this->sedimentCont->getFloat("ZinStep");
        this->numStepsZin = unsigned (24.0 * 60.0 / timeStepZin + 0.5);
        this->readSedProps(); //reading the rainfall_intensity -
            sediment relationships
        size = max - min + 2;
        sumSedi = new float* [this->numStepsZin + 1]; //creates pointer
             array
                for ( int i = 1; i <= this->numStepsZin; i++ ){
                        sumSedi[i] = new float[size+1];
                }
        cout << endl;
}

SedGeneration::~SedGeneration() //destructor
{
}

double SedGeneration::calcSediment(double rainfall, float OFperCell,
    int xcell, int ycell){
//Calculates the amount of erosion (g/(m^2min)) if there is
    OverlandFlow
        double SedPerCell=0;
        int soil;
        rainfall = rainfall / this ->timeStepZin * 60; //transforms the
             input from mm/timestep in mm/h
        if (rainfall == -9999){
                return 0;
        }
        soil = soiltype->getSoiltype(xcell,ycell); //gets the runoff-
            generation-zone-number for the cell
        if (this->isThereOF(OFperCell)){
                switch (this->equationtype[soil]){
                        case 1: SedPerCell = a[soil]*exp(b[soil]*
                            rainfall); //equationtype 1: a * exp(b *
                            rainfall_intensity)
                                break;
                        case 2: SedPerCell = a[soil]*rainfall + b[soil
                            ]; //equationtype 2: a * rainfall_intensity
                             + b
                                break;
                        case 3: SedPerCell = a[soil]*pow(rainfall, b[
                            soil]); //equationtype 3: a * b ^
                            rainfall_intensity
                                break;
```

```
                        case -9999: break; //out of Catchment
                        default: cout << "Fehler\n";
                }
        }
        else SedPerCell = 0;
        return SedPerCell * (this->m2perCell * this->timeStepZin); //
            returns sediment in kg/(timestep * cell)
}

void SedGeneration::readSedProps(){
//reads the properties of the rainfall_intensity-sediment_yield
    relationship from the sediment properties file
//equationtype 1: a * exp(b * rainfall_intensity)
//equationtype 2: a * rainfall_intensity + b
//equationtype 3: a * b ^ rainfall_intensity
        ifstream in;
        int             intRead;
        double  doubleRead;
        string  strDum;
        int i = 1;
        string  evapFile = this->sedimentCont->getPath("SedProps", true
            );
        cout << "reading sediment relationships ... ";
        in.open(evapFile.c_str());
        if (!in)
                throw ReportException(evapFile, 1);
        getline(in, strDum);// header line
        soil.push_back(0);
        equationtype.push_back(0);
        a.push_back(0);
        b.push_back(0);
        while (in >> intRead){
                soil.push_back(intRead);
                in >> intRead;
                equationtype.push_back(intRead);
                in >> doubleRead;
                a.push_back(doubleRead);
                in >> doubleRead;
                b.push_back(doubleRead);
                i++;
        }
        cout << "done!" << endl;
}

//Checks if there is OverlandFlow
bool SedGeneration::isThereOF(float OFSum){
```

```
        bool IsThereOF;
                if (OFSum == 0) {
                IsThereOF = false;
                }
                else {
                        IsThereOF = true;
                }
        return IsThereOF;
}

//sets the value of the SedimentGrid Zero
void SedGeneration::setZero(){
        for (int y=0; y < ySize; y++){
                for (int x=0; x < xSize; x++){
                        sediGrid->putFloatAt(x, y, 0);
                }
        }
}

void SedGeneration::setGridValues(int x, int y, float sedi){
        sedi *= m2perCell; //conversion: g/m2 in g/cell
        sediGrid -> putFloatAt(x, y, sedi);
}

//method for writing the grids of generated sediment/erosion (not
    enabled)
void SedGeneration::writeOutput(string filename, Grid* grid, int m){
        string filenameN;
        ostringstream m_string(ios::in);
        m_string << m;
        filenameN = this->sedimentCont->getPath("Output", true)+ "\\
            sediment\\" + filename + m_string.str() + ".txt";
        grid->writeGrid(filenameN);
}
//calucutaion of the sediment sum per subbasin and timestep
void SedGeneration::sedimentZonalSum(int time, int NoSubbasins){
        float condAux;
        int zoneAux;
        for (int k =1; k < NoSubbasins+1; k++){
                sumSedi[time][k] = 0;
        }
        for (int l = 0; l < ySize; l++){
                for (int k =0; k < xSize; k++){
                        zoneAux = segGrid -> getIntegerAt(k,l);//gets
                            number of the subbasin
                        if (zoneAux != -9999) {
```

```
                    condAux = sediGrid -> getFloatAt(k,l);
                    sumSedi[time][zoneAux]+=condAux;
                    }
            }
    }
}
```

A.4. Model Input data

There are some input files needed for the model. The input data used for this work is presented in this section.

A.4.1. Soil properties file

Table A.4.1.: Contents of the soil properties input file.

type	infCap	inLoss	depth	porEff	PWP	kfSat	lambda	FCap
1	200	6	2	0.42	0.07	0.53	0.35	0.28
2	2	0.8	1.1	0.42	0.07	0.53	0.35	0.28
3	31	3.5	5	0.42	0.07	0.53	0.353	0.28
4	31	2	5	0.42	0.07	0.53	0.353	0.28
5	38.5	4.5	1.1	0.41	0.07	0.46	0.355	0.292
6	38.5	4.5	1.1	0.41	0.07	0.08	0.355	0.29
7	38.5	4.5	1.1	0.41	0.07	0.08	0.355	0.29
8	31	3.5	1.2	0.42	0.07	0.53	0.353	0.28

A.4.2. Erosion properties file

Table A.4.2.: Contents of the channel properties input file.

soiltype	equation_type(1:a*exp(b*X); 2:a*x+b; 3:a*x$\hat{}$b)	parameter_a	parameter_b
1	3	0	0
2	3	5.1345E-05	2.224256
3	3	0.00002934	2.224256
4	3	2.934E-07	2.224256
5	3	0.00002934	2.224256
6	3	0.00002934	2.224256
7	3	0.00002934	2.224256
8	3	0.00002934	2.224256

A.4.3. Channel properties file

Table A.4.3.: Contents of the channel properties input file.

type	alldep	n_mann	varper	full	ni	ki	kb	kf	he	vk	l	antec	T	T0
1	0.01	0.02	0.999	0.6	0.1	0.01	100	0	0.1	0.053	0.1	0.85	100	0
2	0.01	0.035	0.999	1	0.1	0.01	100	0	0.1	0.025	0.1	0.85	100	0
3	0.01	0.035	0.999	1.5	0.1	0.01	100	0	0.1	0.025	0.1	0.85	100	0
4	0.01	0.03	0.999	2	0.1	0.01	100	0	0.1	0.025	0.1	0.85	100	0
5	0.01	0.035	0.999	3	0.1	0.01	100	0	0.1	0.025	0.1	0.85	100	0

A.4.4. Segments properties file

Table A.4.4.: Contents of the segment properties input file.

segment	prev	next	left_trib	right_trib	slope	lenght	width	chan_type	show_seg
1	0	2	0	0	0.23453155	40.08	0.6	1	0
2	1	3	0	0	0.0831678	95.83	0.6	1	0
3	2	4	0	0	0.08091435	119.88	0.6	1	0
4	3	5	0	0	0.12886133	154.74	0.6	1	0
5	4	6	0	0	0.064516	85.56	0.6	1	0
6	5	14	0	0	0.06159049	71.44	0.6	1	0
7	0	8	0	0	0.10421141	377.31	0.6	1	0
8	7	9	0	0	0.07353167	62.83	0.6	1	0
9	8	10	0	0	0.04027867	66.04	0.6	1	0
10	9	11	0	0	0.02839239	65.51	0.6	1	0
11	10	12	0	0	0.06356233	72.37	0.6	1	0
12	11	13	0	0	0.01182409	109.1	0.6	1	0
13	12	14	0	0	0.02230999	116.54	0.6	1	0
14	6	17	13	0	0.09255755	74.44	0.6	1	0
15	0	16	0	0	0.02504101	311.09	0.6	1	0
16	15	17	0	0	0.08478047	63.34	0.6	1	0
17	14	18	16	0	0.05132516	77.35	0.6	1	1
18	17	19	0	0	0.0860038	96.74	2	2	0
19	18	22	0	0	0.06511325	77.25	2	2	0
20	0	21	0	0	0.10102821	128.38	0.6	1	0
21	20	22	0	0	0.09130591	82.47	0.6	1	0
22	19	23	21	0	0.05440978	63.04	2	2	0
23	22	24	0	0	0.04323439	158.67	2.5	3	0
24	23	36	0	0	0.03314407	86.29	2.5	3	0
25	0	26	0	0	0.06960764	143.95	0.6	1	0
26	25	27	0	0	0.08343378	49.62	0.6	1	0
27	26	28	0	0	0.06168294	84.14	0.6	1	0
28	27	29	0	0	0.05494117	112.12	0.6	1	0
29	28	30	0	0	0.03929665	55.73	0.6	1	0
30	29	31	0	0	0.08680324	87.9	0.6	1	0
31	30	32	0	0	0.09497289	57.49	0.6	1	0
32	31	33	0	0	0.05487674	88.38	0.6	1	0
33	32	34	0	0	0.04648688	103.47	0.6	1	0
34	33	35	0	0	0.06184286	88.45	0.6	1	0
35	34	36	0	0	0.04430708	114.88	0.6	1	0
36	24	37	35	0	0.02324797	117.86	2.5	3	0
37	36	50	0	0	0.02094596	72.09	2.5	3	0
38	0	39	0	0	0.06805481	175.3	0.6	1	0
39	38	49	0	0	0.03096061	41.02	0.6	1	0
40	0	41	0	0	0.04267566	602.92	0.6	1	0
41	40	42	0	0	0.0174708	45.79	0.6	1	0

segment	prev	next	left_trib	right_trib	slope	lenght	width	chan_type	show_seg
42	41	43	0	0	0.00381583	47.17	0.6	1	0
43	42	44	0	0	0.09263951	75.13	0.6	1	0
44	43	45	0	0	0.06343069	106.1	0.6	1	0
45	44	49	0	0	0.04239731	139.16	0.6	1	0
46	0	47	0	0	0.09616	184.38	0.6	1	0
47	46	48	0	0	0.08098158	65.2	0.6	1	0
48	47	49	0	0	0.10696723	42.63	0.6	1	0
49	39	50	48	45	0.08795056	131.21	0.6	1	0
50	37	51	49	0	0.02094817	163.26	3	4	0
51	50	52	0	0	0.01992029	97.89	3	4	0
52	51	67	0	0	0.00822272	100.94	3	4	0
53	0	60	0	0	0.12327579	81.2	0.6	1	0
54	0	55	0	0	0.06467295	226.37	0.6	1	0
55	54	56	0	0	0.06160968	116.54	0.6	1	0
56	55	57	0	0	0.12529868	75.34	0.6	1	0
57	56	60	0	0	0.01418552	62.74	0.6	1	0
58	0	59	0	0	0.02948411	142.11	0.6	1	0
59	58	60	0	0	0.06083737	94.35	0.6	1	0
60	53	63	59	57	0.03568726	26.34	0.6	1	0
61	0	62	0	0	0.01523934	260.51	0.6	1	0
62	61	63	0	0	0.01300933	110.69	0.6	1	0
63	60	64	62	0	0.05496267	49.67	0.6	1	0
64	63	65	0	0	0.12323625	45.36	0.6	1	0
65	64	66	0	0	0.05770507	46.27	0.6	1	0
66	65	67	0	0	0.02691612	51.27	0.6	1	0
67	52	78	66	0	0.04344305	73.89	4	5	0
68	0	69	0	0	0.03574546	275.28	0.6	1	0
69	68	72	0	0	0.02796815	90.46	0.6	1	0
70	0	71	0	0	0.03204006	130.15	0.6	1	0
71	70	72	0	0	0.01465686	111.21	0.6	1	0
72	69	73	71	0	0.08959861	109.6	0.6	1	0
73	72	74	0	0	0.07649199	76.74	0.6	1	0
74	73	75	0	0	0.06606597	33.3	0.6	1	0
75	74	76	0	0	0.09584507	57.28	0.6	1	0
76	75	77	0	0	0.06707876	55.01	0.6	1	0
77	76	78	0	0	0.05585492	96.5	0.6	1	0
78	67	102	77	0	0.01769591	111.89	4	5	1
79	0	80	0	0	0.08387698	107.3	0.6	1	0
80	79	81	0	0	0.07445919	133.63	0.6	1	0
81	80	82	0	0	0.15679568	116.84	0.6	1	0
82	81	83	0	0	0.06572502	171.32	0.6	1	0
83	82	84	0	0	0.0467737	106.47	2.5	3	0
84	83	85	0	0	0.0436927	83.08	2.5	3	0
85	84	86	0	0	0.03238404	94.8	2.5	3	0
86	85	98	0	0	0.02733784	113.03	2.5	3	0
87	0	88	0	0	0.0973719	126.32	0.6	1	0
88	87	89	0	0	0.00146382	95.64	0.6	1	0
89	88	90	0	0	0.06281558	77.21	0.6	1	0
90	89	91	0	0	0.09425071	63.66	0.6	1	0
91	90	92	0	0	0.03482516	59.44	0.6	1	0
92	91	93	0	0	0.01858937	75.85	0.6	1	0
93	92	94	0	0	0.08489326	75.86	0.6	1	0
94	93	98	0	0	0.02692584	93.59	0.6	1	0
95	0	96	0	0	0.03476809	552.23	0.6	1	0
96	95	97	0	0	0.68076042	25.78	0.6	1	0
97	96	98	0	0	0.07907506	105.09	0.6	1	0
98	86	99	97	94	0.03172789	43.18	2.5	3	0
99	98	100	0	0	0.02416196	117.54	2.5	3	0
100	99	101	0	0	0.02639677	45.46	2.5	3	0
101	100	102	0	0	0.02444253	139.92	2.5	3	1
102	78	0	101	0	0.02177395	62.46	4	5	1

A.4.5. Subbasins properties file

Table A.4.5.: Contents of the subbasins properties input file.

segment	subbasin	slope	area
1	1	0.0846289	34519
2	2	0.0929271	15075
3	3	0.0749194	19937
4	4	0.0562467	85212
5	5	0.0651691	27806
6	12	0.0605299	41887
7	6	0.113523	11579
8	7	0.0687212	950
9	8	0.131493	1317
10	9	0.178511	1373
11	10	0.114829	10099
12	11	0.0572721	8444
13	0	0.01	0.01
14	14	0.0771396	33257
15	13	0.0592796	18628
16	0	0.01	0.01
17	15	0.164441	1556
18	16	0.0623326	3140
19	17	0.0624598	6185
20	18	0.0780344	9395
21	0	0.01	0.01
22	19	0.0728229	18990
23	20	0.0827202	17731
24	21	0.0692644	17150
25	22	0.0469519	9724
26	23	0.0484537	4569
27	24	0.0623176	13977
28	25	0.0573905	2450
29	26	0.0582477	632
30	27	0.055648	17151
31	28	0.0707245	27260
32	29	0.0534906	30146
33	30	0.0591219	24410
34	0	0.01	0.01
35	0	0.01	0.01
36	31	0.0626289	27566
37	32	0.0681543	50627
38	39	0.0626243	7992
39	38	0.048635	26770
40	33	0.0466398	50913
41	34	0.0821055	2711
42	35	0.0629925	3608
43	36	0.115128	13747
44	37	0.0592065	64130
45	0	0.01	0.01
46	40	0.0710727	13652
47	41	0.0599194	1147
48	0	0.01	0.01
49	0	0.01	0.01
50	42	0.0705823	38388
51	43	0.0742628	20403
52	44	0.0595309	25627
53	46	0.0533093	21018
54	47	0.0451309	11652
55	48	0.0570822	23997
56	0	0.01	0.01
57	0	0.01	0.01
58	45	0.0224571	5870
59	0	0.01	0.01
60	0	0.01	0.01
61	49	0.0435006	9011
62	50	0.0534039	6680

segment	subbasin	slope	area
63	51	0.0604355	25113
64	52	0.223069	419
65	53	0.263492	519
66	0	0.01	0.01
67	54	0.0506234	14308
68	55	0.0961098	7381
69	56	0.0218597	20763
70	57	0.0338919	1891
71	0	0.01	0.01
72	58	0.0824441	3840
73	59	0.0842041	41965
74	60	0.178623	884
75	61	0.112654	26632
76	62	0.275664	648
77	0	0.01	0.01
78	63	0.04432	25443
79	64	0.0485819	28521
80	65	0.0436732	42356
81	66	0.0940847	24490
82	67	0.0598906	6255
83	68	0.0743489	9837
84	69	0.0795305	17017
85	70	0.0632305	16273
86	71	0.072482	21217
87	73	0.0537404	48809
88	74	0.118644	30965
89	0	0.01	0.01
90	76	0.0991937	22812
91	75	0.10718	10890
92	77	0.0577728	3546
93	78	0.241621	782
94	0	0.01	0.01
95	79	0.0316259	42500
96	80	0.129941	32375
97	0	0.01	0.01
98	72	0.0605028	13427
99	81	0.0753504	19169
100	82	0.139875	8976
101	0	0.01	0.01
102	83	0.0503605	11428

A.5. Pictures

Figure A.5.1.: Modified Fluorometer Fl-30 for longtime sediment measurements.

Figure A.5.2.: Sediment at the border of the streets in the Loechernbach catchment.

Figure A.5.3.: The GGun Fl-30 Fluorometer equipped for turbidity measurements in the Loechernbach channel near the catchment outlet at baseflow conditions.

Figure A.5.4.: Configuration of the laboratory measurements for the turbidity-suspended sediment concentration relationship.

Ehrenwörtliche Erklärung:

Hiermit erkläre ich, dass die Arbeit selbständig und nur unter Verwendung der angegebenen Hilfsmittel angefertigt wurde.

Ort, Datum Unterschrift